

https://dspace.org/

A study of the istopic and geochemical gradients in the old granite of the Vredefort Structure with implications for continental heat flow

Hart, R J

2015-08-03
http://hdl.handle.net/10539/18177

Downloaded from a DSpace repository. https://dspace.org/

A STUDY OF THE ISOTOPIC AND GEOCHEMICAL GRADIENTS IN THE OLD GRANITE OF THE VREDEFORT STRUCTURE, WITH IMPLICATIONS FOR CONTINENTAL HEAT FLOW

A thesis submitted for
the degree of
DOCTOR OF PHILOSOPHY
in the
Faculty of Science
University of the Witwatersrand

R.J. Hart

January, 19[illegible].
Johannesburg.

STATEMENT.

All work and interpretation, except where acknowledged in the text, was performed by the author. The work has not been submitted elsewhere for a higher degree.

(Signed) 

ACKNOWLEDGEMENTS

This investigation was undertaken at the Bernard Price Institute for Geophysical Research, University of the Witwatersrand, Johannesburg.

The financial support of the Atomic Energy Board of South Africa is gratefully acknowledged.

I wish to express my sincere thanks to my supervisors, Professor L.O. Nicolaysen and Professor H.L. Allen for their guidance, friendship and often considerable patience throughout the time of this study.

The author wishes to thank Dr. N.H. Cole of the Department of Geology, Oxford University for facilitating the use of irradiation facilities in the DIDO reactor Harwell, England.

To my colleagues at the Bernard Price Institute and the Geology Department, University of the Witwatersrand, goes my sincere gratitude for practical assistance and many stimulating discussions. In particular I would like to thank Dr. H. Welke, Mr. D. Stepto, Dr. S. Richardson, Dr. J. Kramers, Mr. T. McCarthy and Mr. B. Wyatt.

I would also like to thank Mr. W. Netshiluvhi for his able assistance in numerous tasks.

To the secretaries of the B.P.I., Doreen, Linda, Ann and Ros who had to perform the arduous task of typing this thesis, many thanks.

Finally to my wife Adele, thank you for your support and understanding over the past few years.

TABLE OF CONTENTS

CHAPTER			PAGE
1	INTRODUCTION		1
2	GEOLOGICAL OUTLINE		4
	2.1	General geology	4
	2.2	Geology of the basement granite	8
	2.3	Evidence for an overturned crust	12
	2.4	Sequence of events	14
3	ANALYTICAL PROCEDURES		15
	3.1	Sample collection and preparation	15
	3.2	X-ray fluorescence	16
	3.3	Delayed neutron activation	16
	3.4	Water analyses	17
	3.5	Mass spectrometry	17
4	GEOCHEMISTRY		18
	4.1	General theory and discussion	18
	4.2	Data presentation	29
	4.3	Compiling profiles of elemental concentration versus depth in the crust	41
	4.4	Trace element variations	43
	4.5	Averaged trace element profiles	48
	4.6	Major element variations	53
	4.7	Averaged major element profiles	54
	4.8	Interpretation of the geochemical data	56
	4.9	General discussion	58
5	RADIO ELEMENT PROFILES AND HEAT PRODUCTION		72
	5.1	Introduction	72
	5.2	Results	74
	5.3	Th/U, K/U and K/Th profiles	79

5.4 Discussion 81

6 HEAT FLOW/HEAT PRODUCTION IN THE VREDEFORT AND FAR WEST WITWATERSRAND AREAS 84

6.1 Introduction 84

6.2 Geological evidence 85

6.3 Heat flow measurements 86

6.4 Sampling a section through the stratified rocks of the Witwatersrand basin 88

6.5 Heat generation in the stratified rocks 90

6.6 Heat generation in the Vredefort basement granites 90

6.7 Total measured contribution to surface heat flow 94

6.8 Heat production in the lower crust 94

6.9 Estimates of heat flow across the M-discontinuity 97

6.10 Consequences of low mantle heat flow 98

6.11 Conclusions 100

7 GEOCHRONOLOGY OF THE VREDEFORT BASEMENT 101

7.1 Introduction 101

7.2 Results 102

a. Metabasites and metasediments of the Steynskraal Metamorphic zone 104

b. Inlandsee Leucogranofels 109

c. Outer Granite Gneiss 109

d. Central Intrusive Granite 109

e. U-Th-Pb geochronology results 109

7.3 Geological interpretation of whole rock ages and initial ratios 111

7.4 Discussion of results 113

a. Metabasites and metasediments of the Steynskraal Metamorphic zone 113

b. Inlandsee Leucogranofels 114

c. Outer Granite Gneiss 117

d. Central Intrusive Granite 118

7.5 Movement of LIL elements in the Vredefort crust 119

8 INTERPRETATION OF RESULTS 121

8.1 Models for the evolution of the Vredefort crust 121

8.2 Summary and Conclusions 125

a. Geochemistry of the middle Vredefort crust (ILG + SMZ) 125

b. Geochemistry of the Outer Granite Gneiss 126

c. Heat production and the implications for continental heat flow 127

d. Geochronology 128

8.3 Implications for the evolution of the early Precambrian crust 129

APPENDIX

A ISOTOPE DILUTION 135

A.1 Chemical analyses 135

A.2 Instrumentation 137

A.3 Data reduction 138

A.4 Analytical precision and accuracy 140

B X-RAY FLUORESCENCE 142

B.1 Data reduction: precision and accuracy 144

C DELAYED NEUTRON ACTIVATION 147

C.1 Comparison of analytical methods for Uranium and Thorium 147

C.2 Procedure 148

C.3 Interference 150

C.4 Data reduction, precision and accuracy 151

D ANALYSIS OF WATER BY HEATING AND CONDENSATION 155

E PETROGRAPHY OF SOME SELECTED SAMPLES WHICH WERE ANALYSED BY THE ISOTOPE DILUTION METHOD 157

REFERENCES 162

LIST OF FIGURES

Figure		Page
2.1	Vredefort ring structure and the central Witwatersrand basin	5
2.2	View of the northern rim of the Vredefort structure	4
2.3	Detailed geological map of the central Inlandsee area of the Vredefort basement	9
2.4	Section across the Witwatersrand strata and basement granite contact	13
2.5	Section across a sill of the tholeiitic series	13
3.1	Sample locations	15
4.0	K/U ratios as a function of K content for some common rocks	23
4.1	North east radial profile	30
4.2	North west radial profile	33
4.3	South west radial profile	36
4.4	Variation of K/Rb across the Vredefort basement	39
4.5	Variation of Ba/Fb across the Vredefort basement	40
4.6	The Vredefort basement showing one km contour intervals measured inward from the Orange Grove quattzite and the subdivision of the basement into three quadrants	42
4.7	K versus Rb	45
4.8	Ba versus Sr	47
4.9	Averaged trace and major element profiles for the Vredefort basement	49
4.10	Fe versus Ti	55
4.11	Fe versus Zr	55
5.1	Inferred radioelement profiles with depth	72
5.2	Averaged radioelement and heat production profile for the Vredefort basement	76
5.3	Comparison of the degree of fit between a linear and an exponential radioelement distribution function with depth in the Vredefort basement	78

5.4	Averaged Th/U, K/U and K/Rb profiles for the Vredefort basement	80
6.1	Boreholes from which heat flow data has been obtained	87
6.2	Ocean and continental lithosphere	99
7.1	Sample locations	103
7.2	Rb-Sr isochron diagram for the SMZ	107
7.3	Rb-Sr isochron diagram for the ILG	107
7.4	Rb-Sr isochron diagram for the OGG	108
7.5	Rb-Sr isochron diagram for the CIG	108
7.6	Initial Sr^{87}/Sr^{86} ratio versus time diagram	116
8.1	Model I for the evolution of the Vredefort crust	123
8.2	Model II for the evolution of the Vredefort crust	123

LIST OF TABLES

Table		Page
4.1	Trace element concentrations and ratios for rocks from the Vredefort basement	61
4.2	Major and select trace elements : Traverse 1	66
4.3	Major and select trace elements : Traverse 2	69
4.4	Major and select trace elements : Traverse 3	71
4.5	Averaged major and trace element profiles for the Vredefort basement	44
5.1	Averaged radioelement concentrations and heat production for the Vredefort basement (excl. S-W quad.)	75
5.2	Conversion of radioelement concentrations to heat production	74
5.3	Average concentration of U, Th and K from granulites of the Musgrave range (south-west Australia) and from north Norway	80
5.4	Average Th/U, K/U and K/Th ratios for Precambrian shield rocks	81
5.5	U, Th and K for the mafic granulites for the Vredefort basement	82
5.6	Comparison of K/Th and K/U ratios between pyroxene granulites and amphibolite facies rocks from the southwest Australian shield	82
6.1	Comparison of U, Th and K concentrations from the southwest Australian shield, the upper Vredefort basement and the basement rocks of the eastern Transvaal and Swaziland	86
6.2	Heat flow measurements in the Transvaal and Orange Free State	89
6.3	Radioelement concentrations for the stratified rocks of the Witwatersrand basin	91
6.4	Average radioelement concentrations and heat productions (expressed in cal. $cm^{-3} sec^{-1} \times 10^{-13}$) for the stratified rocks of the Witwatersrand basin	92
6.5	The thickness of the lithological units for the boreholes in Figure 6.1	93
6.6	Average radioelement and heat production for the Vredefort basement (including S.W. quadrant)	95

6.7	Models for the heat production for the lower 16 Km of the crust	97
6.8	Heat production model for a three layered lithosphere	97
7.1	Rb-Sr isotopic data for the Steynskraal Metasediments and Metabasites	105
7.2	Rb-Sr isotopic data for the Inlandsee Leucogranofels	105
7.3	Rb-Sr isotopic data for the Outer Granite Gneiss	106
7.4	Rb-Sr isotopic data for the Central Intrusive Granite	106
7.5	Summary of the Th-Pb, U-Pb and Pb-Pb isotopic data	110
8.1	Summary of Models for the evolution of the Vredefort crust	122

ABSTRACT

The presence of granite of pre-Witwatersrand age forming the core of an updomed and overturned sequence of strata at Vredefort, South Africa, has been known for over seventy years. It is only recent geophysical, geochemical and geological evidence that has given rise to the proposal that the basement core has also been overturned, presenting a section of the earth's granitic crust to view. Comprehensive geochemical and isotopic studies on this section are presented in this thesis.

Two distinct annular zones which were identified by their geologic and petrographic character have distinct major element attributes. The deepest crustal levels, exposed in the central parts of the dome, are represented by the highly siliceous Inlandsee leucogranofels (ILG) which is characterised by the absence of ferro-magnesium minerals, and a strongly marked tectonic fabric. Inclusions of metasedimentary supracrustals and pyroxene granulites occur interlayered with the Inlandsee leucogranofels. The outer granite gneiss (OGG) forms a 10 km wide peripheral zone to the inner core. The gneisses vary in composition, and in general show a progressive increase in cafemic character from the margins inwards: the geochemical variations suggest a partial melting model for the development of the outer 10 km of the Vredefort crust.

Detailed trace element profiles across the granite basement indicate that (i) the central part of the core is depleted in the large ion lithophile elements U, Th and Rb, relative to the perimeter, (ii) the concentrations of U, Th and Rb falls off regularly from the granite margin inwards, and the distribution of these elements over the outer 8 km is consistent with an exponential depth-function, and (iii) the central part of the core is characterised by high K/Rb, Th/U, K/U, K/Th, Ba/Rb and low Rb/Sr ratios, and it is only the outer 5 km of the basement core that has elemental ratios which approach those found in "normal" surface granites.

The heat generation from the entire exposed vertical section of the Vredefort granite, together with heat production in the overlying stratified rocks, has been examined. By comparing the heat production in the crust to heat flow in the nearby Far West Witwatersrand goldfield, a reasonable estimate of the heat flow from the mantle has been made. A value of between .25 and .36 HFU has been estimated. The mantle heat flow has an important bearing on the depth of the lithosphere - asthenosphere boundary. On the basis of the mantle heat flow value, the depth to the low velocity zone beneath the Southern African sub-continent has been estimated at approximately 300 km.

Whole rock Rb-Sr, Th-Pb and U-Pb isotopic investigations were made on the granite and basic rocks of the Vredefort basement. The measured ages and initial ratios provide evidence that well preserved remnants of sedimentary supracrustals and basic to intermediate volcanics existed as a protocrust in pre-3.5 b.y. times. Further, these results have a direct bearing on the question of movement of material between mantle and crust in Archaean times, and suggest that a major phase of sialic differentiation from the mantle occurred close to 3.5 b.y. ago.

It is argued that circa 2.8 b.y. ago high grade metamorphic conditions in the felsic rocks (IIG) of the lower Vredefort crust effected complete isotopic rehomogenization of the Rb-Sr isotopic system. It was during this period that uranium depletion occurred in both the felsic and mafic rocks of the lower Vredefort crust. The Th-Pb system of the felsic rocks was partially effected but the mafic rocks have remained a closed system with respect to both Rb-Sr and Th-Pb.

In the upper Vredefort crust (OGG) good whole rock isochron ages of $\sim$ 3.0 b.y. are obtained for Rb-Sr, Th-Pb and U-Pb isotopic systems. The primary ratios for both Rb-Sr and U-Pb suggest that the OGG was derived from the mantle shortly before 3.0 b.y. However, evidence of a complex tectonic and thermal history, and an anomalously low Pb^{208}/Pb^{206} initial

ratio has led to the conclusion that prior to 3.0 b.y. ago the OGG participated in a crustal history of about 550 m.y., characterised by relatively low Rb/Sr ratios and low μ and $\kappa\mu$ values (before taking on their present-day values).

1 INTRODUCTION

The Vredefort granitic basement lying near the centre of the Witwatersrand basin, is one of numerous basement domes found in the southern Transvaal and northern Orange Free State in South Africa. The Vredefort structure, however, is unique in that the collar strata, which form prominent semi-circular series of ridges around the central granite core, are largely overturned. This striking feature of Vredefort geology has attracted the attention of geologists since the turn of the century.

The first description of some of the features of the Vredefort dome was made by Hall and Molengraaf (1925). A detailed map and geological description was presented by Nel (1927). A later detailed petrographic and chemical investigation on the Archaean granite was made by Willemse (1937). These investigations showed that the granite core neither intruded nor metamorphosed the collar sediments, indicating that the granite margins were solid and cold at the time of updoming. A detailed petrographic study of the post-Witwatersrand igneous and metamorphic phenomena in and around the Vredefort structure was made by Bisschoff (1969).

The origin of the Vredefort dome is controversial and has been the subject of disputes for several decades. A meteorite impact origin was proposed by Daly (1947) and was later augmented by Dietz (1961), who claimed that shatter cones, found in the Vredefort area (Hargraves, 1961), are unique to meteorite impact sites. The principle arguments for and against a meteorite impact origin for the Vredefort structure are outlined by Hargraves (1970).

Poldervaart (1962) first drew attention to the possibility of singularities in the age patterns of the old basement granite. He suggested that during uplift the extreme margins of the central granite may have been partially recrystallised, thus enabling the age of the updoming event to be dated. Slawson (1976) tested this theory.

A Rb-Sr whole isochron for the basement granite obtained by Slawson (1976) yields an age of 2850 ± 60 m.y. These data "show that on the scale of the whole rock samples the geochemical regime of the Vredefort granite as set prior to the 'extrusion' and has been retained for the elements Rb, Sr and K."

Although Slawson's study provides no further clue as to the age of the Vredefort structure, an additional dividend arising from his work was the remarkable "bulls eye" pattern of the Rb/Sr and K/Rb ratios, that led him to suggest that the rocks at the centre may be representative of a deeper section of the earth's granitic crust than those at the perimeter. If this interpretation is correct, "it would appear that Vredefort provides a unique opportunity for geochemical and geophysical examination of a deep section of the earth's granitic crust" (Slawson 1976).

In this present work, it was not anticipated that any single geochemical or isotopic study could provide definitive evidence for a "crust on edge model", although the integrated results, taken in the context of the geological evidence were expected to provide a reasonable test. In essence, the study was directed at these questions: will detailed work confirm Slawson's conjecture?, and if the conjecture is confirmed, what behaviour will be exhibited by the major and trace elements in a deep crustal section? Particular attention was given to the radio-elements, with a view to improving our knowledge on some of the problems of terrestrial heat flow and the temperature distribution within the crust.

The presence of basic to intermediate rocks occurring in the granulite facies from the interior of the basement core was described by Hall and Molengraaf (1925) and Nel (1927). The existence of rocks of varying lithologic character indicated the need to re-examine the Rb-Sr whole rock isotopic data as presented by Slawson. Furthermore, additional Rb-Sr isotope analyses were carried out for the purpose of observing the effects

of depth and increasing metamorphic grade on this isotopic system.

The U-Th-Pb isotopic results from the Vredefort basement have a significant bearing on the reconstruction of the chronological history of the Precambrian crust. These results, which are reported in a paper by Welke et al. (Ms. in preparation), are discussed here in depth.

2 GEOLOGICAL OUTLINE

2.1 General geology

A brief review of some of the principal published investigations on the Vredefort structure has already been given in the previous chapter. The geological observations provide the framework upon which more recent geophysical and geochemical studies have been carried out, and a brief geological description is now given. A detailed description of the geology and structural setting is available from Haughton (1969).

The Vredefort structure is located ~ 110 km south-west of Johannesburg and is centred around the towns of Vredefort and Parys (Figure 2.1). The basement granitic core which is about 50 km in diameter, outcrops near the centre of the Witwatersrand Basin. The southern and eastern portions of the structure are covered with flat-lying Palaeozoic Karroo strata. On the northern and western sides of the dome overturned Precambrian strata of the Lower Witwatersrand Group form a rim around the central hub of Archaean granite. These Precambrian strata reach a total thickness of about 15 km and where inverted, are seen to be dipping



FIGURE 2.2 View of the northern rim of the Vredefort structure.



FIGURE 2.1 Vredefort ring structure and the central Witwatersrand basin

(after Borchers, 1961)

steeply inwards towards the granite core (Figure 2.2). Elsewhere around the collar the sediments are more vertical in attitude.

The mantling strata of the collar must have undergone striking structural disturbances in order to accommodate the structure (Nicolaysen, personal communication). The outcrop length of the Lower Witwatersrand sediments has been considerably shortened by oblique faulting. Over the exposed portion of the Orange Grove quartzite the amount of shortening is about 7% (Manton, 1962). Before uplift the present surface exposure of the unit was evidently located on an arc of greater radius than the present perimeter. Similar measurements on strata that occur higher up in the sequence indicated that the relative crustal shortening decreases with radial distance from the centre.

Bishopp (1941) noted that the stratigraphic thicknesses of the collar strata are closely comparable with those measured elsewhere in the Witwatersrand basin. The collar strata thus appear to have behaved in a competent fashion during updoming and any mechanism of updoming requires either extensive lateral faulting or shattering of the collar strata (Nicolaysen, personal communication).

A number of intrusive rocks of different ages, petrography and mode of emplacement occur within the granite basement and surrounding strata. These intrusives have been described in detail by Bisschoff (1969) and others; their main features are summarised below:

(i) Tholeiitic sills occur within the granite and the Lower Witwatersrand sediments. These sills, which are cut by faults produced during updoming, appear to be conformable with the bedding planes of the sediments and are vertical or near vertical in attitude. Some of the tholeiitic bodies show evidence of having been differentiated while in a horizontal position, and now show features of upturned sills.

(ii) Genetically related alkalic granites and nepheline syenites have been intruded into the northern portion of the overturned rim sediments. The tholeiitic and the alkalic intrusives contain pseudotachylite, shatter cones and microscopic evidence of shock deformation (Hargraves, 1970; Bisschoff, 1969). The Roodekraal igneous complex is intruded into the Pretoria Series strata of the Transvaal Group to the southeast of Potchefstroom. It consists of diabasic, dioritic and syenitic rocks. It is probably an intrusive mass of the same suite.

(iii) Over the northwestern arc of the dome a thin, vertical discontinuous dyke of bronzite granophyre closely follows the contact between the sediments and the Archaean granite. The dyke cuts across all the faults produced during the formation of the dome. Other shorter dykes of bronzite granophyre are found in the Archaean granite near the town of Vredefort.

A most conspicuous feature of the Vredefort dome is the presence of pseudotachylite and shatter cones. It is generally agreed that these features are closely related to the formation of the Vredefort structure.

(i) Pseudotachylite, a term used by Shand (1916) to describe an ultra-mylonitised rock is similar in appearance to tachylite and cuts most of the rock types in the Vredefort area, with the exception of the bronzite granophyre dyke. The pseudotachylites of the Vredefort dome have been described in a paper by Bisschoff (1961).

(ii) The widespread development of shattercones in the collar rocks of the Vredefort dome was first described by Hargraves (1961) and later by Manton (1962). The orientations of the shattercones are such that when the rocks of the collar are restored

to their original horizontal position, the apices of the cones point inwards to a central focus.

2.2 Geology of the basement granite

The most common rock types in the Vredefort basement are granitic in composition. In the central region of the Vredefort dome mafic to intermediate Archaean rocks occur as xenoliths within the felsic rocks (Stepto Ms. in preparation). The mafic xenoliths vary in size from small pods to large outcrops between 1 and 2 kilometres in length. The margins of the mafic bodies generally appear to be conformable with the foliation of the surrounding felsic rocks.

The Steynskraal metamorphic zone (SMZ), which is the type area for the mafic metamorphic suite, occurs about 10 km from the outer margin of the basement granite and appears to extend as a collar around the inner core of the dome (Figure 2.3). The Steynskraal metamorphic zone not only marks the beginning of the occurrence of metabasite and metasedimentary inclusions, but it is also the transition zone between the Inlandsee leucogranophyre (ILG) and the outer granite gneiss (GGG).

In the Steynskraal area the xenoliths are predominantly banded ironstones and restricted cherts, whereas in the vicinity of the Inlandsee near the centre of the dome metasediments account for only a minor amount of the mafic rocks, which are mainly metagabbros and metanorites. The metasediments and metabasites occur as distinct units interlayered with the ILG and account for between 3 and 10% of the basement rocks in the Steynskraal zone and in the central core of the dome. It should be emphasised that apart from the SMZ, the outcrops in the central part of the dome are exceedingly poor, and generally the more mafic rocks are preferentially weathered (Stepto, personal communication). This makes it difficult to give a true assessment of the proportion of mafic and felsic rocks in this area.



FIGURE 2.3 Detailed geological map of the central Inlandsee area of the Vredefort Basement (after Stepto, MS in preparation)

High grade granulite facies rocks from the interior of the granite core were mentioned by Hall and Molengraaf (1925) and Nel (1927). The variation of metamorphic grade across the dome has now been described in detail by Stepto (Ms. in preparation). The OGG exhibit a lower grade amphibolite facies metamorphism. The transformation from hydrous to anhydrous mineral assemblages is quite apparent in the outer regions of the ILG. Details of the transition are best observed in the SMZ. Within this zone the mineralogy of the mafic inclusions changes from amphibolites through pyroxene to pyroxene granulites. These changes occur over a di tance of about 5 km.

Apart from the fact that the ILG exhibits a higher grade of metamorphism than the OGG, the most striking difference between the two suites of rocks is the almost complete lack of mafic mineral phases in the former. The ILG consists essentially of quartz and feldspar. Ilmenite, zircon, monazite and rutile occur as accessories. Minor amounts of hypersthene have been encountered in heavy mineral separates, although not in thin section (a detailed account of thin section and mineral separate studies of some selected samples is given in Appendix E).

In many outcrops, especially toward the centre of the dome in the vicinity of the Inlandsee, the leucogranofels a striking appearance. A strong planar tectonic fabric is often evident on these outcrops. This is due to flattened lenticular aggregates of quartz. In thin section these aggregates display a well developed glomerogranular texture. In all cases the quartz is completely recrystallised into aggregates of equant 5 or 6-sided polyhedra. The larger grains form the cores, and the smaller ones the margins of such aggregates. Striking granophyric textures are developed marginal to the quartz aggregates in the most central rocks of the dome (Nicolaysen, Ms. in preparation).

Although on a hand specimen scale the outer granite gneisses are not tectonites, the only obvious deformation in thin section being a

faint undulatory extinction of quartz crystals, there are a number of features in the field which indicate a complex tectonic and metamorphic history.

Firstly, the outer granite gneiss varies considerably in colour, texture and mineralogy from strongly banded and layered biotite-rich rocks through gneissic rocks with a weak foliation to rocks of granitic texture which may be termed massive and homogeneous. The typical granite gneisses, which predominate, consist essentially of quartz, pink orthoclase, plagioclase, biotite with minor amounts of sphene and apatite. Towards the inner margins of the OGG there are numerous outcrops which suggest that a pre-existing more basic rock type has been invaded and replaced by a more felsic component, and even towards the outer margin where the rocks are generally massive, remnants of basic material that have been incompletely incorporated are distinguishable. Discordant quartz feldspar veins are prevalent throughout the OGG and vary from single strings of quartz and felspar crystals, to pegmatite veins which are ~ two metres in width.

Secondly, at least two phases of deformation are evident in the field. On many outcrops the OGG appears to be massive, but in substantial pavements and all blasted exposures it has a heterogeneous and streaky character; a pronounced banding and mineral orientation (related to incomplete assimilation of relict rocks) is often evident. At least one period of folding that has resulted in a local duplication of strata occurred.

In the vicinity of the Inlandsee, a small outcrop of intrusive biotite granite has been noted by Stepto (Ms. in preparation). Although the outcrop extends over only a few metres, its intrusive nature and distinctly different mineralogy and texture from that of the surrounding basement rocks, is of considerable interest for this study. The granite's texture is massive, and it is not a tectonite, as there is no evidence of any deformation. Quartz, feldspar and large (5 mm) light brown biotite

flakes make up the essential minerals. The lack of any deformation textures suggest that this rock postdates the updoming event, and could thus supply valuable information as to the time of emplacement of the Vredefort structure.

2.3 Evidence for an overturned crust

The depth of penetration of a radial profile across the dome, which is based largely on the geological evidence for an overturned crust, is discussed in some detail in chapter 4, section 4.3.

However it is convenient at this stage to outline briefly some of the features of an overturned crust. It has been observed that the dips of the rim sediments change in a regular fashion as one proceeds from the granite contact outwards (Hanton, 1962; Bisschoff, 1969). This regular dip change manifests a basic mechanical characteristic of the 15 km thick stratified column during overturning. If this mechanical "style" were to continue inwards into the granite basement, that is if the regular diminution in the degree of overturning continues steadily into the interior of the structure, then a considerable vertical section must be exposed to view (Fig. 2.4).

Bisschoff (1969) first drew attention to the fact that a sill of the tholeiitic series emplaced into the basement over 1 km inwards from the Orange Grove quartzite has an inverted sequence of differentiates (Fig. 2.5). This sill (and several others) were clearly intruded in a near horizontal attitude, differentiated and then updomed and overturned. The surrounding basement must also have been overturned.

At about 10 km from the granite margin there is still reason to believe that the attitude of the basement is still steeply inclined. This is demonstrated by the fact that in traversing inwards through the SMZ, one is continuously passing into new and deeper crustal units, as reflected by the changing metamorphic grade (i.e. from amphibolites into garnet pyroxene granulite over a distance of about 5 km).

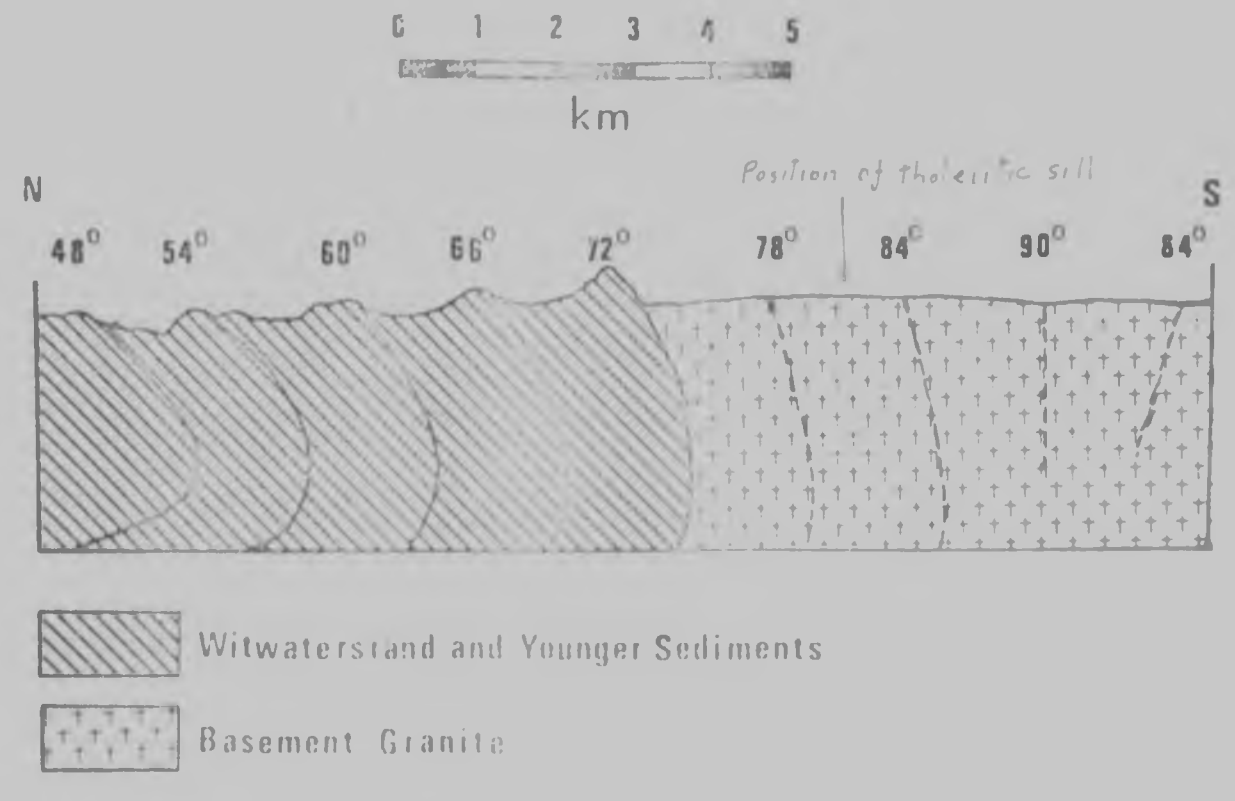


FIGURE 2.4 Section across the Witwatersrand strata and basement granite contact

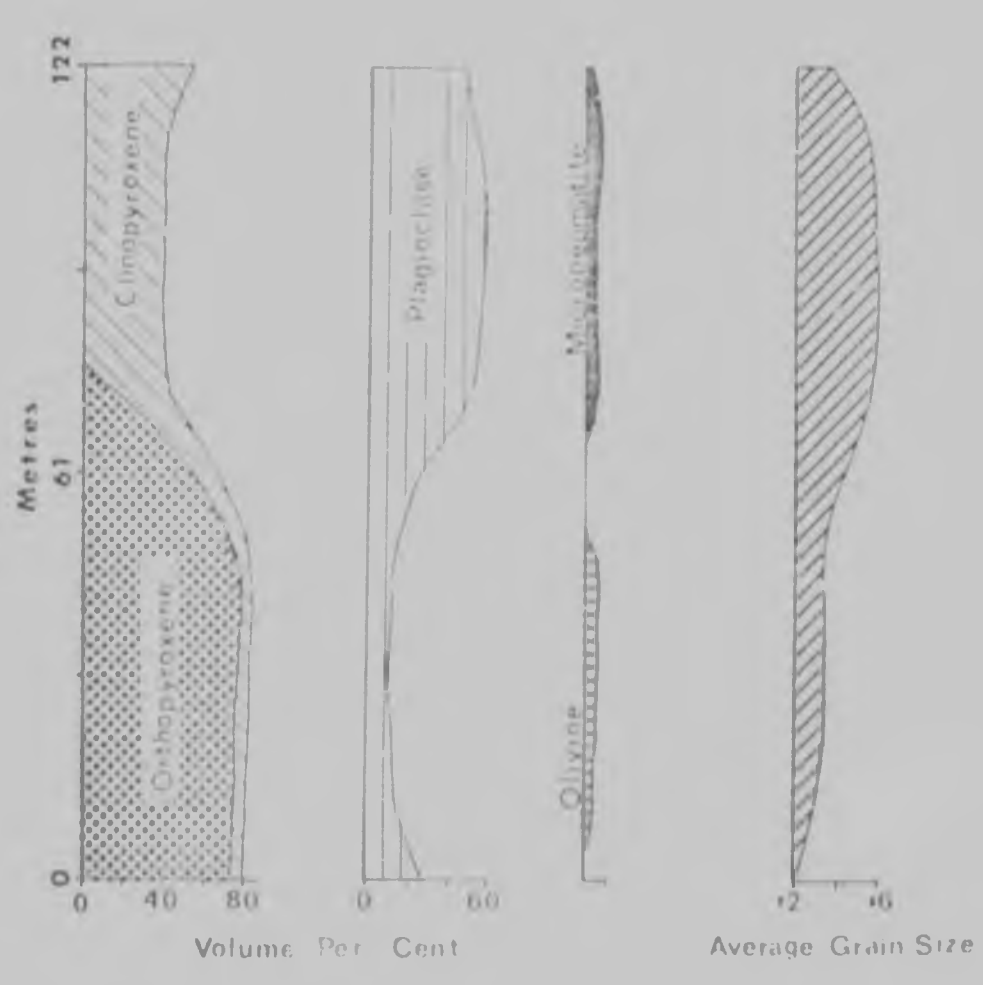


FIGURE 2.5 Section across a sill of the tholeiitic series (after Bischoff, 1969)

In a later chapter (8) it will be demonstrated that this granulite facies metamorphism was completed at least c. 2800 m.y. ago, long before deposition of the Transvaal Supergroup (of the upturned collar strata); thus it is highly likely that the granulite metamorphism was completed when the crustal section was essentially horizontal.

2.4 Sequence of events

The field relationships, and the time of emplacement of the alkali granites and associated syenites, and the basic granophyre dyke, are crucial in determining the time of updoming of the Vredefort structure.

The alkali granites are extensively cut by veins of pseudotachylite and contain abundant shatter cones. Dietz (1961) contends that these features provide evidence for meteorite impact, which in turn implies that the alkali granites were intruded into essentially flat lying sediments prior to the development of the Vredefort structure. However the field relationships indicate that the alkali granites were emplaced after the overturning, and hence that their shock features are unrelated to the mechanism of overturning (Bisschoff 1969). On the other hand the intrusion of the basic granophyre dyke is clearly post-overturning. The basic granophyres do not contain shock deformation features, and the nature of the outcrop is clearly transgressive to all features such as radial faults which might be closely associated with the formation of the structure. Radiometric age determinations on the alkali granite give an age which is no more than 70 m.y. older than the age of 1970 m.y. for the basic granophyre (Nicolaysen et al. 1963).

Summarizing the known facts, the updoming postdates deposition of the Transvaal Supergroup and the tholeiite sill intrusions, and predates the intrusion of the basic granophyre dykes. The time of updoming relative to the intrusion of the alkalic suite is not known.

3 ANALYTICAL PROCEDURE

3.1 Sample collection and preparation

150 rock samples of between 5 and 10 kg each, were collected at the points shown in Figure 3.1. Samples of this size were considered large enough to represent closed systems for whole rock isotope analyses and geochemical studies. 80 samples were collected on near linear traverses extending radially across the circular massif, as indicated in Figure 3.1.

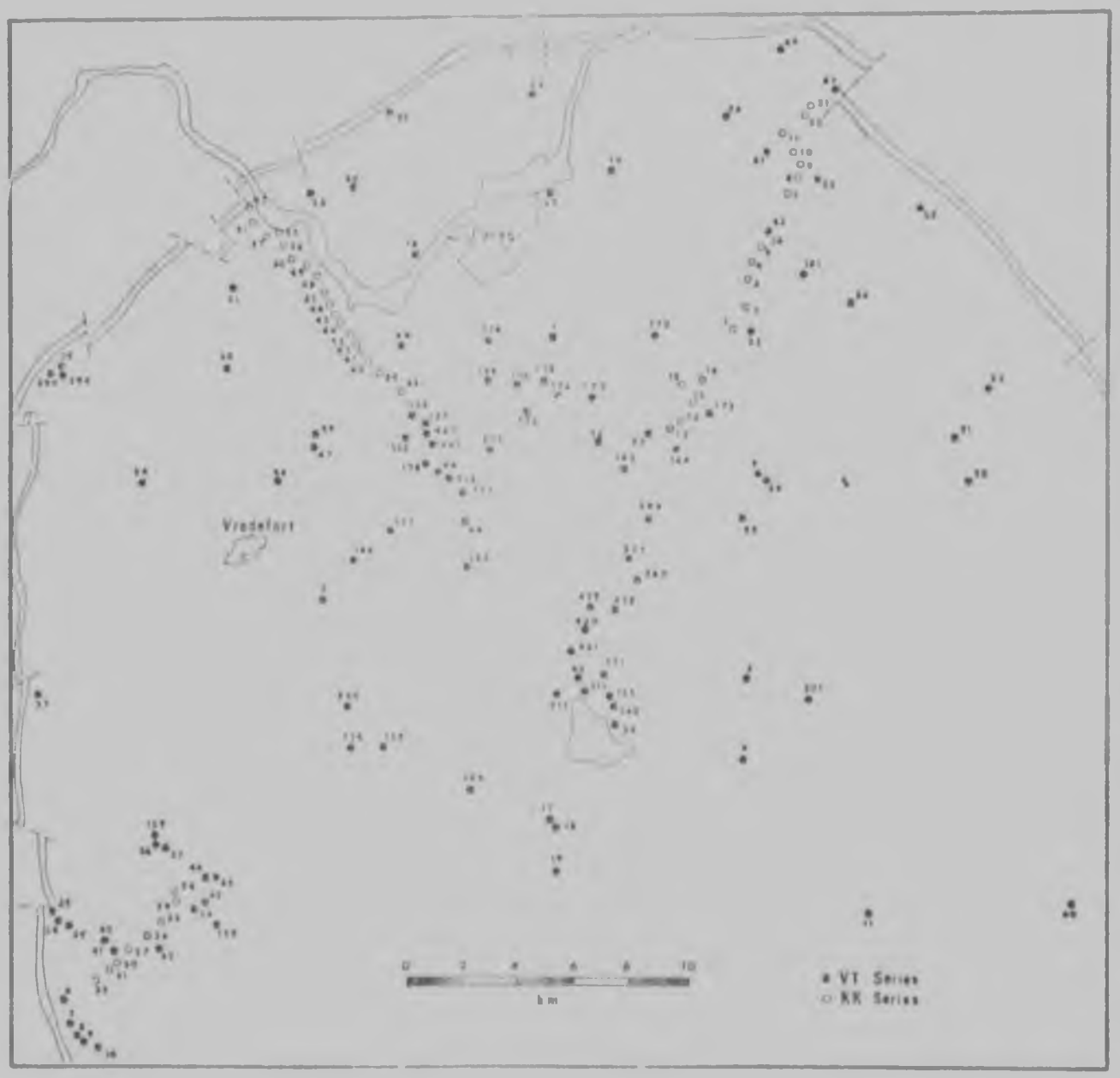


FIGURE 3.1 Sample Locations.

These samples were collected at approximately ½ km intervals along three traverses avoiding a systematic bias towards a specific petrography. Rocks of granitic composition are overwhelmingly the most common type in the Vredefort basement. Seven samples of the mafic metamorphic suite of rocks were collected. The samples which are representative of this suite are indicated in the chemical tables.

Fresh, cleaned (visibly altered portions of any rock were discarded prior to crushing) samples were crushed sufficiently so as to pass through a mesh size of about 6 mm. At this stage a representative fraction of approximately 100 gm was split off. This portion was powdered and homogenised in a Sieb chrome-stainless steel cylindrical crusher. Portions from the same rock powder were used for all the analytical techniques applied in this study.

3.2 X-ray fluorescence

All samples collected were analysed for Rb, Sr, K, Na and Ba by XRF. In addition 80 selected samples from the 3 linear radial traverses were analysed for Yt, Nb and Zr by XRF. The results are presented in Tables 4.1, 4.2, 4.3 and 4.4. These trace elements were determined by the author on a Phillips P1410 X-ray fluorescence spectrometer, following the procedures described by Cherry et al. (1970).

The XRF data were processed with the aid of an IBM 360/50 computer, using programs written with the assistance of T.S. McCarthy, D. Crampton and B. Wyatt. Further details on running conditions, data reduction and analytical precision and accuracy are given in Appendix 2. Major element analyses presented in this study were performed by the General Superintendence Co. Pty. Ltd.

3.3 Delayed neutron activation

Thorium and uranium concentrations were determined by means of the delayed neutron activation method. The analyses were carried out by the

author, using one of the pneumatic transfer tubes of the DIDO reactor at the Atomic Research Centre, Harwell, England. The counting equipment was set up by N.H. Gale of the Department of Geology, Oxford University. The method used in this study follows a similar procedure to that described by Gale (1967). Details are given in Appendix C.

3.4 Water analyses

Analyses of the water content (H_2O^+) of the 80 samples collected from the radial traverses were carried out (on apparatus set up at the Bernard Price Institute of Geophysical Research, Johannesburg). The method, involving heating and condensation, follows that of Maxwell (1968) and has been modified to suit the needs of this study. Details of the method are given in Appendix D.

3.5 Mass spectrometry

The techniques employed in the analysis of Rb and Sr in whole rock powders follow closely those reported by Allsopp et al. (1968). The chemical procedure and instrumentation used in this investigation are briefly described in Appendix A, where details of data reduction, precision and accuracy are also given.

Isotope dilution analyses of U and Pb were carried out by Welke following the procedure outlined by Welke et al. (Ms. in preparation). Descriptions of the chemical methods and mass spectrometry are not given in this work and are fully described elsewhere. Three Th analyses were carried out by Kramers at the National Bureau of Standards Laboratory in Washington in order to check the delayed neutron activation results. The methods used were similar to those used for uranium by Garner et al. (1971).

author, using one of the pneumatic transfer tubes of the DIDO reactor at the Atomic Research Centre, Harwell, England. The counting equipment was set up by N.H. Gale of the Department of Geology, Oxford University. The method used in this study follows a similar procedure to that described by Gale (1967). Details are given in Appendix C.

3.4 Water analyses

Analyses of the water content (H_2O^+) of the 80 samples collected from the radial traverses were carried out (on apparatus set up at the Bernard Price Institute of Geophysical Research, Johannesburg). The method, involving heating and condensation, follows that of Maxwell (1968) and has been modified to suit the needs of this study. Details of the method are given in Appendix D.

3.5 Mass spectrometry

The techniques employed in the analysis of Rb and Sr in whole rock powders follow closely those reported by Allsopp et al. (1968). The chemical procedure and instrumentation used in this investigation are briefly described in Appendix A, where details of data reduction, precision and accuracy are also given.

Isotope dilution analyses of U and Pb were carried out by Welke following the procedure outlined by Welke et al. (Ms. in preparation). Descriptions of the chemical methods and mass spectrometry are not given in this work and are fully described elsewhere. Three Th analyses were carried out by Kramers at the National Bureau of Standards Laboratory in Washington in order to check the delayed neutron activation results. The methods used were similar to those used for uranium by Garner et al. (1971).

4 GEOCHEMISTRY

4.1 General theory and discussion

The main emphasis of the present geochemical investigation concerns the distribution of Th, U,K, Rb, Sr and Ba within the Vredefort basement. All rock samples collected from the basement granite were analysed for these elements. The results are listed in Table 4.1 (Tables 4.1 to 4.4 are to be found at the end of this chapter pp 61 to 71).

A more detailed geochemical study, which includes the major oxides and the trace elements Yt, Nb and Zr, was carried out on the rocks along the radial traverses. The results are given in Tables 4.2, 4.3 and 4.4. Before presenting the geochemical data obtained in this study, the literature on the general geochemistry of selected trace elements is discussed. This provides a background on the behaviour of trace elements during igneous and metamorphic processes operating in high grade granulite and granite gneiss terrains. Although the literature mainly covers investigations on specific igneous rock suites, the information most relevant to this study comes from work on high grade metamorphic rocks occurring in deeply eroded Archaean basement terrains.

(a) Potassium and Rubidium

The behaviour of the alkali metal pair K-Rb is reviewed by Erlank (1968), who includes a summary of all reliable data available up to 1967. Rubidium and potassium provide a good example of geochemical coherence because of the similarity in ionic radii and chemical behaviour. This similarity is demonstrated by the fact that Rb is always incorporated in K-minerals, and forms no mineral of its own. It follows that the most important Rb accepting minerals are the micas and K-feldspars. The Rb content of these minerals increase with increasing differentiation of the host rock, and is at a maximum in late stage pegmatites and K-minerals.

The Rb^+ ion is larger than the K^+ ion, and is preferentially accepted in the 12 coordinated potassium site in the micas. Consequently K/Rb ratios are always lower in mica than K-feldspars. Mainly because of the larger ionic size Rb is enriched relative to K in low temperature K-minerals and in fractional crystallisation Rb will be preferentially concentrated in the felsic fractions, and the K/Rb ratios will decrease in a sequence from mafic to felsic rocks.

The relationship between K/Rb ratios and metamorphic grade in metamorphic rocks are at present not as well documented as the corresponding trends in igneous rock suites. The average K/Rb ratios from granulite facies rocks varies considerably and generally values are significantly higher than the accepted crustal average of 230 (Taylor et al. 1956). Sighinolfi (1971) reports an average value of 636 for high pressure granulite rocks from the Brazilian shield. This value is in good agreement with the data obtained from other granulite terrains by Lambert and Heier (1968) and Heier and Thompson (1971). The granulites of the Lewisian gneisses of the Scottish mainland have K/Rb ratios in excess of a 1000 (Holland and Lambert, 1969).

(b) Uranium and Thorium

Geochemical coherence between uranium and thorium, as predicted by the similarity in ionic properties, has been reported by Heier and Rogers, 1963; Heier and Adams, 1965 and Rogers and Adams, 1969.

Like K and Rb, Th and U also increase in concentration during normal magmatic differentiation. However, unlike K and Rb, the precise location of the radioactive elements in rock forming minerals is more varied. The classical method for studying the mode of occurrence of the alpha-emitting elements in rock-forming minerals is by autoradiography which involves the use of thin films or plates of alpha-sensitive emulsion. The principle conclusions derived from autoradiographic studies of igneous rocks are summarized by Rogers and Adams (1969), as follows:

(i) Most granites have a major portion of their alpha activity concentrated in small grains of accessory minerals, such as zircon, allanite, huttonite and monazite, the thorium and uranium occupying one or more of the cation sites in the lattice as a major constituent. In many granites, however, there is also appreciable concentration on grain borders or disseminated through the minerals. In minerals such as K-feldspar it is uncertain whether the U and Th occur in lattice sites, interstitial positions, sub-microscopic defects or perhaps in the form of individual small grains of Th and U minerals.

(ii) Gabbros and other basic igneous rocks have their alpha activity distributed fairly evenly among the various major constituents. From these facts Rogers and Adams (1969) conclude that most minerals containing appreciable amounts of thorium and uranium form quite late in the igneous crystallization sequence.

Thorium and uranium concentrations vary considerably in any particular rock type and rather than listing average values, Rogers and Adams (1969) indicate the general range of Th and U concentrations for major rock types: In granites the radioactive elements show extreme variation from one type of plutonic acid rock to another. Rogers and Adams (1969) give a general range of between 10 and 20 ppm for thorium and 1 to 4 ppm for uranium in granitic rocks.

The average Th and U concentrations of the continental crust may be estimated from concentration data given for the major rock types, provided that the proportions of the various rock types which make up the crust are known. Rogers and Adams (1969) estimated that less than 50% of the exposed earth's crust is granite and that most of the remaining continental rock types contain less thorium and uranium than granite. The average Th content of the crust is thus estimated at 6 to 10 ppm, whereas U is estimated at about 2 ppm (Rogers and Adams, 1969).

(i) Most granites have a major portion of their alpha activity concentrated in small grains of accessory minerals, such as zircon, allanite, huttonite and monazite, the thorium and uranium occupying one or more of the cation sites in the lattice as a major constituent. In many granites, however, there is also appreciable concentration on grain borders or disseminated through the minerals. In minerals such as K-feldspar it is uncertain whether the U and Th occur in lattice sites, interstitial positions, sub-microscopic defects or perhaps in the form of individual small grains of Th and U minerals.

(ii) Gabbros and other basic igneous rocks have their alpha activity distributed fairly evenly among the various major constituents. From these facts Rogers and Adams (1969) conclude that most minerals containing appreciable amounts of thorium and uranium form quite late in the igneous crystallization sequence.

Thorium and uranium concentrations vary considerably in any particular rock type and rather than listing average values, Rogers and Adams (1969) indicate the general range of Th and U concentrations for major rock types. In granites the radioactive elements show extreme variation from one type of plutonic acid rock to another. Rogers and Adams (1969) give a general range of between 10 and 20 ppm for thorium and 1 to 4 ppm for uranium in granitic rocks.

The average Th and U concentrations of the continental crust may be estimated from concentration data given for the major rock types, provided that the proportions of the various rock types which make up the crust are known. Rogers and Adams (1969) estimated that less than 5% of the exposed earth's crust is granite and that most of the remaining continental rock types contain less thorium and uranium than granite. The average Th content of the crust is thus estimated at 6 to 10 ppm, whereas U is estimated at about 2 ppm (Rogers and Adams, 1969).

A more realistic study by Lambert (1971) is based on a detailed investigation of the radioelement concentrations in high pressure granulite facies rocks from the South West Australian shield. Radioelement concentrations in the granulites are statistically compared to abundances in more "normal" surface granites. The crustal abundance of U and Th calculated on the basis of this model are significantly lower than previous estimates (U = 1.1 ppm and Th = 4.5 ppm).

Analogous to the K/Rb system, small variations in the Th/U ratio would reflect a general coherency in the geochemistry of Th and U. The average Th/U ratios for a variety of different igneous rock types were reviewed by Rogers and Adams (1969). All the reported Th/U ratios fell within a range of 2.2 to 6.3. The varied rock types covered include ocean floor basalts and granites. An average of 3 to 4 is generally accepted.

Lambert and Heier (1967) found that the Th/U ratio tended to be greater than 4 in low grade metamorphic rocks, whilst it is generally less than 4 in pyroxene granulite facies rocks. Furthermore, it has been noted that uranium and thorium concentrations in pyroxene granulite rocks are significantly depleted relative to amphibolite facies rocks of comparable major element chemistry (Heier and Thoresen, 1970; Lambert and Heier, 1967, 1968; Sighinolfi, 1971; Lambert, 1971). These authors suggest that the variations of the radioelements with metamorphic grade are consistent with partial melting during deep crustal metamorphism; specifically water, thorium and uranium are believed to move preferentially into granitic magmas which migrate to higher crustal levels.

Heier and Adams (1965) also found that there was a possible decrease of the average Th/U ratio with increasing metamorphism. This effect, however, was obscured by the fact that in gneissic rocks of different metamorphic grade Th/U ratios varied within wide limits and that the ratios were often higher than the commonly accepted ratios of 3 to 4. The

variations in ratios were largely attributed to fluctuations in U concentrations, as high ratios appear to relate to much lower than "normal" U content rather than to high Th content.

A characteristic feature of uranium is its ability to be oxidized to the highly soluble uranyl ion (UO_2^{++}). The solubility of the oxidized uranyl complex ion renders U more mobile in metamorphic processes. Heier and Adams (1965) attribute the observed variations in Th/U ratios to urarium oxidation and its subsequent removal in metamorphic processes. Erlank (1971) came to a similar conclusion, and suggested that Th/U ratios may be used in evaluating oxidation conditions (eg. open versus closed systems).

Inferred radioelement distribution profiles with depth, based on the average abundances in the surface shield rocks of South West Australia and the Musgrave Range granulites, have been calculated by Lambert (1971), (Figure 5.1). On the basis that "normal" Th/U ratios (eg. values around 3 to 4) are found in both the surface shield rocks and the granulites (which presumably are representative of the lower crust), Lambert (1971) contends that "normal" Th/U ratios extend over most of a 30 km profile through the continental crust. Lambert concluded that the oxidation and depletion of uranium at low metamorphic grades, and the subsequent concentration of this element (relative to Th) in near surface rocks, has not occurred to any great extent.

(c) Potassium, Thorium and Uranium

The close geochemical relationship existing between K, Th and U was first established by Heier and Rogers (1963). The near constancy of the K/Th and K/U ratios was claimed in the older reviews by Wedepohl et al. (1964) and Shaw (1968). With respect to K and U, Gast (1968) noted: "it is indeed remarkable that two such chemically dissimilar elements show so little variation in their relative abundance in rocks". Figure 4.0

variations in ratios were largely attributed to fluctuations in U concentrations, as high ratios appear to relate to much lower than "normal" U content rather than to high Th content.

A characteristic feature of uranium is its ability to be oxidized to the highly soluble uranyl ion (UO_2^{++}). The solubility of the oxidized uranyl complex ion renders U more mobile in metamorphic processes. Heier and Adams (1965) attribute the observed variations in Th/U ratios to uranium oxidation and its subsequent removal in metamorphic processes. Erlank (1971) came to a similar conclusion, and suggested that Th/U ratios may be used in evaluating oxidation conditions (e.g. open versus closed systems).

Inferred radioelement distribution profiles with depth, based on the average abundances in the surface shield rocks of South West Australia and the Musgrave Range granulites, have been calculated by Lambert (1971), (Figure 5.1). On the basis that "normal" Th/U ratios (e.g. values about 3 to 4) are found in both the surface shield rocks and the granulites (which presumably are representative of the lower crust), Lambert (1971) contends that "normal" Th/U ratios extend over most of a 40 km profile through the continental crust. Lambert concluded that the oxidation and depletion of uranium at low metamorphic grades, and the subsequent concentration of this element (relative to Th) in near surface rocks, has not occurred to any great extent.

(c) Potassium, Thorium and Uranium

The close geochemical relationship existing between K, Th and U was first established by Heier and Rogers (1963). The near constancy of the K/Th and K/U ratios was claimed in the older reviews by Wedepohl et al. (1964) and Shaw (1968). With respect to K and U, Gast (1968) noted: "It is indeed remarkable that two such chemically dissimilar elements show so little variation in their relative abundance in rocks". Figure 4.0

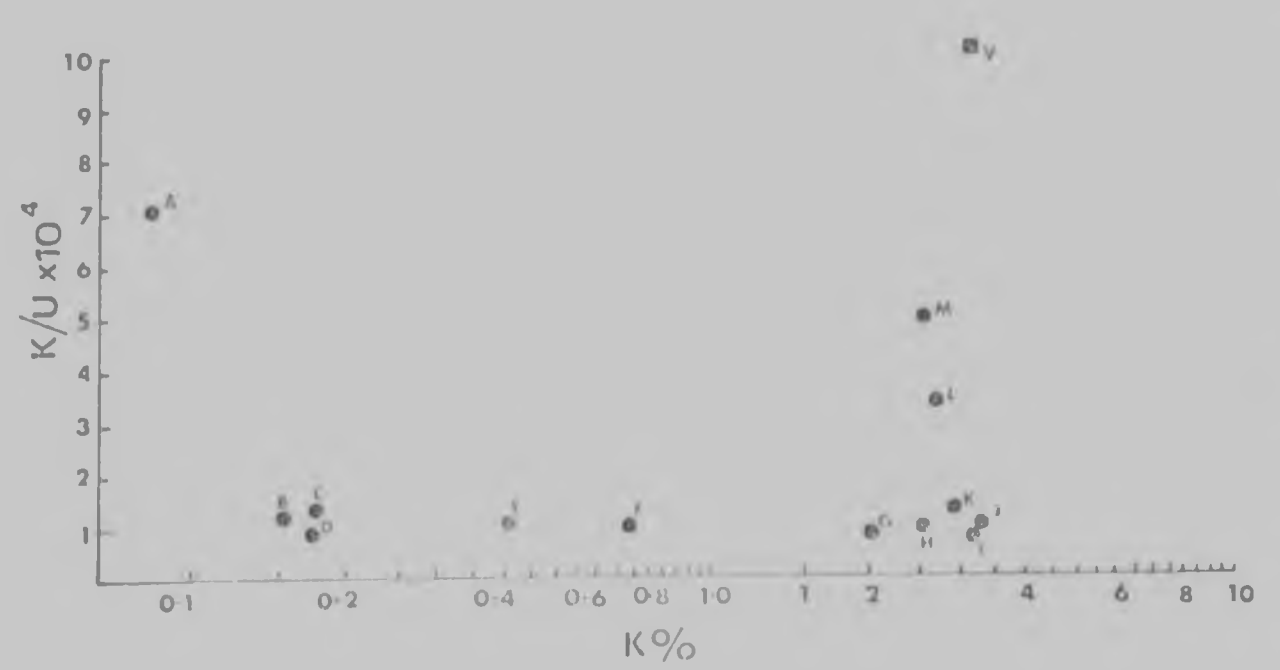
variations in ratios were largely attributed to fluctuation in U concentrations, as high ratios appear to relate to much lower than "normal" U content rather than to high Th content.

A characteristic feature of uranium is its ability to be oxidized to the highly soluble uranyl ion (UO_2^{++}). The solubility of the oxidized uranyl complex ion renders U more mobile in metamorphic processes. Heier and Adams (1965) attribute the observed variations in Th/U ratios to uranium oxidation and its subsequent removal in metamorphic processes. Erlank (1971) came to a similar conclusion, and suggested that Th/U ratios may be used in evaluating oxidation conditions (eg. open versus closed systems).

Inferred radioelement distribution profiles with depth, based on the average abundances in the surface shield rocks of South West Australia and the Musgrave Range granulites, have been calculated by Lambert (1971), (Figure 5.1). On the basis that "normal" Th/U ratios (eg. values around 3 to 4) are found in both the surface shield rocks and the granulites (which presumably are representative of the lower crust), Lambert (1971) contends that "normal" Th/U ratios extend over most of a 30 km profile through the continental crust. Lambert concluded that the oxidation and depletion of uranium at low metamorphic grades, and the subsequent concentration of this element (relative to Th) in near surface rocks, has not occurred to any great extent.

(c) Potassium, Thorium and Uranium

The close geochemical relationship existing between K, Th and U was first established by Heier and Rogers (1963). The near constancy of the K/Th and K/U ratios was claimed in the older reviews by Wedepohl et al. (1964) and Shaw (1968). With respect to K and U, Gast (1968) noted: "it is indeed remarkable that two such chemically dissimilar elements show so little variation in their relative abundance in rocks". Figure 4.0



A Chondrite

B Average for Alkali Basalt
(Basalt, Pacific Coast [illegible])

C Average Abyssal Tholeiite

D Average crust

E Composite Snake River Basalt

F Average for Hawaii Lava

G Average Crust

H Average Canadian Shield

I Rhyolite Composite

J Granite Composite I

K Amphibolite Gneiss (North Norway)

L Banded Granulites (North Norway)

M Musgrave Range Granulites

V Average for the Vredefort Basement (this study)

A,E,I, and J Gast,1968

B Erlank,1971

C Tatsumoto et. al.,1965

D Hurley,1968

F Heier et. al.,1964

G Taylor,1969

H Shaw,1968,1969

K and L Heier and Thoresen,1970

M Lambert and Heier 1967

V This Study

FIGURE 4.0 K/U ratios as a function of K content for some common rocks (modified after Gast, 1968)

shows the variation of K/U ratios as a function of K in a number of rock types given by Gast (1968). The mean K/U and K/Th ratios for the Canadian shield are 1.05×10^4 and 0.25×10^4 respectively (Shaw, 1968). Wasserburg et al. (1964) suggested that a K/U ratio of 1×10^4 is characteristic of terrestrial material.

In the high grade metamorphic rocks of the South West Australian Shield, Lambert and Heier (1967) noted that whereas the K/U and K/Th ratios in the mafic rocks of the pyroxene granulite subfacies are consistent with other areas (K/U = 1.0×10^4 and K/Th = 0.25×10^4), the values in the felsic rocks of the pyroxene subfacies are significantly higher (K/U = 6.67×10^4 and K/Th = 1.7×10^4). This indicates that U and Th are depleted relative to K in these latter rocks.

(d) Barium and Strontium

A close geochemical relationship exists between barium and strontium. Although much of the relevant literature is devoted to Ba geochemistry, similar considerations apply to Sr. Both elements occur in the 2+ cation form, and have similar ionic radii. The concentrations of Ba and Sr in continental crustal rocks are significantly higher than the abundances in the mantle derived volcanics of the ocean floor, (Gast, 1968), indicating that these elements are concentrated in the continental crust.

In igneous rocks Ba and Sr occur as trace elements distributed mainly amongst the feldspars and rarely do not form minerals of their own. For Ba the most important substitution is for potassium due to nearly identical ion size (Fischer and Puchalt, 1972; Hall, 1967) and consequently the K feldspars are the most important Ba carriers. In acid rocks free of K-feldspar, biotite is often the main Ba carrier (Fischer and Puchalt, 1972). In basic to intermediate rocks Ba substitutes mainly for Ca in plagioclase. This substitution occurs less readily than the substitution for K in alkali feldspars and micas.

Although Ba and Sr are highly enriched in the continental crust, their behaviour shows association with refractory phases during normal magmatic differentiation. In basic rocks, however, such as a basaltic magma (Fischer and Puchalt, 1972), Ba is initially enriched in the liquid phase. With progressing crystallisation Ba is incorporated in K-feldspars and micas. These minerals extract Ba from the melt as crystallization proceeds. The last stages of a differentiation series are consequently impoverished in Ba.

McCarthy (1976) considered the distribution of Ba, Sr and Rb between partial melts and residues during the progressive melting of a gneiss in some theoretical models based on partition coefficient equations. The models demonstrate that for a gneiss consisting of only potash feldspar, sodic plagioclase and quartz, when 50% of the rock is melted, Rb is strongly fractionated into the melt, while Ba and Sr are largely retained in the residue. If 5% biotite (which does not melt) is present, the effect is to remove the content of both Rb and Ba in the partial melt, because of the large partition coefficients of both Ba and Rb in biotite. The addition of biotite has little effect on the Sr content of the melt. When these models are applied to a suite of low-pressure granulite facies rocks in Namaqualand, South Africa, which are thought to have been derived by extensive melting of underlying gneisses, McCarthy (1976) demonstrates that the interelement relationship in this district reflect solid-melt equilibria, Ba and Sr being retained in the residue.

Hall (1967) notes that in the Roses granite complex which is interpreted as being formed by a process involving the formation of granitic magma by progressive partial fusion, Ba is most abundant in the mafic members and falls below the limit of detection in the most felsic rocks.

In the high grade metamorphic terrain of the Brazilian shield Sighinolfi (1971) observes that the deeper crust is significantly enriched in Ba and Sr by comparison with intermediate rocks of the upper

crust. These observation[illegible] in agreement with results obtained from Norwegian granulites (Hei[illegible] Heier and Thoresen (1970) [illegible] Sr concentrations in the [illegible] of the granitophile elements, [illegible] granulite which is significantly enriched in Ba and [illegible] metamorphic rocks of the upper crust.

(b) Yttrium

In a review [illegible] geochemistry [illegible] in calciferous [illegible] and metamorphic [illegible] investigation the development of Y geochemistry [illegible] member of the rare earth [illegible] authors to have investigated Y [illegible] (1953, 1956).

Yttrium exists only in the [illegible] and has an ionic radius between that of [illegible] and [illegible] latter. Y enters nearly all Ca-silicates [illegible] rarely is found as a trace element in non Ca-[illegible] (mainly silicates, [illegible] sphene are the most important Y [illegible] and have low Ca/Y ratios, whereas [illegible] and have high Ca/Y ratios (Hermann, 1970).

The distribution of Y in [illegible] Hermann (1970). A comparison of the distribution [illegible] origin shows that [illegible] systematic variation. Hermann (1970) [illegible] there are notable changes in the concentration of Y and Ln - and the relative distribution of Y (lanthanides [illegible] the sequence from granites to

hydrothermal veins, formed during the emplacement of granitic massifs.

Lambert and Holland (1974) contend that Y behaves systematically in igneous, metamorphic and sedimentary rock series, due to its incorporation in a predictable and uniform manner in Ca-minerals. In all igneous series Ca/Y falls as Ca falls. In metamorphic processes Y is inert, and Lambert and Holland suggest that the Ca and Y contents in metamorphic rocks (including granite gneisses) are related to the original igneous or sedimentary complexes from which they were derived.

(f) Niobium

An extensive report on the geochemistry of niobium and tantalum, which show a strong geochemical coherence, is given by Parker and Fleischer (1968). This report summarizes what is known of the geochemical characteristics of these elements and their occurrence in various types of minerals and rocks. The following information is taken from the above report:

Niobium and tantalum commonly substitute for one another in minerals because they both have similar ionic radii, and occur mainly in the quinquivalent state. Both elements are lithophile and are enriched in the silicate crust of the earth. The average abundance of niobium in the crust is about 20 ppm but abundances in different rock types are highly variable. Twenty-eight granitic plutons from throughout the world have an average Nb content of 16 ppm, ranging from 0.9 to 30 ppm. However, crustal abundances as well as abundances in various rock types are subject to considerable uncertainty because of limitations imposed by the availability of analytical data.

Most occurrences of niobium and tantalum are as oxides of these elements. Niobium and tantalum, however, occur in minor amounts in many oxide, tungstate, phosphate and silicate minerals of other elements. In these minerals, niobium and tantalum are closely associated with titanium, tungsten, tin, zirconium and hafnium for which they commonly substitute

isomorphously, by virtue of the similarity of their ionic radii and other physical properties. Uranium and thorium commonly occur in the same minerals as niobium and tantalum.

Isomorphous substitution of niobium for titanium is common, and the geochemical behaviour of niobium in granitic rocks depends to a certain extent on the paragenesis of the titanium minerals in which niobium occurs. Monazite-bearing granites containing ilmenite and rutile commonly contain niobium in accessory biotite, whereas allanite-bearing granites containing sphene and magnetite commonly have niobium concentrated in sphene with only subordinate amounts in the biotite. This suggests that the calcium content of the whole rock may be an important factor in determining the distribution of niobium in the rock-forming minerals. In some granites hornblende has also been shown to contain a large percentage of the total niobium content of the rock.

In felsic rocks, niobium generally accumulates in the later differentiates during the crystallisation of a magma. High concentrations of niobium occur in granitic pegmatites in the lattices of mica, garnet, tourmaline, ilmenite and zircon.

(g) Zirconium

Zirconium occurs only in the Zr^{4+} form in the mineral zircon. Zirconium does not substitute into any of the major phases of felsic plutonic rocks, that is quartz, feldspars or micas and its distribution cannot be interpreted in terms of their abundances.

On petrographic evicence, Hall (1967) notes that zircon is one of the earliest minerals to crystallise from a granite magma and it resists fusion during the experimental melting of granites (Kranck and Oja, 1960). Zirconium would not therefore be a constituent of the minimum melting temperature mixture. This is demonstrated by the fact that zirconium falls to zero in the most felsic rocks of the Roses granite (Hall, 1967).

Investigations on three granitic plutons in the Southern Black Forest by Hahn-Weinheimer and Johanning (1968) show a close linear relationship between Zr and Ti. Each pluton shows its own characteristic linear relationship and plots in a specific Ti-Zr field. In these granites the Ti occurs mainly in biotite and it is suggested that biotite and zircon belong to the early crystallizing minerals in the three granite plutons.

4.2 Data presentation

The variation of major and trace element chemistry across the Vredefort granite is shown for the three radial traverses in Fig. 4.1 to 4.3 (radial distance from the margin versus concentration). These profiles permit a preliminary appraisal of the results.

Ratios of elements such as K/Rb and Ba/Rb which are particularly sensitive as geochemical indicators have been contoured as shown in Fig. 4.4 and 4.5. This method of data presentation illustrates the broad trace element geochemical features of the basement granite.

For the major part of the discussion, it has been found desirable to compile an average section through the Vredefort crust, presenting the data as a single vector file with depth in the crust for each element. An averaging process has proved beneficial in an understanding of the variation of the radioelement chemistry with depth.

It is only once the radioelement abundances across the Vredefort basement are averaged out, that it becomes possible to fit mathematical models to the depth distribution profiles. This is perhaps not surprising as one would expect that rock sequences should conform only at the broadest possible scale to convenient mathematical representations. Because of their significance with regard to terrestrial heat flow, the radioelement data are discussed in detail in the following chapter.

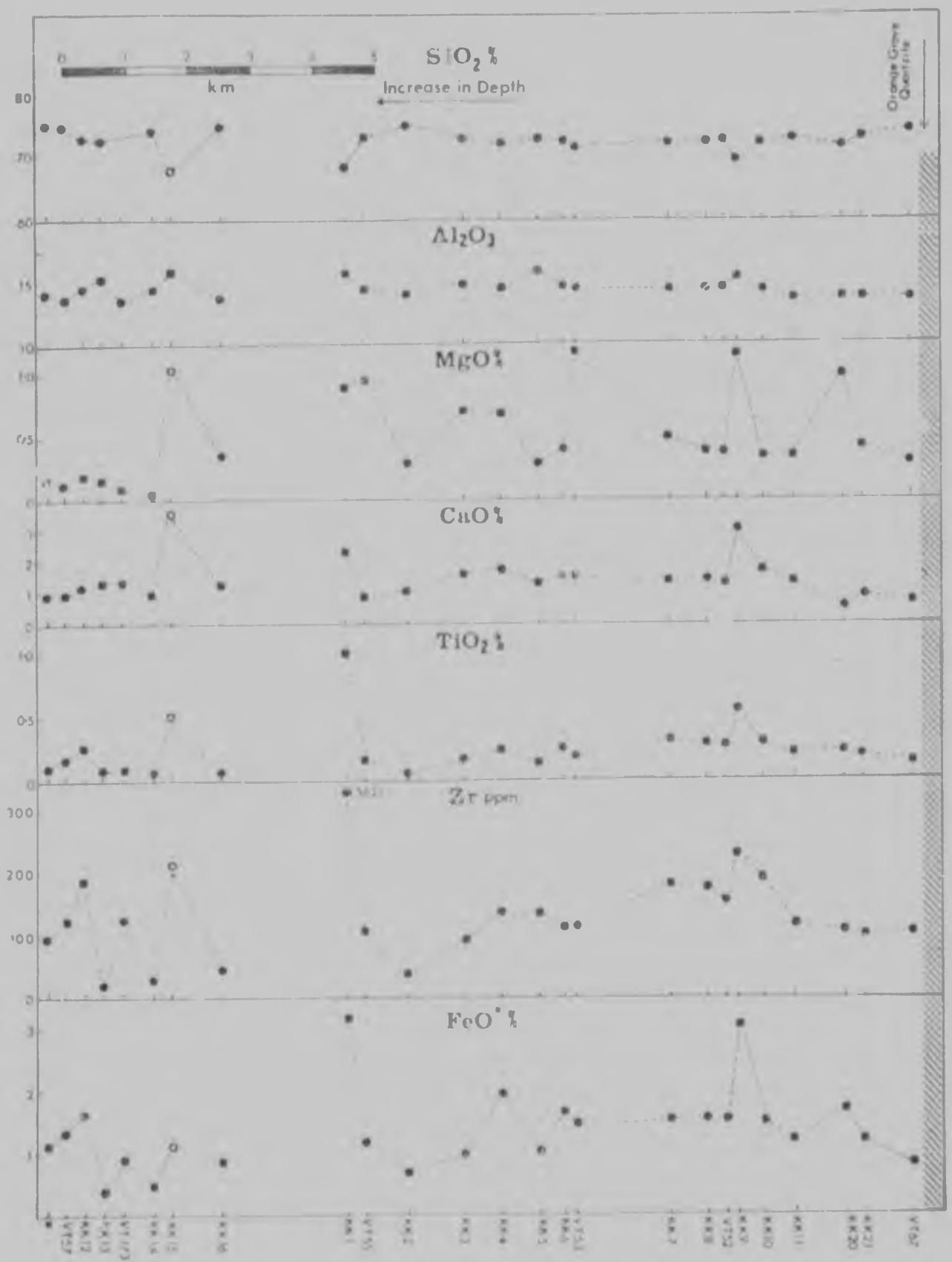


FIGURE 4.1 Northeast radial profile

Open circles: mafic granulites

* Composite sample including VT142, 144, 393, 380, 428, 431, 211

● Total iron expressed as FeO

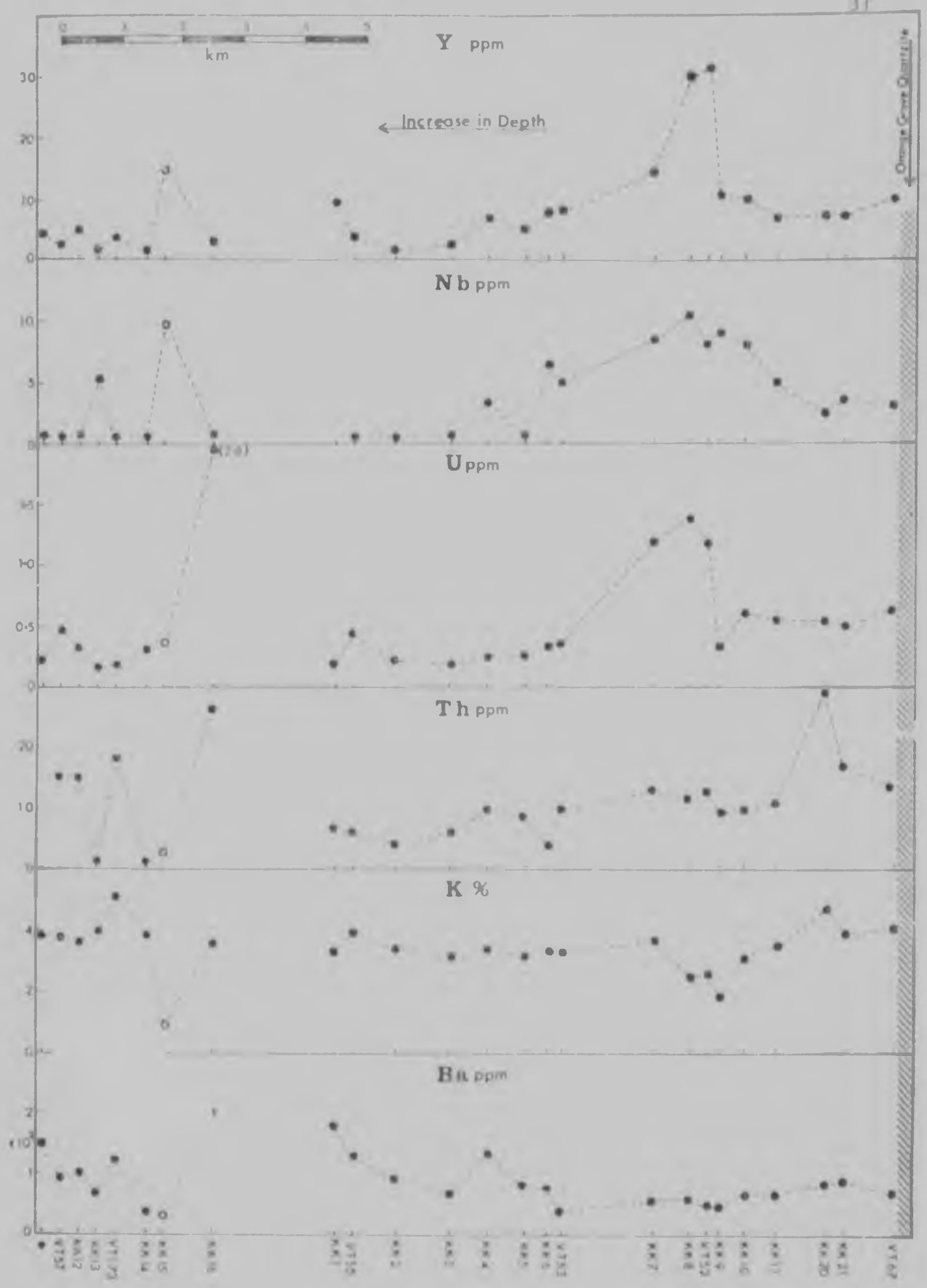


FIGURE 4.1 (Cont'd.

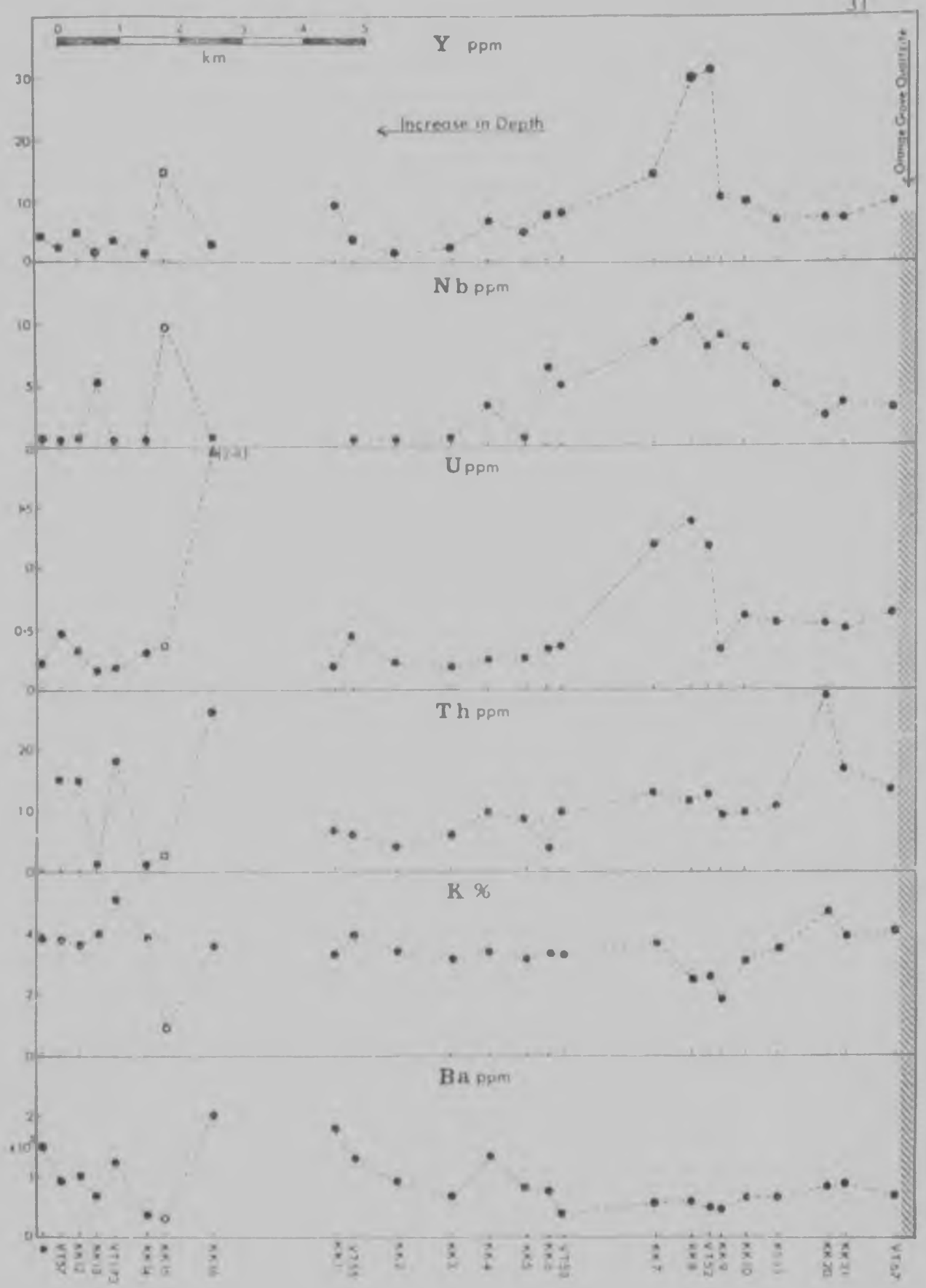


FIGURE 4.1 Contd.

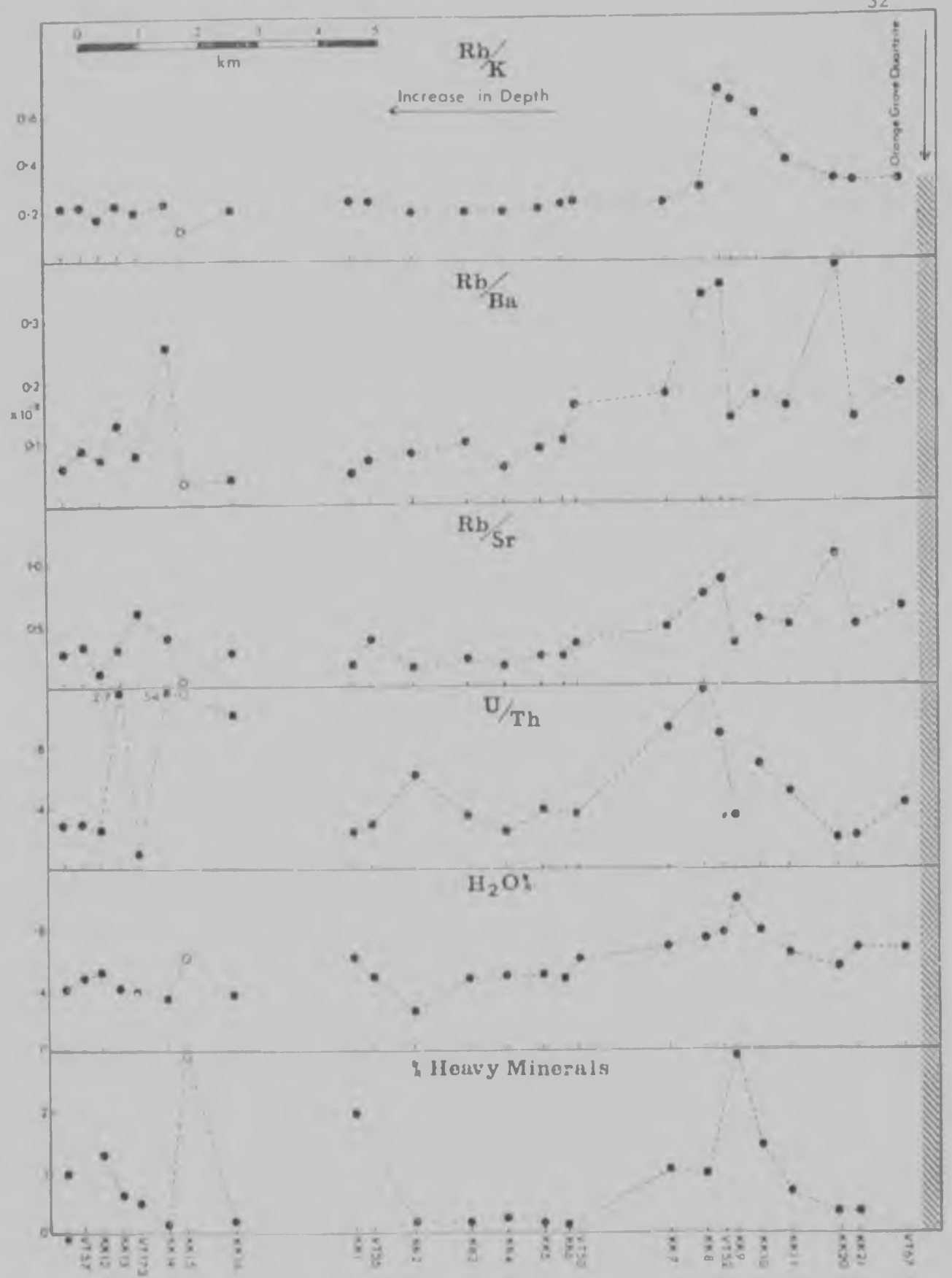


FIGURE 4.1 (contd.

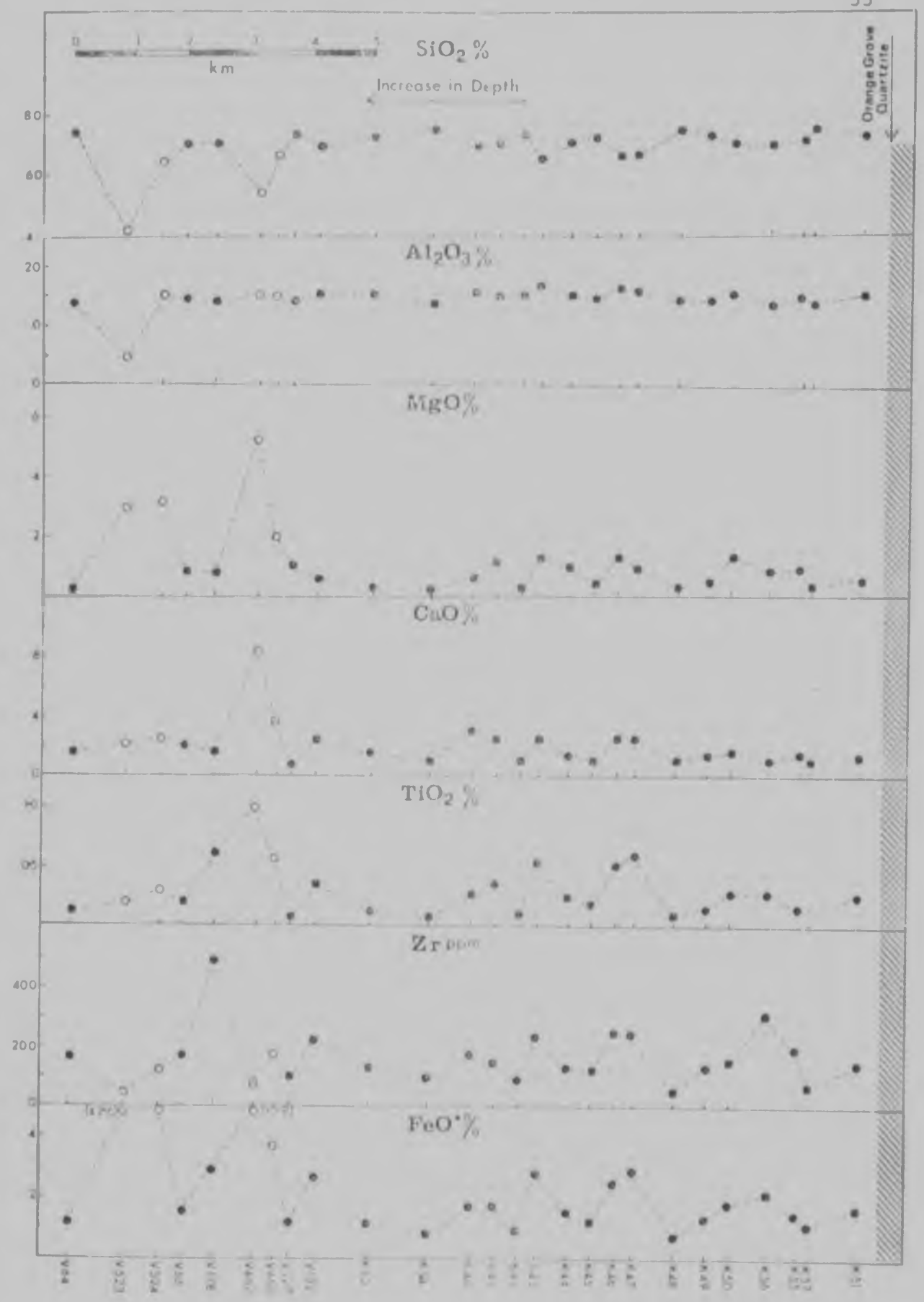


FIGURE 4.2 Northwest radial profile

Open circles: mafic granulites

* Total iron expressed as FeO

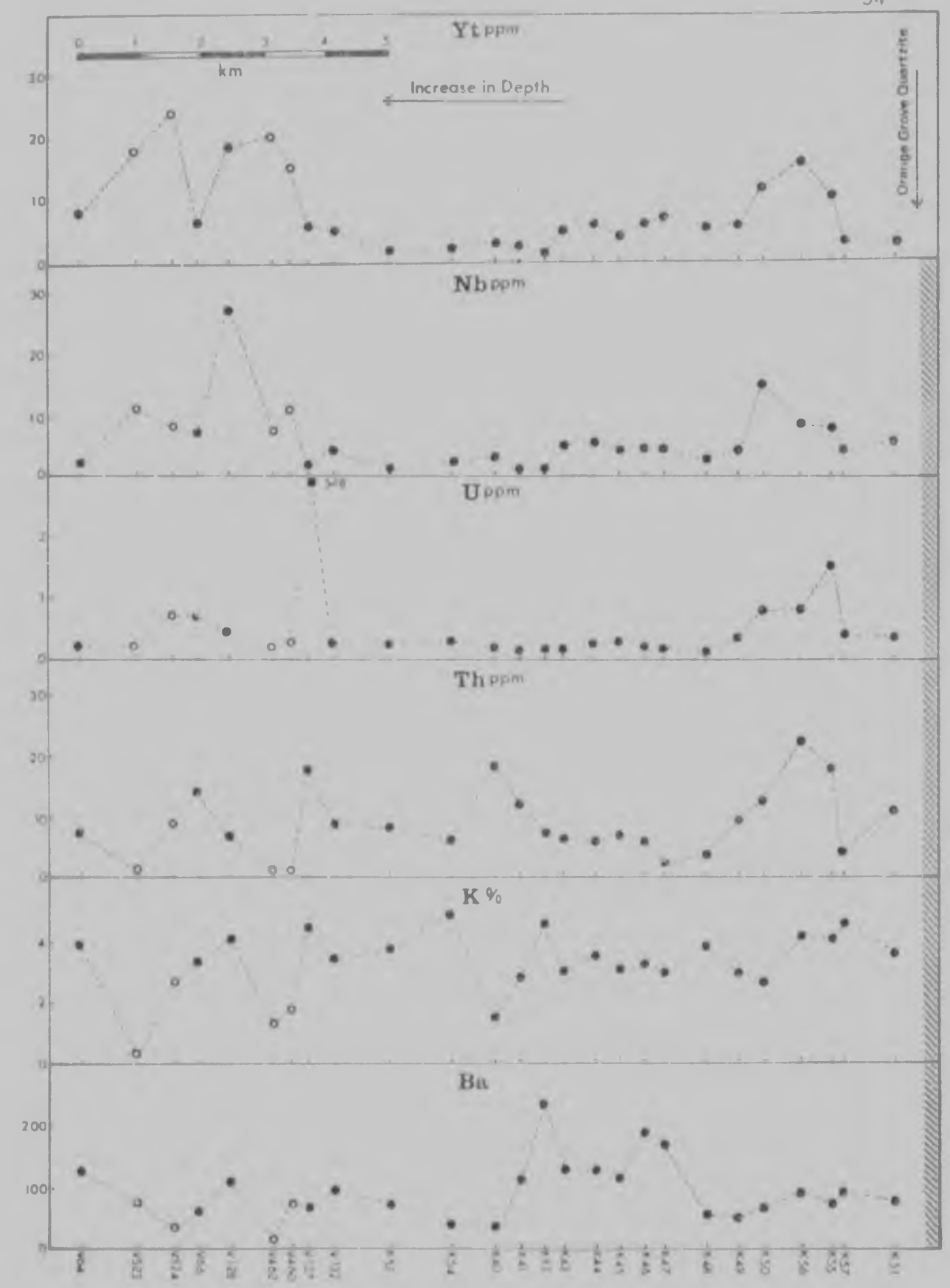


FIGURE 4.2 Contd.

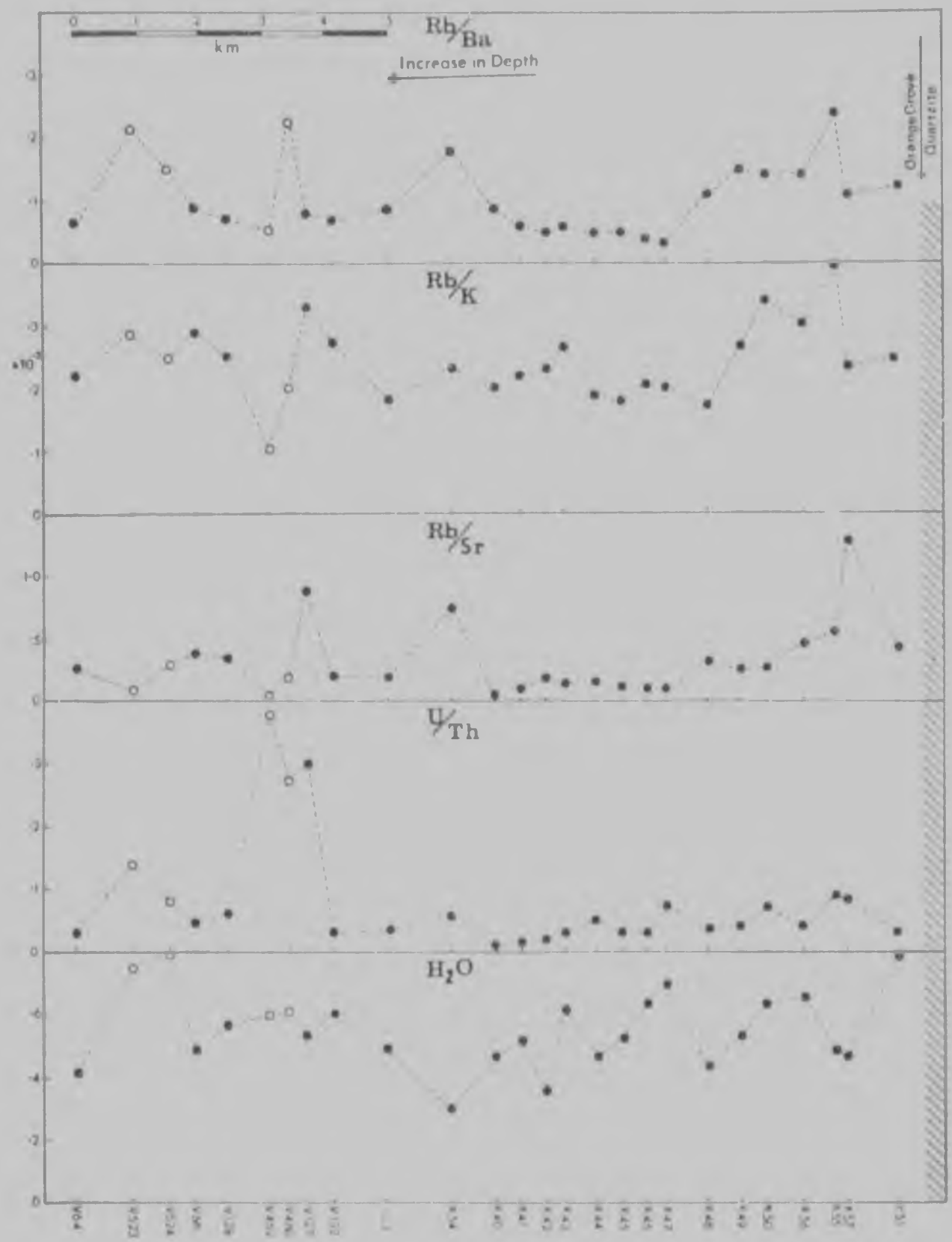


FIGURE 4.2 Contd.

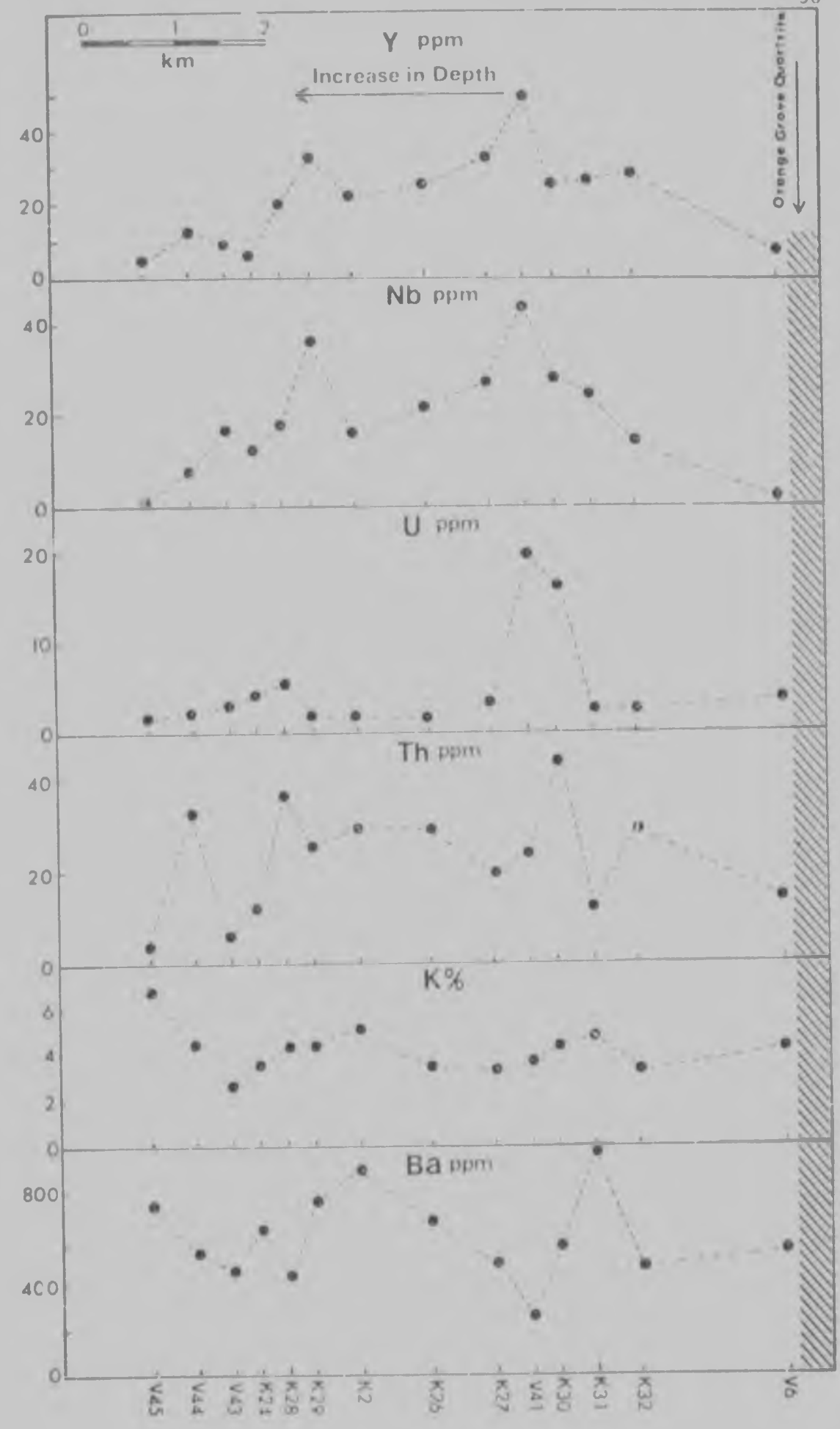


FIGURE 4.3 Southwest radial profile

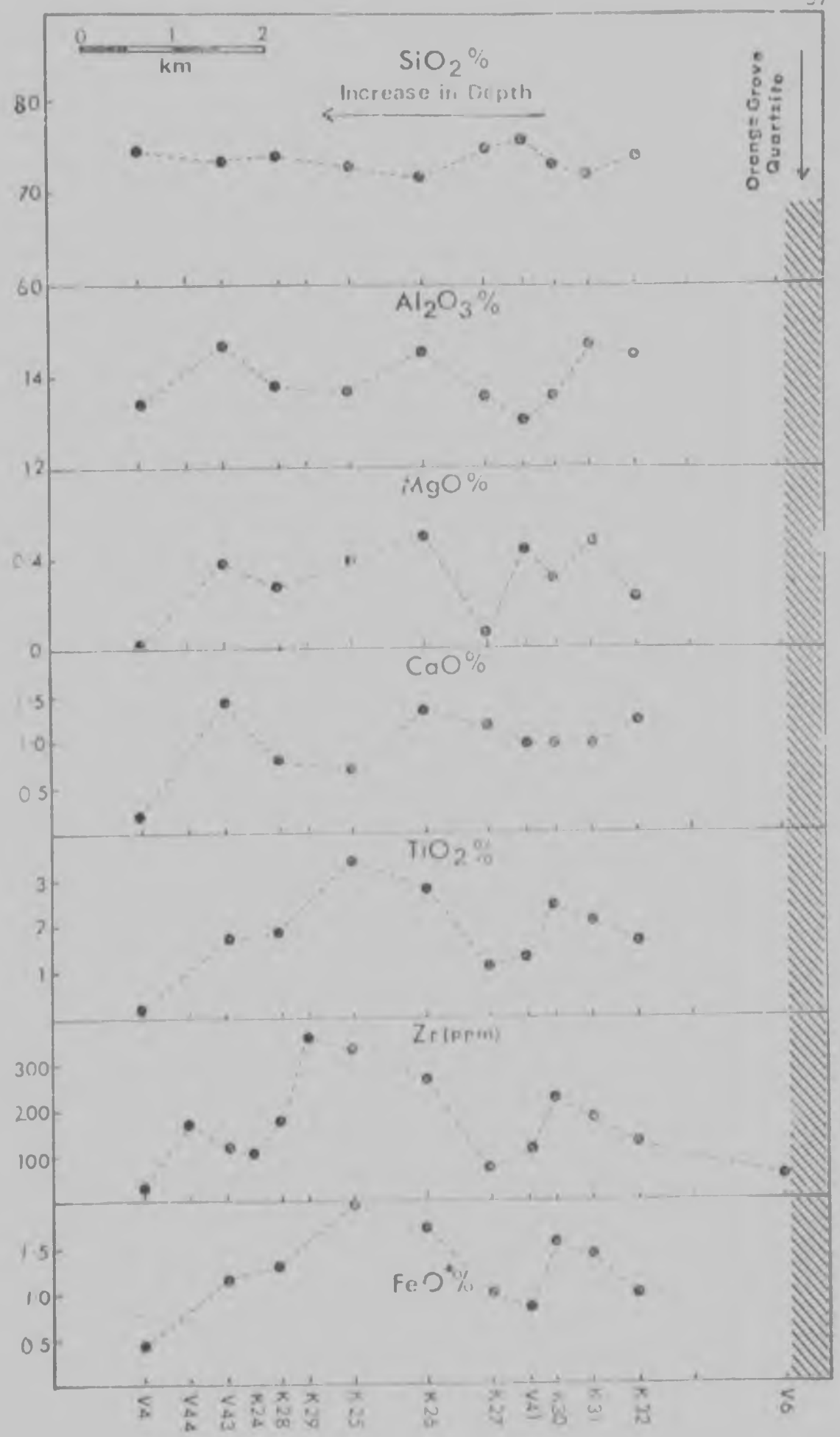


FIGURE 4.3 Contd.

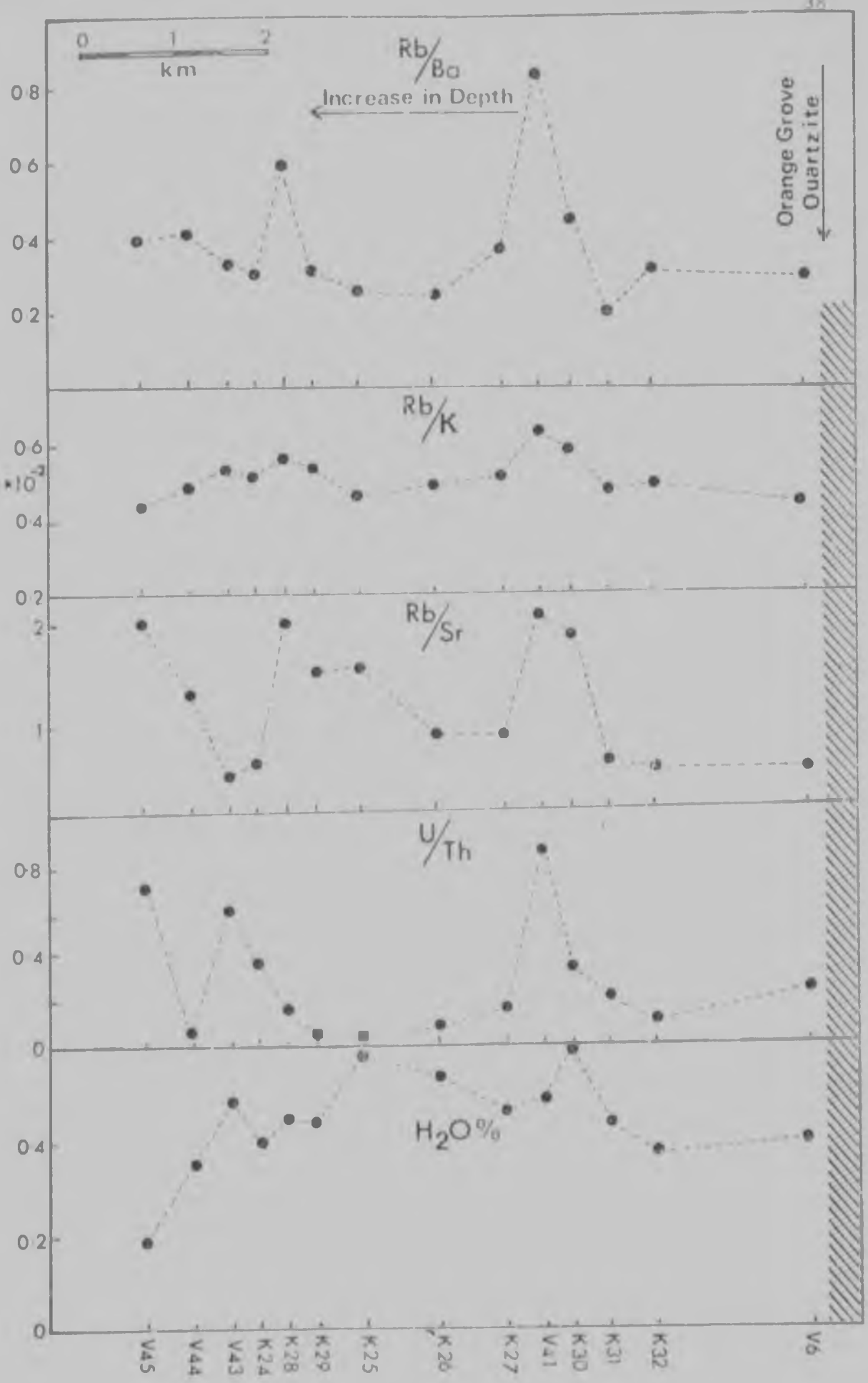


FIGURE 4.3 Contd.

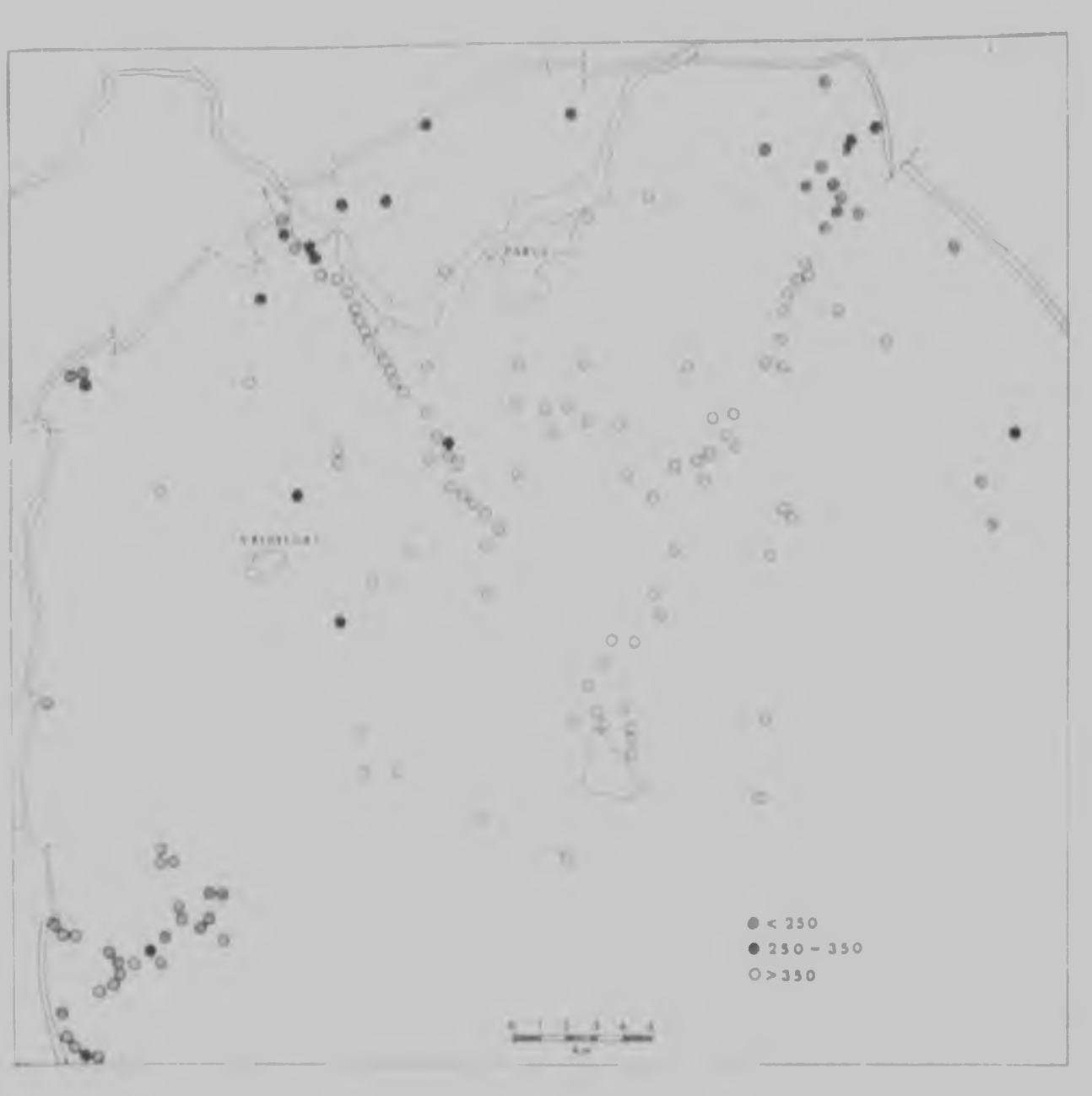


FIGURE 4.4 Variations of K/Rb ratios

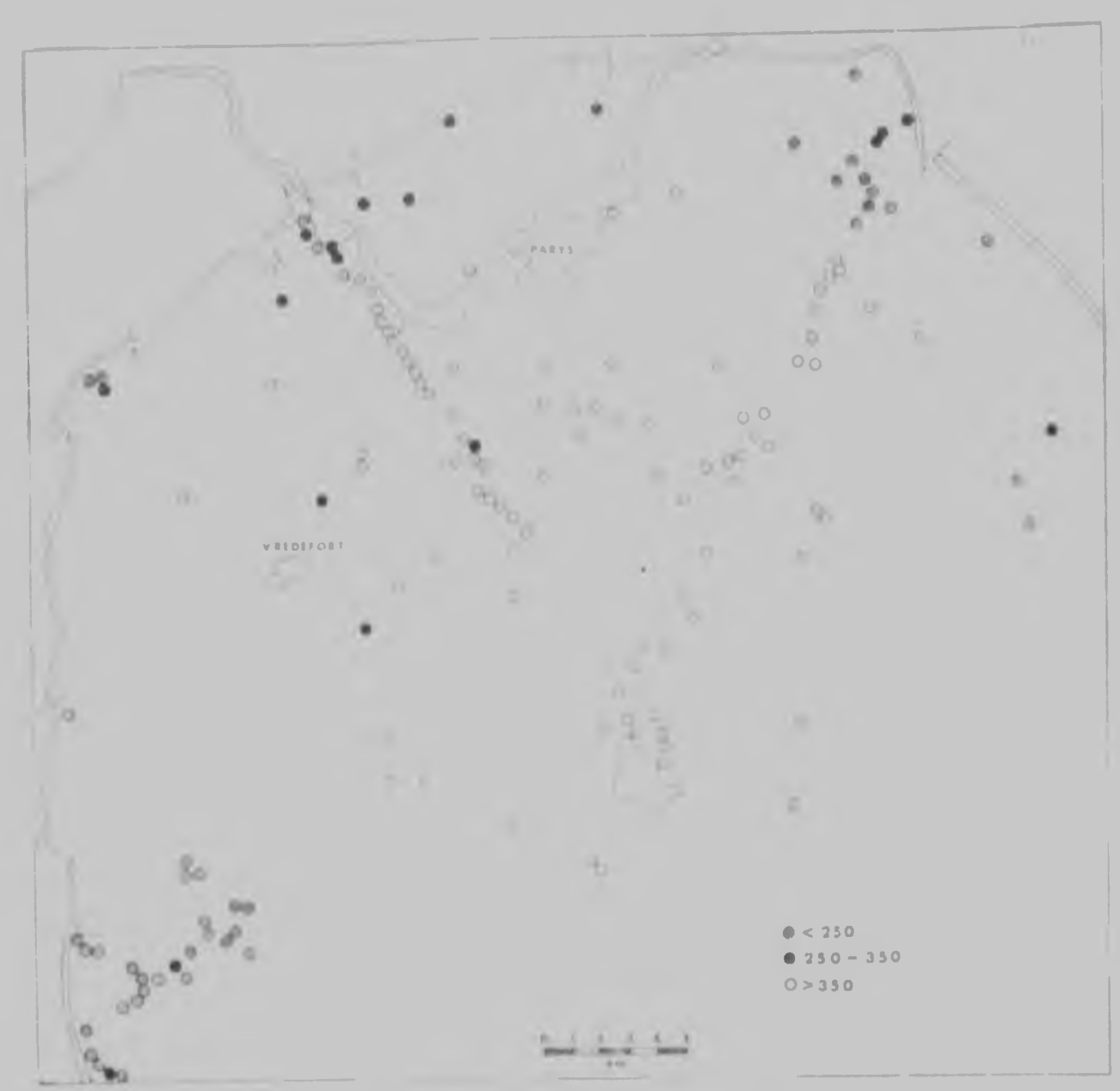


FIGURE 4.4 Variations in K/Rb ratios

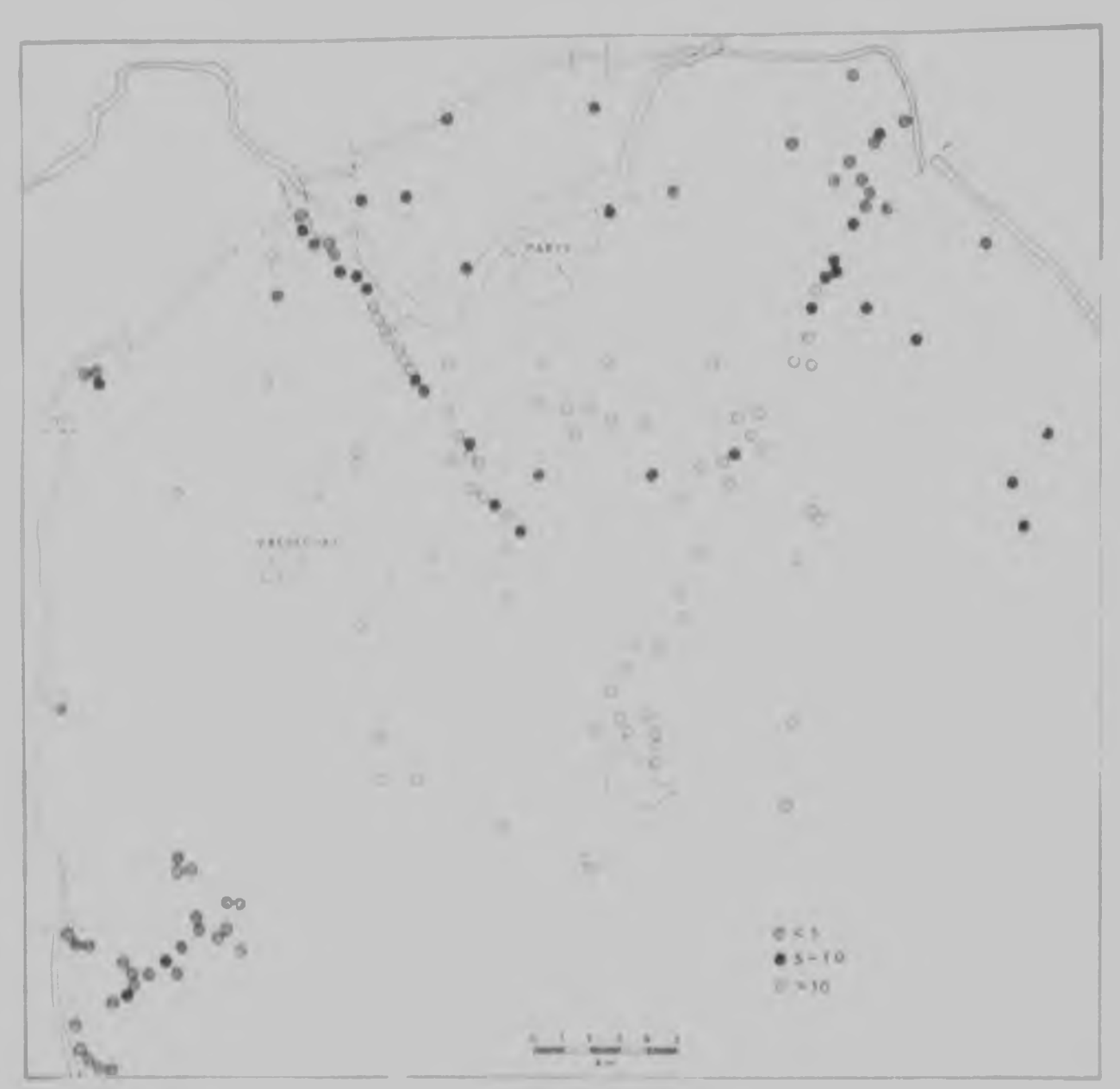


FIGURE 4.5 Variations of Ba/Rb ratios

4.3 Compiling profiles of elemental concentration versus depth in the crust

The perpose of the averaging procedures is to discern and highlight overall trends, which might otherwise be obscured by local geological variations within the individual traverses. Before the data were averaged, contours of 1 km horizontal distance intervals were measured inwards from the Orange Grove Quartzite. The peripheral outline of the basement-collar contact was reproduced closely near the contact. Near the centre, more circular contours were drawn. How do these contours relate to depth in the Archaean basement, measured vertically below the Orange Grove Quartzite? This problem is analysed in N. Clayton (Ms. in preparation). This paper presents the relation between (vertical) penetration and horizontal distance for two radically different models for the uplift of the basement core. One model assumes no radial strain within the basement (all strains either tangential or vertical) and the other model reproduces the internal (basement) deformations of a laboratory diapir, with large radial strains near the centre. For the outermost basement annulus (extending 8 km inward from the contact there is very close matching between contour horizontal distance (the contours of Fig. 4.6 of this study) and depth of penetration into the crust. For the inner suite of contours (from the 9 km level to the 13 km level) shown in Figure 4.6, the difference between contour level and vertical penetration may be as little as 2 to 3 km, if the mechanics of Vredefort basement uplift are approximated by either of the models referred to. In the light of the above discussion the 14 km profile (radial distance) adopted in this study will from now on represent a vertical section of 14 km through the continental crust.

To present the data as a single averaged depth-profile, the dome was first divided into three portions - NE, NW, SW in Fig. 4.6. Taking each quadrant separately, the average major and trace element concentrations



FIGURE 4.6 The Vredefort basement at one km contour intervals measured inwards from the Orange Grove Quartzite and the subdivision of the basement into three quadrants

within each particular contour were obtained by a 3-point moving average procedure. Because the SW sector is enriched in the large radius incompatible elements such as U, Th and Rb, and depleted in the more refractory trace elements such as Ba and Sr relative to the rest of the dome, and as the sampling in the SW quadrant did not extend further inward than this contour, the averaging of the 3 quadrants created a step at the 6 km contour. Thus, to obtain the realistic portrayal of the fall-off of elements and elemental ratios with depth in the crust only the NW and NE quadrants were averaged (Table 4.5 and 5.1). To calculate the overall crustal concentrations of the [illegible] required for modelling of heat flow problems, averaging of all three segments - NE, NW and SW is required (chapter 6).

4.4 Trace element variations

The broad geochemical features (illustrated in Figures 4.4 to 4.5) are now critically examined in particular to ascertain whether the data are consistent with the "crust on edge" model proposed by Tarney (1976).

The K/Rb ratios in the Vredefort basement display a six fold range of values. Those in the central zone (below 5 km) (the average being about 480) and approximate to results obtained from the Brazilian and Australian granulite facies terrains. The rocks from the periphery*, however, have low K/Rb ratios ranging from 150 to 350, the average being about 240. It is only in the outer 5 km that the K/Rb ratios approximate the crustal average of 230.

The geochemical coherence expected from the alkali metal pair is demonstrated in a K versus Rb plot (Fig. 4.7). However, only the rocks from the central part of the dome show a strong positive correlation. The deviation from the linear K-Rb relationship and the low K/Rb ratios around the margins are attributed to Rb enrichment.

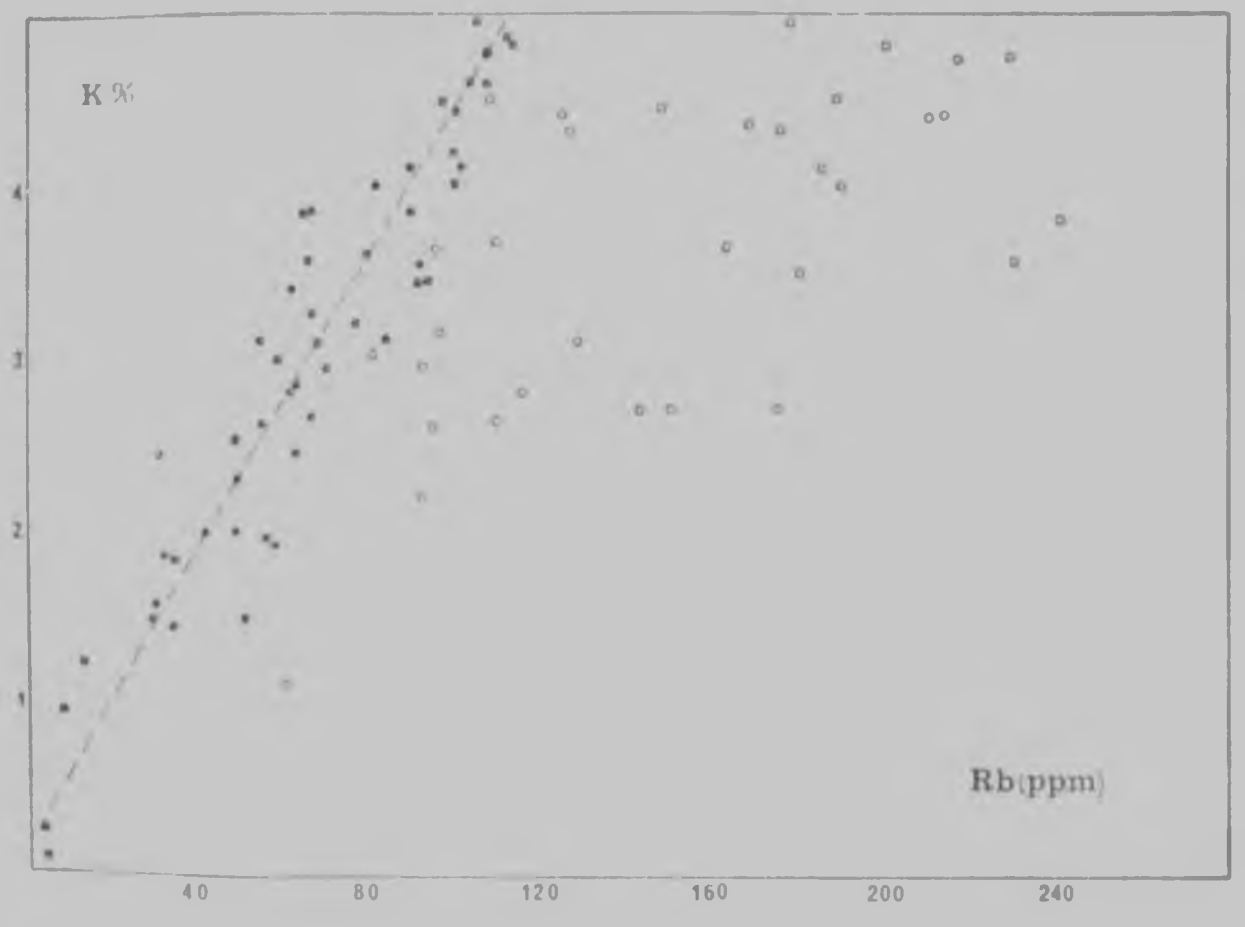
Details of the variation of K and Rb are presented in a plot of Rb/K versus depth for NE and SW radial profiles (Figures 4.1 and 4.3). Both profiles show the same general pattern: moving outwards, at about

* For the purposes of discussion the marginal granites include all rocks occurring in the outer 5 km.

Table 4.3 Averaged Major and Trace Element Analyses for the Vendeburn Basanite

No.																	
SiO_2*																	
Al_2O_3																	
Fe_2O_3																	
MgO																	
MnO																	
CaO																	
Na_2O																	
K_2O																	
TiO_2																	
P_2O_5																	
Ba**																	
Sr																	
Rb																	
Th																	
U																	
Nb																	
Ta																	
Zr																	
Hf																	
Y																	
Sc																	
V																	
Cr																	
Co																	
Ni																	
Cu																	
Zn																	
Ga																	
Pb																	
La																	
Ce																	
Nd																	
Sm																	
Eu																	
Gd																	
Dy																	
Er																	
Yb																	
Lu																	
Mg/Mg+Fe																	
Ba/Rb																	
K/Rb																	
Zr/Y																	
La_N/Yb_N																	
K_2O/P_2O_5																	

FIGURE 4.7 K VERSUS Rb



...tures - Mafic granulites

...les - Outer 5 m of the felsic rocks

...les - Central felsic rocks

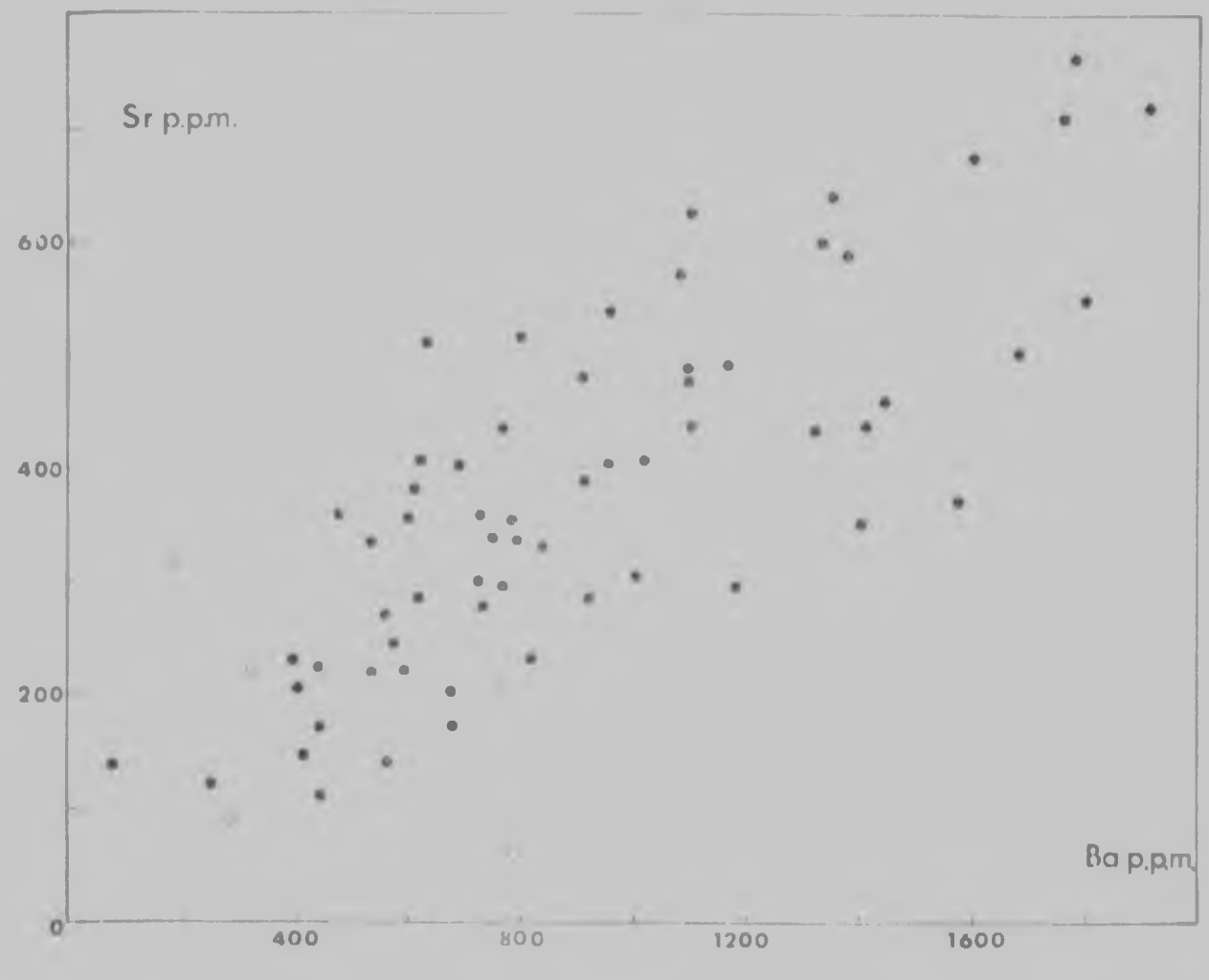
3 to 4 km from the outer margin there is a sharp increase in the Rb/K values of the rocks. These high Rb/K ratios do not persist, but drop off steeply towards the outer margin. Apart from the peripheral zone, there is very little variation over the remai[illegible] f the profiles, except for the mafic granulites, which are charac[illegible]l by low Rb/K (high K/Rb) ratios.

The broad feature[illegible] of the Ba/Rb rati[illegible] (Figure 4.5) are similar to those of K/Rb, the values in the centre being consistently higher than those around the margins. Unlike K which shows little variation a[illegible]ross the dome, Ba increa[illegible] centrally, and is similar to Sr in its geochemical behaviour (Fig. 4.8). Except for the mafic gr[illegible]nulite[illegible] which have low Ba and Sr concentrations, the concentrations of these elements are g[illegible]nerally high in the centre (Ba > 1000, Sr > 350) and decre[illegible]e steadily towards the margins.

The distributi[illegible]n pattern[illegible] of Ba and Sr differ fr[illegible] the other [illegible]latively refractory trace elements Y and Nb. The latter pair are highly c[illegible]ncentrated in rocks with a high percentage of heavy minerals (Fig. 4.1; e.g. KK1, 7, 8, 9 and 15) as well as the mafic granulite[illegible]. In these rocks Ba and Sr concentrations are low and although Ba and Sr [illegible]how no strict correlation with any of the major oxides, these elements are almost certainly controlled by the feldspar[illegible], which is to be expected (Bray, 1942; Shimer, 1943; Duchesne, 1968; Hall, 1967).

Another significant feature of the distribution of trace elements throughout the profile[illegible] (Fig. 4.1 to 4.3) is that although the mo[illegible]e incompatible elements such as Rb, U and Th reach a maximum concentration in the region where the percentage of H_2O and heavy minerals are at their greatest, it is not the more mafic rocks such as KK9 which have the greatest concentrations of Rb, U and Th, but rather the felsic rocks which occur in close proximity. This is also seen in the zone where the mafic granulites occur. Samples such as KK16 (Figure 4.1) and VT 127 (Figure

FIGURE 4.8 Ba VERSUS Sr



Open circles : Mafic granulite

4.2) have anomalously high Rb, U and Th concentrations relative to any of the surrounding rocks. Whereas the proportion of mafic minerals correlate with the concentration of certain trace elements (Y and Nb) along the radial profiles, the proportion of these minerals have no correlation with the concentration of the incompatible elements such as Rb, Th and U.

In the case of Rb, as has already been mentioned, the major control is most probably the K-feldspars and the micas. This is demonstrated by the correlation between Rb and K. The exact location of U and Th is not known although they are thought to occur interstitially or in minerals such as zircon and monazite. However, it does appear that on average, the regions along the radial profiles (Fig. 4.1) characterised by a high percentage of mafic minerals, and consequently a high volatile content, have some indirect control on the relative position at which high concentrations of incompatible elements occur.

4.5 Averaged trace element profiles

The variation of U and Th (Figure 4.9) is similar to that of Rb, the other large radius cation that has been studied. All three elements increase steadily from a depth of 7 km towards the margin, although the gradient for U is almost twice that for Th and Rb. The main difference between the Rb and the Th and U distribution, occurs in the lower half of the profiles on the outer margin of the Steynskraal metamorphic belt (at about 10 km depth); a peak occurs showing an increase in concentration of both U and Th. This feature is not exhibited in the Rb concentrations.

Ba and Sr, which behave in a similar fashion, show trends which are opposite to that of the incompatible elements. That is, both these elements are relatively abundant in the lower half of the profiles, and then show a steady diminution over the outer 7 km. Like U and Th, Ba and Sr exhibit important variations in the lower half of the profile: the concentrations of Ba and Sr decrease to a minimum at about 12 km, which correspond (approximately) to the centre of the Steynskraal metamorphic zone and then

4.2) have anomalously high Rb, U and Th concentrations relative to any of the surrounding rocks. Whereas the proportion of mafic minerals correlate with the concentration of certain trace elements (Y and Nb) along the radial profiles, the proportion of these minerals have no correlation with the concentration of the incompatible elements such as Rb, Th and U.

In the case of Rb, as has already been mentioned, the major control is most probably the K-feldspars and the micas. This is demonstrated by the correlation between Rb and K. The exact location of U and Th is not known although they are thought to occur interstitially or in minerals such as zircon and monazite. However, it does appear that on average, the regions along the radial profiles (Fig. 4.1) characterised by a high percentage of mafic minerals, and consequently a high volatile content, have some indirect control on the relative position at which high concentrations of incompatible elements occur.

4.5 Averaged trace element profiles

The variation of U and Th (Figure 4.9) is similar to that of Rb, the other large radius cation that has been studied. All three elements increase steadily from a depth of 7 km towards the margin, although the gradient for U is almost twice that for Th and Rb. The main difference between the Rb and the Th and U distribution, occurs in the lower half of the profiles on the outer margin of the Steynskraal metamorphic belt (at about 10 km depth); a peak occurs showing an increase in concentration of both U and Th. This feature is not exhibited in the Rb concentrations.

Ba and Sr, which behave in a similar fashion, show trends which are opposite to that of the incompatible elements. That is, both these elements are relatively abundant in the lower half of the profiles, and then show a steady diminution over the outer 7 km. Like U and Th, Ba and Sr exhibit important variations in the lower half of the profile: the concentrations of Ba and Sr decrease to a minimum at about 12 km, which correspond (approximately) to the centre of the Steynskraal metamorphic zone and then

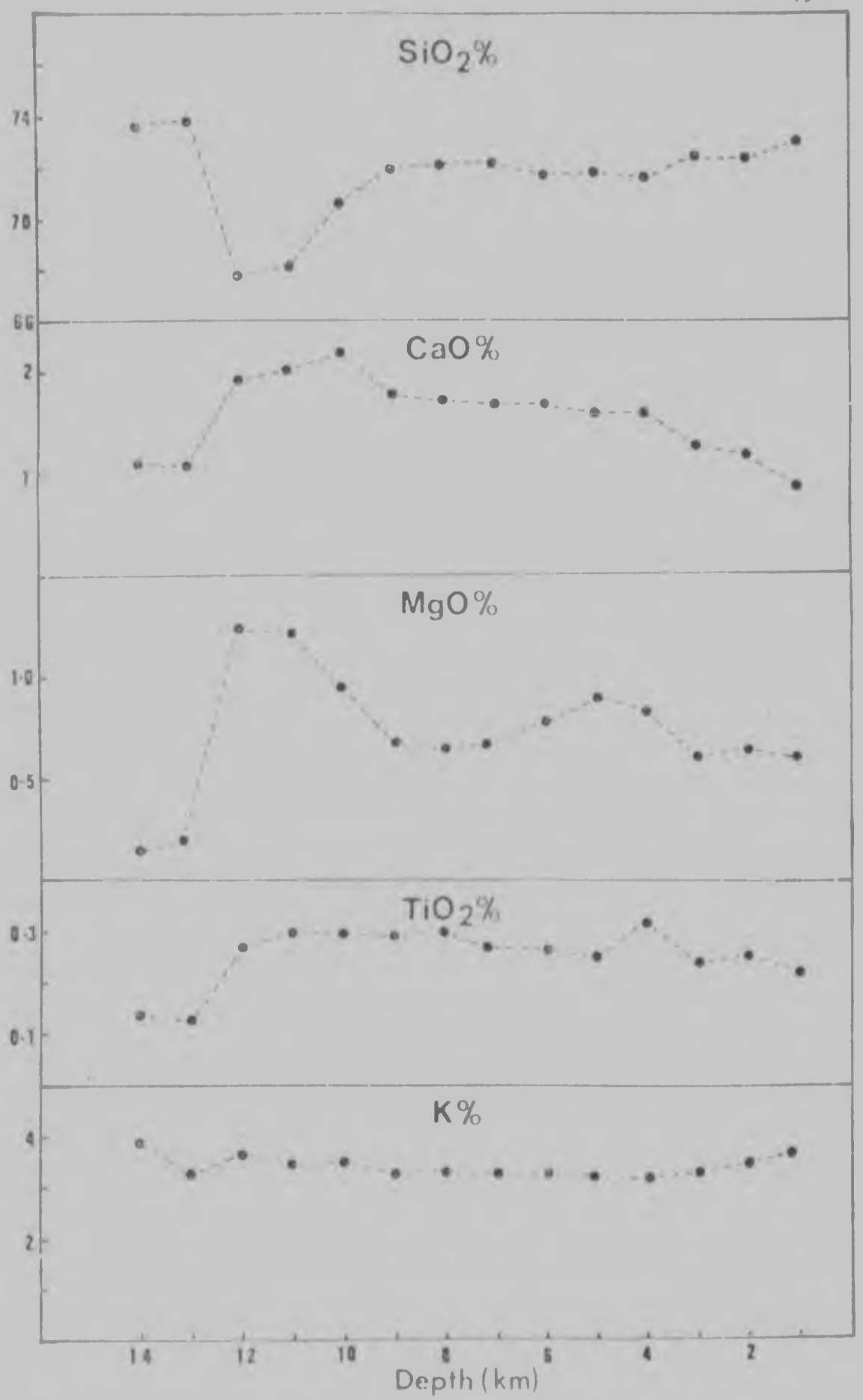


FIGURE 4.9 Averaged major and trace element profiles for the Vredefort basement

1 to 10 km Outer Granite Gneiss
11 and 12 km Mafic metamorphic inclusions
13 and 14 km Inlandsee leucogranite

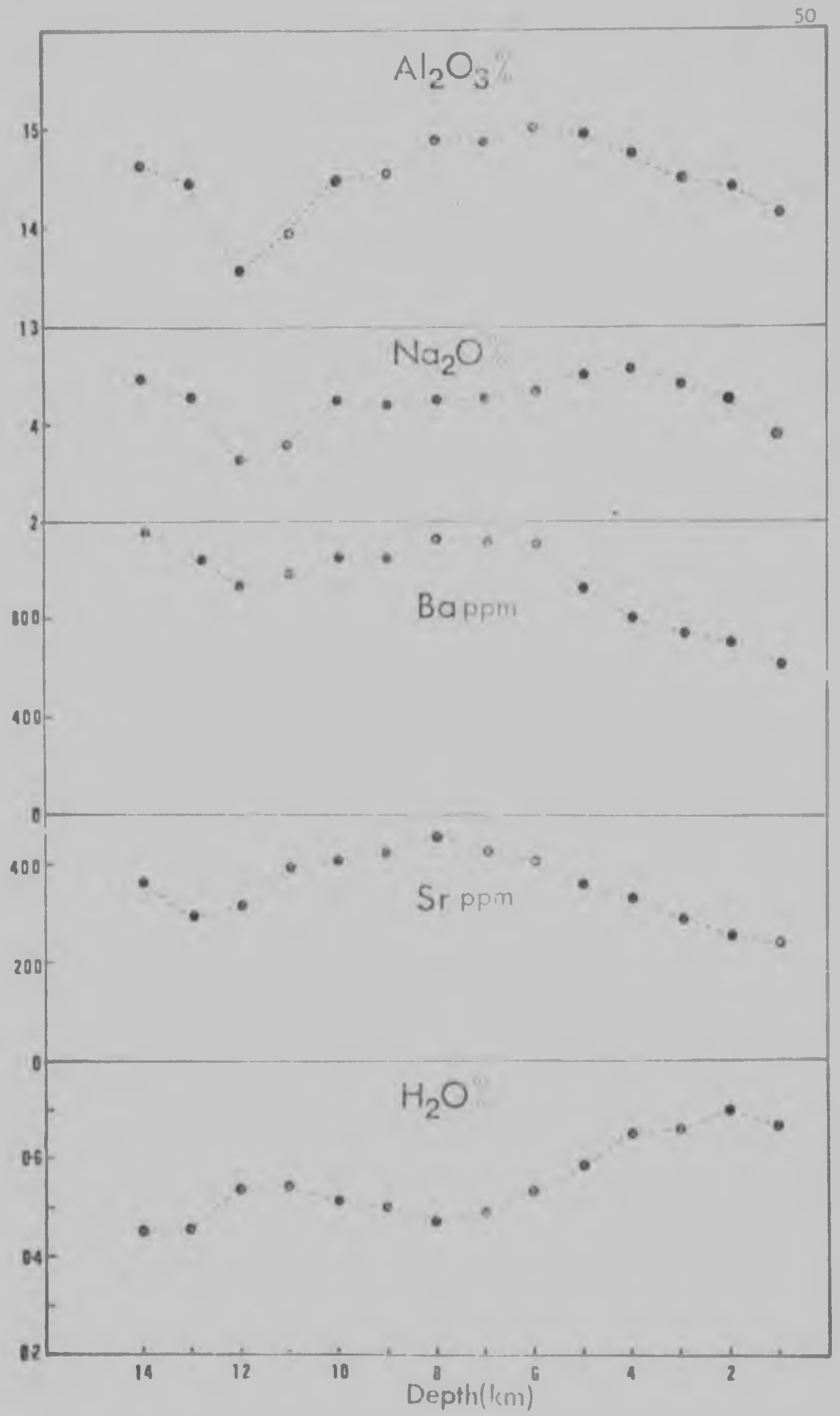


FIGURE 4.9 Contd.

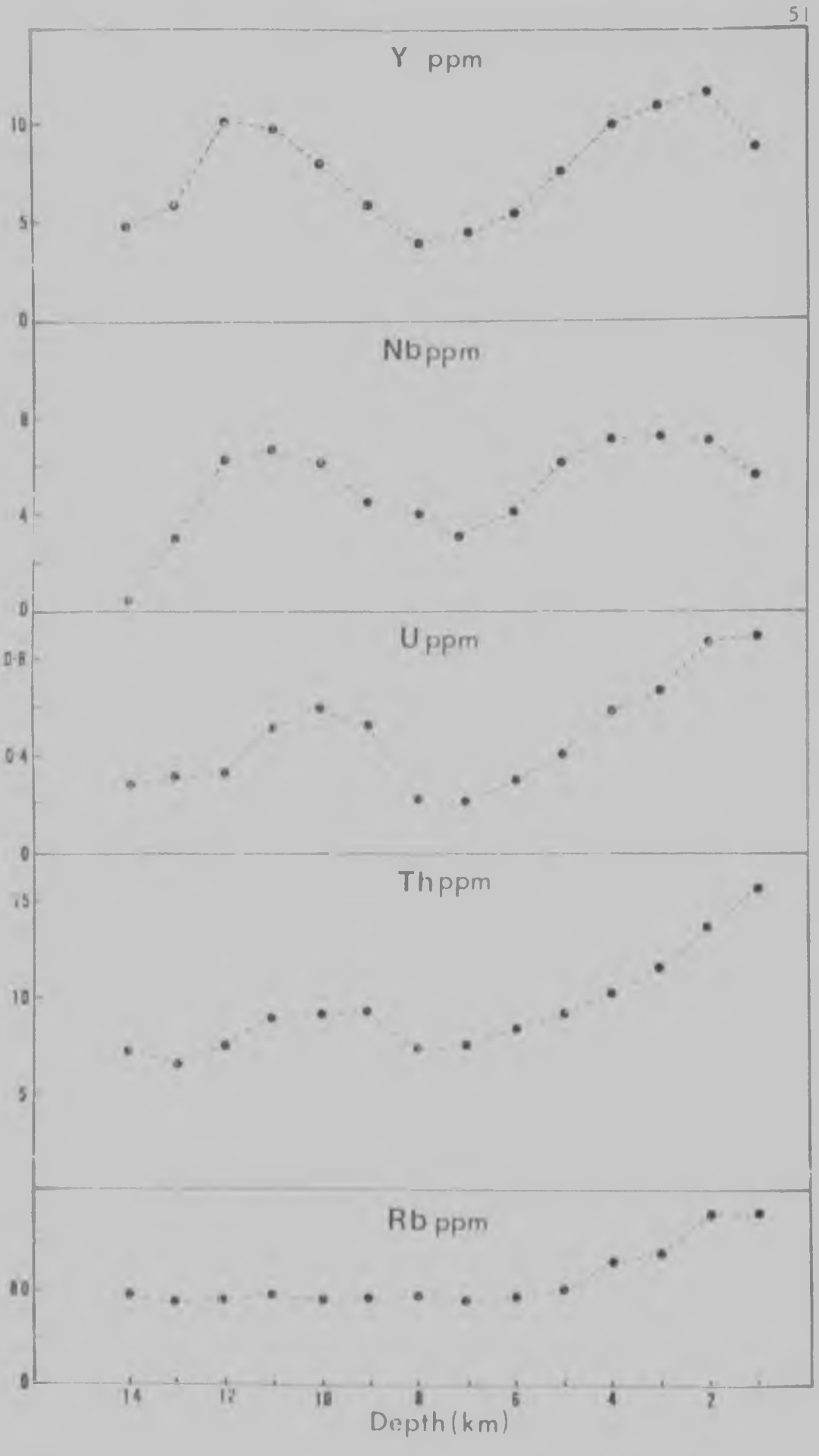


FIGURE 4.9 Cont.d.

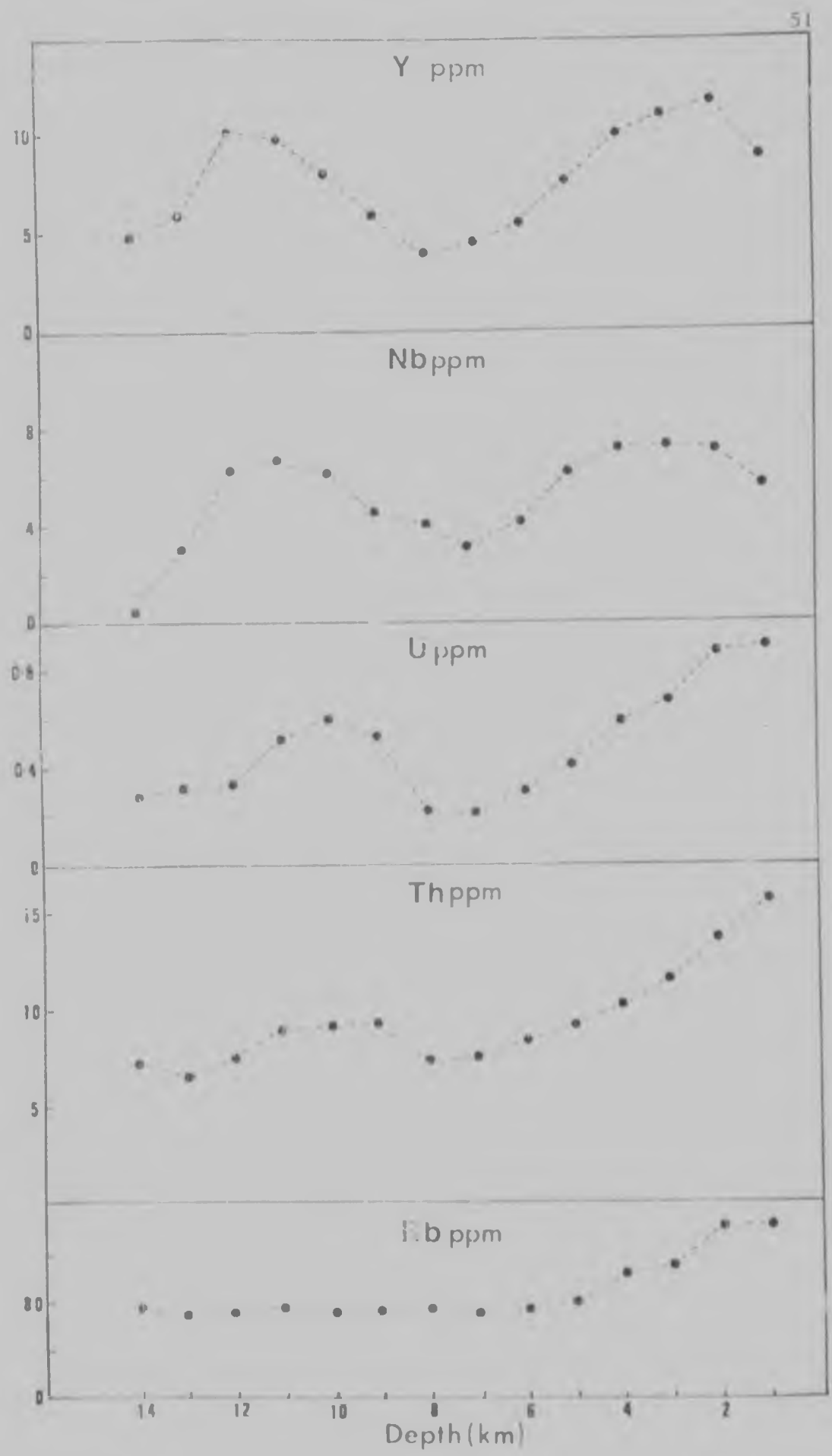


FIGURE 4.9 Contd.

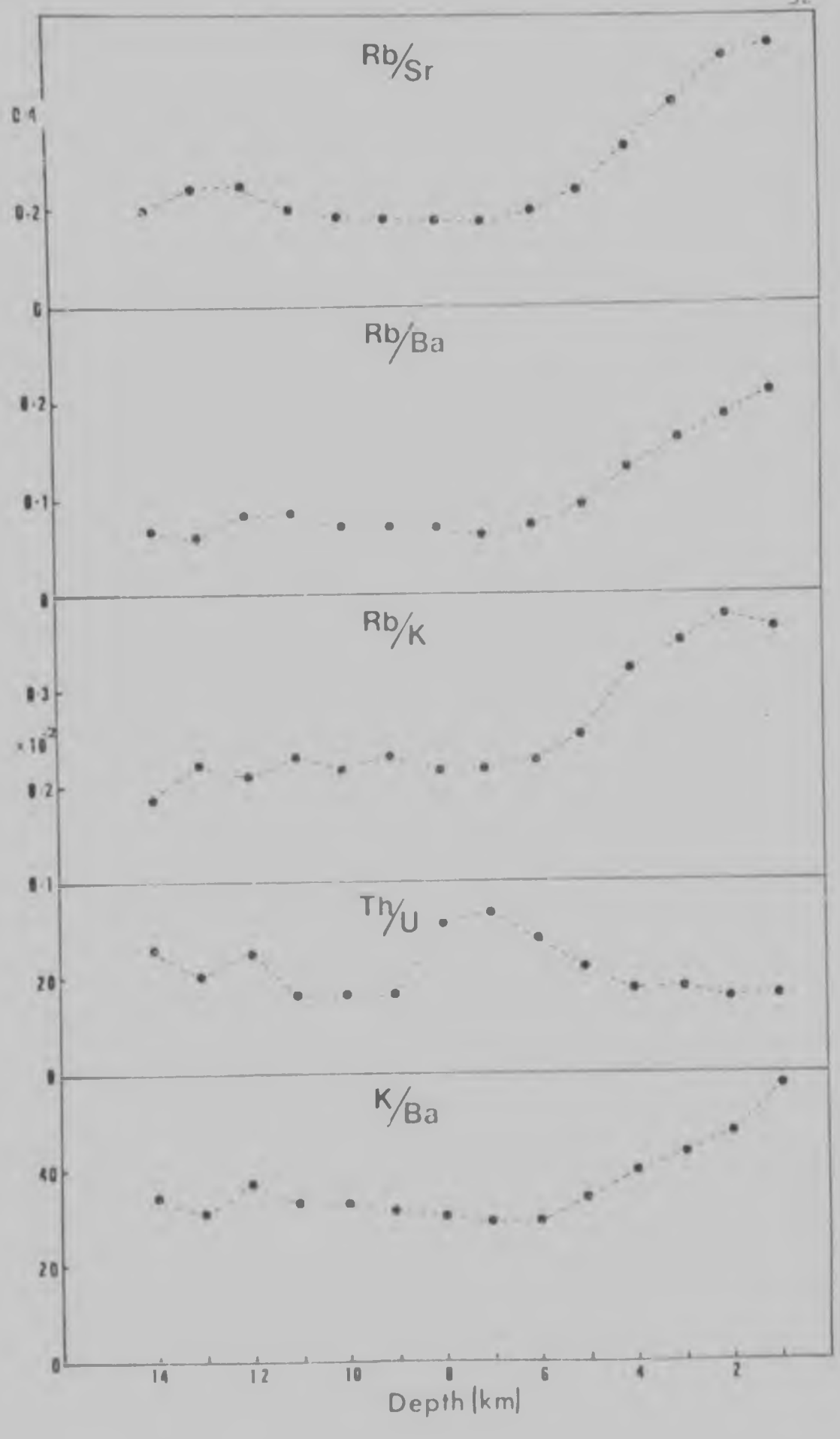


FIGURE 4.9 Contd .

once again increase at the base of the profile.

Rb/Sr, Rb/Ba, Rb/K and K/Ba all show little or no variation over the lower half of the profiles at 7 km from the granite margin there is a steady increase outwards towards the granite contact. In the lower half of these profiles the elemental ratios are in keeping with those reported for other high grade metamorphic rocks; whereas the outer 3 to 5 km have trace element concentrations and interelement ratios approximating to average crustal values.

The average distribution curves for Yt and Nb are in many ways similar to those of U and Th and some of the other trace elements. But there are significant differences; like the radioelements, Yt and Nb indicate two distinct regions of relatively high concentrations along the profile. In the lower half of the profiles (7 to 14 km) the maximum concentrations of Yt and Nb occur within the SMZ whereas the highest concentration of Th and U occur in the felsic rocks lying immediately above this zone of mafic inclusions.

In the outer 7 km of the granite dome the lithophile elements show a steady increase towards the margin, the distribution being roughly exponential in form (see Chapter 5). Yt and Nb pass through a maximum at about 2 to 3 km from the margin. It is noted that the average distribution of H_2O^+ very closely approximates the curves for Yt and Nb, thus tending to verify the suggestion that the concentrations of these elements are controlled by the hydrous minerals. For the outer granite gneisses biotite is the dominant hydrous mineral, whereas in the mafic xenoliths amphiboles, and accessory minerals such as allanite and sphene are the controlling phases.

4.6 Major element variations

It is convenient at this stage to point out some of the detailed features with regard to the major element concentrations, and the relationship of these features to anomalies in the trace element variations.

The broader aspects of the major element distribution are discussed in the following section.

The sympathetic relationship between Ti, Zr and Fe is evident in all three traverses (Figures 4.1, 4.2 and 4.3). The positive correlation between Ti and Fe (Figure 4.10) is probably due to these elements being taken up in ilmenite (and biotite) as very little magnetite occurs in these rocks. An average total Fe/Ti ratio of 9.5 is estimated from the slope of the trend (Figure 4.10). It is only in those rocks which have been identified as metasediments in the field (Stepto, Ms in preparation) such as VT523 and 524 (Figure 4.2), that this correlation does not apply. The metasediments exhibit higher and more variable total Fe/Ti ratios.

Because Zr only occurs in the mineral zircon, and the Fe and Ti content of the rocks are associated with the minerals ilmenite and biotite, it is contended that the behaviour of these minerals during igneous and metamorphic processes is reflected by the respective elements. Zircon, ilmenite and biotite are refractory in nature as they resist melting. It is therefore possible that the relative concentrations of Ti, Fe and Zr reflect the degree of partial melting that has occurred. This expected decrease in the overall abundance of Zr, Ti and Fe from mafic to felsic rocks of the Vredefort basement is apparent from the averaged major element profiles.

4.7 Averaged major element profiles

On the basis of the geochemical parameters discussed up to this point, it has not been possible to distinguish unambiguously the different basement rocks previously mentioned in this study (Chapter 2) namely: Inlandsee leucogranofels (ILG), metabasite and metasedimentary inclusions of the SMZ and the outer granite gneiss (OGG). For example although Y and Nb are at a maximum in the SMZ, as a result of the mafic xenoliths present, these high concentrations are not unique to this zone as they also occur at higher levels in the profile. However, the averaged major element chemistry clearly delineates three annular zones, each characterised by distinctive

The broader aspects of the major element distribution are discussed in the following section.

The sympathetic relationship between Ti, Zr and Fe is evident in all three traverses (Figures 4.1, 4.2 and 4.3). The positive correlation between Ti and Fe (Figure 4.10) is probably due to these elements being taken up in ilmenite (and biotite) as very little magnetite occurs in these rocks. An average total Fe/Ti ratio of 5.5 is estimated from the slope of the trend (Figure 4.10). It is only in those rocks which have been identified as metasediments in the field (Stepto, Ms in preparation) such as VT523 and 524 (Figure 4.2), that this correlation does not apply. The metasediments exhibit higher and more variable total Fe/Ti ratios.

Because Zr only occurs in the mineral zircon, and the Fe and Ti content of the rocks are associated with the mineral ilmenite and biotite, it is contended that the behaviour of these minerals during igneous and metamorphic processes is reflected by the respective elements. Zircon, ilmenite and biotite are refractory in nature and they resist melting. It is therefore possible that the relative concentrations of Ti, Fe and Zr reflect the degree of partial melting that has occurred. This expected decrease in the overall abundances of Zr, Ti and Fe from mafic to felsic rocks of the Vredefort basement is apparent from the averaged major element profiles.

4.7 Averaged major element profiles

On the basis of the geochemical parameters discussed up to this point, it has not been possible to distinguish unambiguously the different basement rocks previously mentioned in this study (Chapter 2) namely: Inlandsee leucogranofels (ILG), metabasite and metasedimentary inclusions of the SMZ and the outer granite gneiss (OGG). For example although Y and Nb are at a maximum in the SMZ, as a result of the mafic xenoliths present, these high concentrations are not unique to this zone as they also occur at higher levels in the profile. However, the averaged major element chemistry clearly delineates three annular zones, each characterised by distinctive

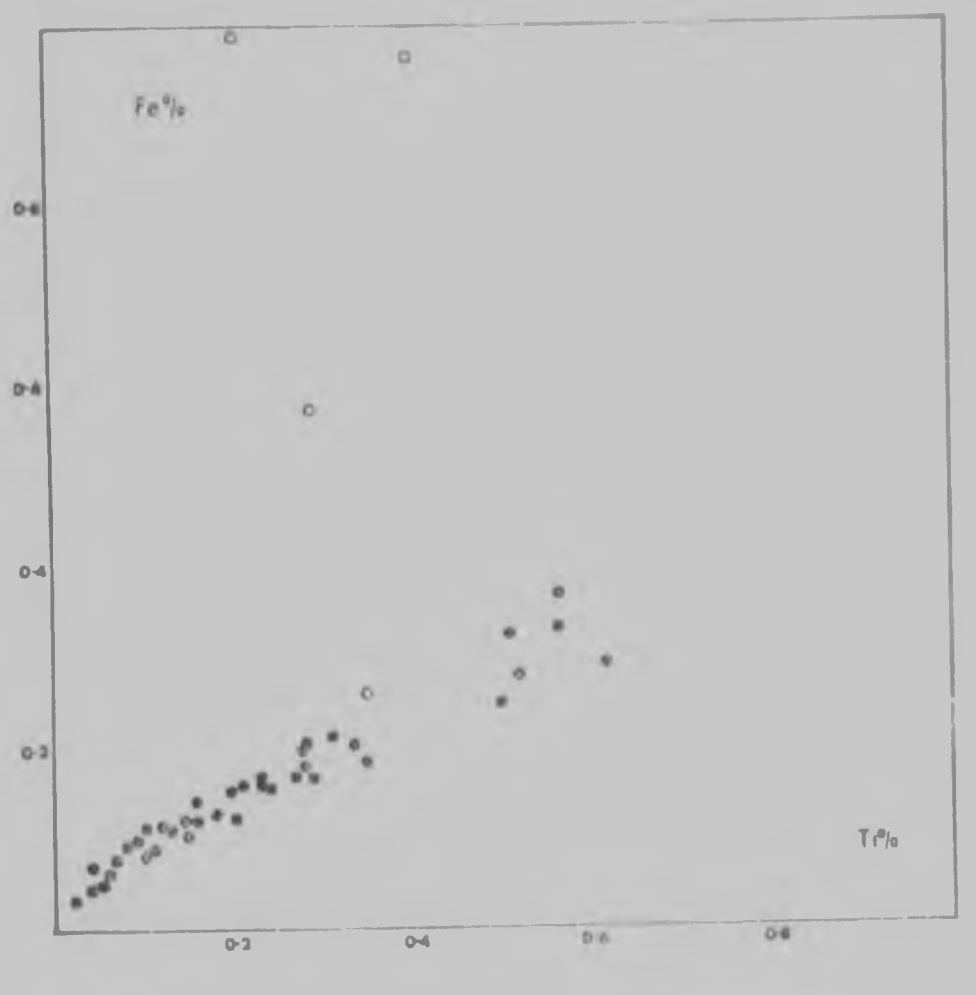


FIGURE 4.10
Fe VERSUS Ti

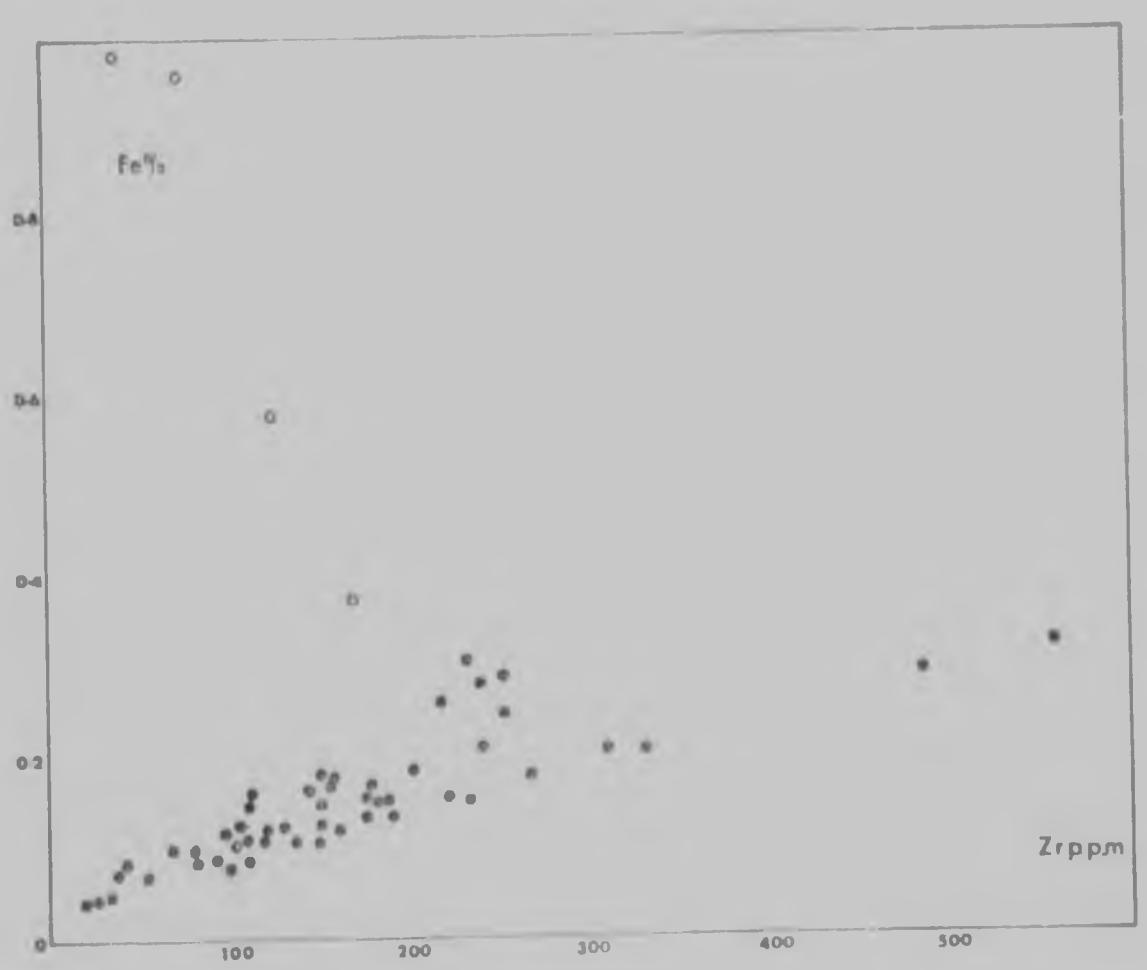


FIGURE 4.11 Fe VERSUS Zr
Open circles :Mafic granulites

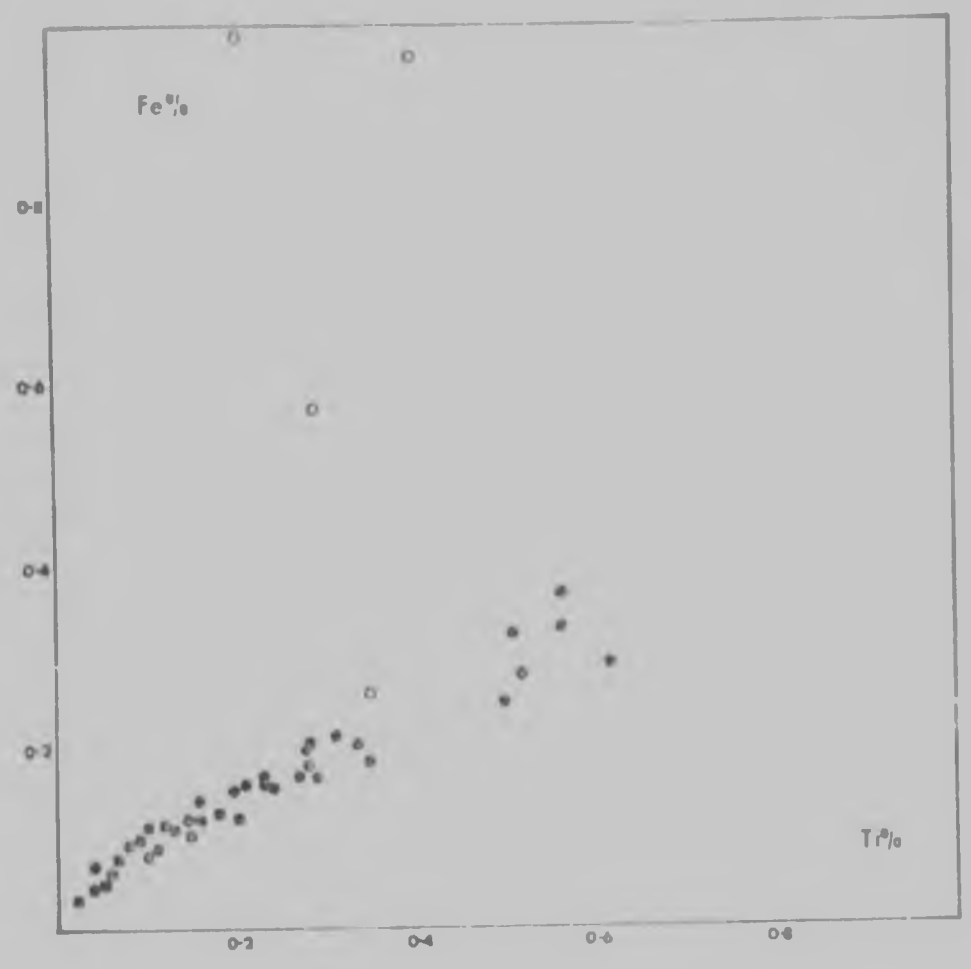


FIGURE 4.10
Fe VERSUS Ti

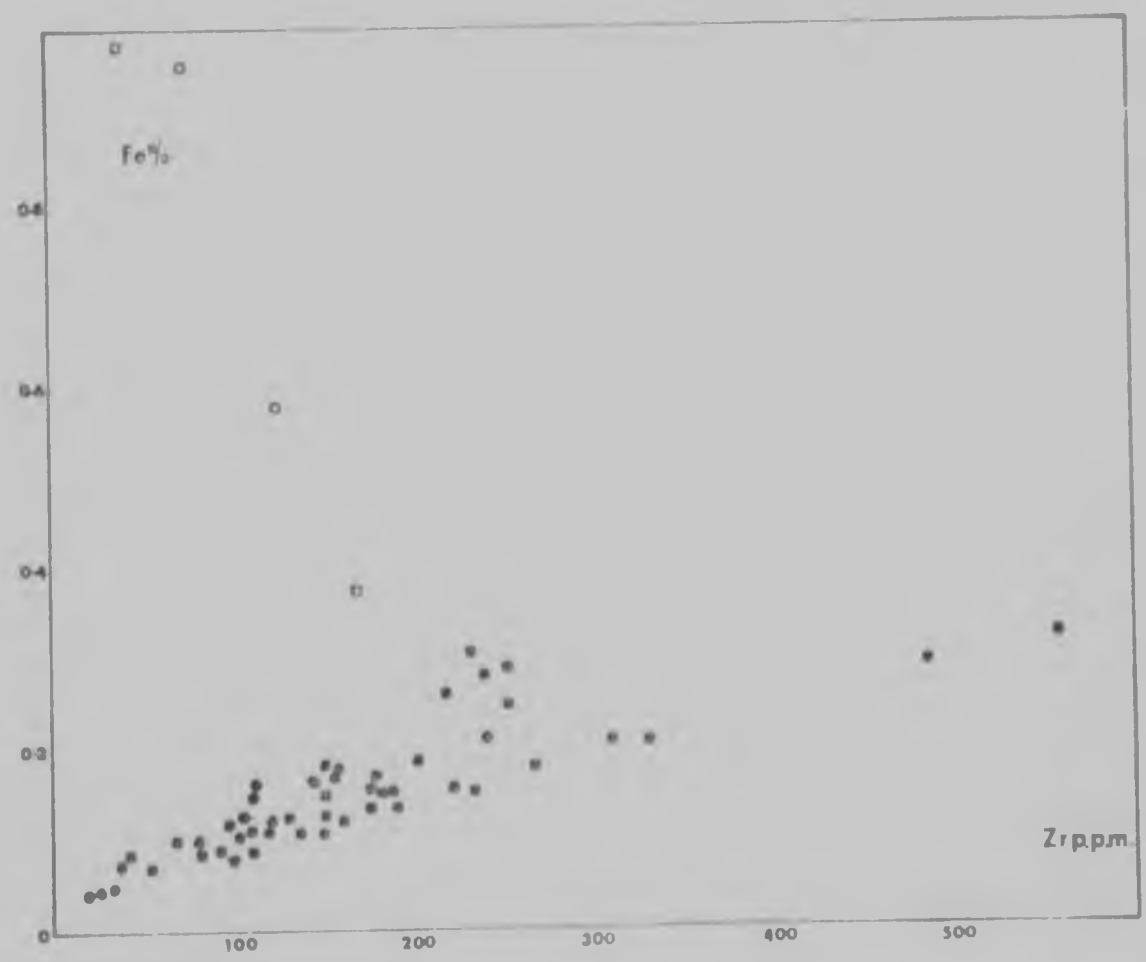


FIGURE 4.11 Fe VERSUS Zr
Open circles :Mafic granulites

geochemical features.

Firstly, the profiles clearly reflect the mafic character of the rocks of the SMZ*, and distinguish the metabasites and metasediments from the felsic rocks of the Vredefort basement. One interesting and unexpected feature arising from the averaged major element data is the difference in composition between the felsic rocks occurring in the central zone of the dome (the ILG) to that of the OGG.

In the OGG both CaO and MgO increase steadily from the margin towards the centre, as would be expected from a traverse through the upper crust. (These trends however do not continue into the Inlandsee leucogranofels, which has a chemistry that is significantly more felsic than the OGG.) The Inlandsee granite is highly depleted in CaO, MgO, FeO and TiO_2 (Figure 4.9) whereas SiO_2 values are significantly higher than in the OGG (73.66 as opposed to 71.88).

The averaged profiles have provided an additional dividend of further controls on some of the trace element distribution patterns. The averaged profiles indicate a strong correlation between the major elements sodium and aluminium and trace elements Ba and Sr. In rocks of granitic composition most, if not all, of the Na and Al is taken up in the feldspar mineralogy. These observations support earlier suggestions with respect to the controls that the feldspar mineralogy has on Ba and Sr. Further, the averaged data imply that plagioclase is the most probable host for these elements.

4.8 Interpretation of the geochemical data

Before discussing the implications of the geochemical data, it is important to examine whether the averaged profiles are truly representative

*Footnote

Since the completion of this study, many more mafic to intermediate rock types from the Vredefort basement have been analysed and that the major element data presented here does not necessarily represent the full range in composition of these rocks. A more comprehensive report on the chemistry of the metabasites and metasediments is given by Stepto (ms. in preparation).

geochemical features.

Firstly, the profiles clearly reflect the mafic character of the rocks of the SMZ*, and distinguish the metabasites and metasediments from the felsic rocks of the Vredefort basement. One interesting and unexpected feature arising from the averaged major element data is the difference in composition between the felsic rocks occurring in the central zone of the dome (the ILG) to that of the OGG.

In the OGG both CaO and MgO increase steadily from the margin towards the centre, as would be expected from a traverse through the upper crust. (These trends however do not continue into the Inlandsee leucogranofels, which has a chemistry that is significantly more felsic than the OGG.) The Inlandsee granite is highly depleted in CaO, MgO, FeO and TiO_2 (Figure 4.9) whereas SiO_2 values are significantly higher than in the OGG (73.66 as opposed to 71.88).

The averaged profiles have provided additional dividend of further controls on some of the trace element distribution patterns. The averaged profiles indicate a strong correlation between the major elements sodium and aluminium and trace element Ba and Sr. In rocks of granitic composition most, if not all, of the Na and Al is taken up in the feldspar mineralogy. These observations support earlier suggestions with respect to the controls that the feldspar mineralogy has on Ba and Sr. Further, the averaged data imply that plagioclase is the most probable host for these elements.

4.8 Interpretation of the geochemical data

Before discussing the implications of the geochemical data, it is important to examine whether the averaged profiles are truly representative

*Footnote

Since the completion of this study, many more mafic to intermediate rock types from the Vredefort basement have been analysed and that the major element data presented here does not necessarily represent the full range in composition of these rocks. A more comprehensive report on the chemistry of the metabasites and metasediments is given by Stepto (ms. in preparation).

of the Vredefort crust.

The averaged major element profiles suggest that the Vredefort crust consists essentially of two felsic layers, the upper (the OGG) approximately 9 km thick and the lower of undefinable thickness, separated by a zone characterised by rocks of a more mafic composition. However such an over simplified first model of the Vredefort crust could lead to a gross misrepresentation of crustal structure and a more realistic appraisal of the data is essential.

The reason for this approach is best illustrated by referring to Fig. 2.3 and 3.1 respectively. A large part of the southern and central portions of the dome are covered by palaeozoic sediments and dolerite sills. The geochemical data which make up the averaged profiles comes in the main from two northerly trending traverses (Fig. 3.1). Samples from the OGG are well represented on both traverses, whereas the felsic rocks of the ILG occur only along the NE traverse. (The exposures along this traverse are generally poor with only a limited outcrop of mafic rocks.) This traverse samples a narrow basement tongue penetrating through the younger stratified cover which represents an arc of about 20° and the question now arises; is the inner 8 km of this traverse representative of the interior of the basement core? The NW traverse does not continue into the interior of the dome, because of the presence of the younger strata which cover the innermost boundary of the SMZ. All but one of the mafic samples lie along this traverse. If the NW traverse were to continue under the Palaeozoic cover it is conjectural whether or not one would pass into a unit typified by the felsic rocks samples on the NE traverse or a more heterogeneous unit containing a greater proportion of mafic inclusions. This implies a second model for the lower Vredefort crust. That is, the ILG interleaved with mafic pods, the proportion of mafics possibly increasing with depth.

As yet there is no definitive independent evidence, such as from

boreholes through the thin cover of stratified rock, to test either model. The latter model is however considered more realistic in view of the general increase in mafic components with depth in the crust in world wide granulite terrains.

4.9 General Discussion

There is a progressive increase in metamorphic grade with depth in the continental crust; the progression from medium to high grade mineral assemblages during centrally-directed traverses in the Vredefort basement must reflect rocks formed at increasing depth. That is, low grade amphibolite facies rocks grade downwards through amphibolites and hornblende granulites into pyroxene granulites in the lower part of the crust. Where exposed by erosion, granulite facies rocks provide valuable information on the composition of rocks which presumably were once buried deeply in the crust.

On the basis of extensive geochemical studies in granulite facies terrains, and statistical comparisons of the chemical compositions of granulite facies rocks with that of more normal surface granite, the concept of a geochemically layered continental crust has been developed. This crust consists of a granitic rich layer overlying rocks of intermediate average composition (Lambert and Heier, 1967; 1968; Eade et al., 1966; Sighinolfi, 1971; Lambert, 1971). It has been held that during high grade regional metamorphism and conditions of partial melting, melts of granitic composition migrate upwards leaving a depleted lower crust to crystallise under granulite facies conditions. Indeed, estimates of density based on seismic velocities (Pakiser and Robinson, 1967; Christensen and Fountain, 1975) and high pressure experimental studies (Green 1970) suggest that anhydrous phase assemblages with an intermediate composition must predominate in the lower crust. However, it is generally agreed that the lower crust consists of rocks of extremely variable composition with an overall average intermediate composition,

rather than discrete homogeneous layers.

In a recent review of the geochemical characteristics of the high grade gneissic terrain of the northern Atlantic craton, Tarney (1976) recognises three main Archaean gneissic groups: granodioritic grey gneiss, high grade metasedimentary supracrustals and pyroxene granulites. In all three groups the range in composition varies between ultramafic and acid, although rocks of acid composition dominate the amphibolite facies terrain, whereas the granulites are distinctly more mafic.

In the light of the above discussion an examination of the geochemical characteristics from the exposed vertical profiles seen at Vredefort show some common features and also some very striking differences which are detailed below.

a) At Vredefort the principal metamorphic facies lie in their expected vertical sequences (Stepto, ms. in preparation). The main components, felsic amphibolites, metasediments, supracrustals and mafic pyroxene granulites recognised in other Archaean cratons, are also present. The variation of major element chemistry with depth is however not altogether consistent with the recent publications (quoted above) dealing with crustal structures.

b) Although the range in composition is small, the progressive increase in cafemic character of the OGG with depth, provides strong evidence for the development of the upper Vredefort crust by processes of partial melting; inter-element trends specifically Rb versus Sr, and Zr versus Ti, support this conclusion. The trends defined by the OGG do not characterise either the ILG or the mafic inclusions of the lower Vredefort crust, which have a different geochemical signature.

c) There is no convincing evidence from this middle crustal zone which might suggest that the OGG was formed at depth as a result of partial melting and the subsequent upward migration of granite fluids leaving a depleted lower crust. The author contends that partial melting processes

were largely restricted to the upper crust, and that the OGG formed as a result of "in situ" processes.

d) The lower zone consists of rocks of extremely variable composition. The heterogeneities are such that they preclude partial melting as a mechanism for their development. A possible model for the development of the lower Vredefort crust is discussed in Chapter 7 after the isotopic data is presented.

TABLE 4.1 Trace Element Concentrations and Ratios for Rocks from the Verdefuel Dunesuite

Sample	Rb	Sr	Zr	Nb	Ba	Th	U	Rb/Sr	K/Rb	Ba/Rb	Th/U	K/U*	K/Th*	K/Ba
VT1	42	348	1.43	1.20	705	1.04	0.13	0.12	548	16.58	8.00	26.15	3.27	1.08
VT2	62	874	1.43	4.74	878	11.97	0.32	0.07	774	13.90	8.00	4.64	0.39	0.40
VT3	91	193	3.49	9.16	879	13.43	0.63	0.47	638	9.33	16.00	5.64	0.42	1.09
VT4	82	412	4.04	9.03	731	10.08	0.41	0.16	548	8.40	10.00	8.83	0.27	1.48
VT5	41	1313	1.54	4.08	1887	18.82	0.09	0.18	903	46.03	22.00	1.48	0.19	0.80
VT6	161	300	1.47	9.18	181	42.00	0.26	0.243	219	8.59	1.00	1.04	0.06	1.12
VT7	141	333	1.21	4.28	387	13.00	2.19	0.42	1103	7.78	10.67	1.82	0.13	0.73
VT8	131	411	2.32	7.07	511	15.00	0.79	0.32	1103	7.78	10.67	1.82	0.13	0.73
VT9	118	242	0.23	5.84	1111	13.67	4.93	0.49	1203	10.14	1.00	1.18	0.81	1.98
VT10	130	1401	4.74	9.71	490	84.000	1.04	1.6	1304	3.78	11.0	4.32	0.33	1.74
VT11	131	131	2.11	4.08	852	8.10	5.61	0.18	243	6.41	0.33	0.46	0.89	0.26
VT12	131	141	2.11	4.08	852	8.10	5.61	0.18	243	6.41	0.33	0.46	0.89	0.26
VT13	131	141	2.11	4.08	852	8.10	5.61	0.18	243	6.41	0.33	0.46	0.89	0.26
VT14	131	141	2.11	4.08	852	8.10	5.61	0.18	243	6.41	0.33	0.46	0.89	0.26
VT15	131	141	2.11	4.08	852	8.10	5.61	0.18	243	6.41	0.33	0.46	0.89	0.26
VT16	131	141	2.11	4.08	852	8.10	5.61	0.18	243	6.41	0.33	0.46	0.89	0.26
VT17	131	141	2.11	4.08	852	8.10	5.61	0.18	243	6.41	0.33	0.46	0.89	0.26
VT18	131	141	2.11	4.08	852	8.10	5.61	0.18	243	6.41	0.33	0.46	0.89	0.26
VT19	131	141	2.11	4.08	852	8.10	5.61	0.18	243	6.41	0.33	0.46	0.89	0.26
VT20	131	141	2.11	4.08	852	8.10	5.61	0.18	243	6.41	0.33	0.46	0.89	0.26
VT21	131	141	2.11	4.08	852	8.10	5.61	0.18	243	6.41	0.33	0.46	0.89	0.26
VT22	131	141	2.11	4.08	852	8.10	5.61	0.18	243	6.41	0.33	0.46	0.89	0.26
VT23	131	141	2.11	4.08	852	8.10	5.61	0.18	243	6.41	0.33	0.46	0.89	0.26
VT24	131	141	2.11	4.08	852	8.10	5.61	0.18	243	6.41	0.33	0.46	0.89	0.26
VT25	131	141	2.11	4.08	852	8.10	5.61	0.18	243	6.41	0.33	0.46	0.89	0.26
VT26	131	141	2.11	4.08	852	8.10	5.61	0.18	243	6.41	0.33	0.46	0.89	0.26
VT27	131	141	2.11	4.08	852	8.10	5.61	0.18	243	6.41	0.33	0.46	0.89	0.26
VT28	131	141	2.11	4.08	852	8.10	5.61	0.18	243	6.41	0.33	0.46	0.89	0.26
VT29	131	141	2.11	4.08	852	8.10	5.61	0.18	243	6.41	0.33	0.46	0.89	0.26
VT30	131	141	2.11	4.08	852	8.10	5.61	0.18	243	6.41	0.33	0.46	0.89	0.26
VT31	131	141	2.11	4.08	852	8.10	5.61	0.18	243	6.41	0.33	0.46	0.89	0.26
VT32	131	141	2.11	4.08	852	8.10	5.61	0.18	243	6.41	0.33	0.46	0.89	0.26
VT33	131	141	2.11	4.08	852	8.10	5.61	0.18	243	6.41	0.33	0.46	0.89	0.26
VT34	131	141	2.11	4.08	852	8.10	5.61	0.18	243	6.41	0.33	0.46	0.89	0.26
VT35	131	141	2.11	4.08	852	8.10	5.61	0.18	243	6.41	0.33	0.46	0.89	0.26
VT36	131	141	2.11	4.08	852	8.10	5.61	0.18	243	6.41	0.33	0.46	0.89	0.26
VT37	131	141	2.11	4.08	852	8.10	5.61	0.18	243	6.41	0.33	0.46	0.89	0.26
VT38	131	141	2.11	4.08	852	8.10	5.61	0.18	243	6.41	0.33	0.46	0.89	0.26
VT39	131	141	2.11	4.08	852	8.10	5.61	0.18	243	6.41	0.33	0.46	0.89	0.26
VT40	131	141	2.11	4.08	852	8.10	5.61	0.18	243	6.41	0.33	0.46	0.89	0.26
VT41	131	141	2.11	4.08	852	8.10	5.61	0.18	243	6.41	0.33	0.46	0.89	0.26
VT42	131	141	2.11	4.08	852	8.10	5.61	0.18	243	6.41	0.33	0.46	0.89	0.26
VT43	131	141	2.11	4.08	852	8.10	5.61	0.18	243	6.41	0.33	0.46	0.89	0.26
VT44	131	141	2.11	4.08	852	8.10	5.61	0.18	243	6.41	0.33	0.46	0.89	0.26
VT45	131	141	2.11	4.08	852	8.10	5.61	0.18	243	6.41	0.33	0.46	0.89	0.26
VT46	131	141	2.11	4.08	852	8.10	5.61	0.18	243	6.41	0.33	0.46	0.89	0.26
VT47	131	141	2.11	4.08	852	8.10	5.61	0.18	243	6.41	0.33	0.46	0.89	0.26
VT48	131	141	2.11	4.08	852	8.10	5.61	0.18	243	6.41	0.33	0.46	0.89	0.26
VT49	131	141	2.11	4.08	852	8.10	5.61	0.18	243	6.41	0.33	0.46	0.89	0.26
VT50	131	141	2.11	4.08	852	8.10	5.61	0.18	243	6.41	0.33	0.46	0.89	0.26
VT51	131	141	2.11	4.08	852	8.10	5.61	0.18	243	6.41	0.33	0.46	0.89	0.26
VT52	131	141	2.11	4.08	852	8.10	5.61	0.18	243	6.41	0.33	0.46	0.89	0.26
VT53	131	141	2.11	4.08	852	8.10	5.61	0.18	243	6.41	0.33	0.46	0.89	0.26
VT54	131	141	2.11	4.08	852	8.10	5.61	0.18	243	6.41	0.33	0.46	0.89	0.26
VT55	131	141	2.11	4.08	852	8.10	5.61	0.18	243	6.41	0.33	0.46	0.89	0.26
VT56	131	141	2.11	4.08	852	8.10	5.61	0.18	243	6.41	0.33	0.46	0.89	0.26
VT57	131	141	2.11	4.08	852	8.10	5.61	0.18	243	6.41	0.33	0.46	0.89	0.26
VT58	131	141	2.11	4.08	852	8.10	5.61	0.18	243	6.41	0.33	0.46	0.89	0.26
VT59	131	141	2.11	4.08	852	8.10	5.61	0.18	243	6.41	0.33	0.46	0.89	0.26
VT60	131	141	2.11	4.08	852	8.10	5.61	0.18	243	6.41	0.33	0.46	0.89	0.26
VT61	131	141	2.11	4.08	852	8.10	5.61	0.18	243	6.41	0.33	0.46	0.89	0.26
VT62	131	141	2.11	4.08	852	8.10	5.61	0.18	243	6.41	0.33	0.46	0.89	0.26
VT63	131	141	2.11	4.08	852	8.10	5.61	0.18	243	6.41	0.33	0.46	0.89	0.26
VT64	131	141	2.11	4.08	852	8.10	5.61	0.18	243	6.41	0.33	0.46	0.89	0.26
VT65	131	141	2.11	4.08	852	8.10	5.61	0.18	243	6.41	0.33	0.46	0.89	0.26
VT66	131	141	2.11	4.08	852	8.10	5.61	0.18	243	6.41	0.33	0.46	0.89	0.26
VT67	131	141	2.11	4.08	852	8.10	5.61	0.18	243	6.41	0.33	0.46	0.89	0.26
VT68	131	141	2.11	4.08	852	8.10	5.61	0.18	243	6.41	0.33	0.46	0.89	0.26
VT69	131	141	2.11	4.08	852	8.10	5.61	0.18	243	6.41	0.33	0.46	0.89	0.26
VT70	131	141	2.11	4.08	852	8.10	5.61	0.18	243	6.41	0.33	0.46	0.89	0.26
VT71	131	141	2.11	4.08	852	8.10	5.61	0.18	243	6.41	0.33	0.46	0.89	0.26
VT72	131	141	2.11	4.08	852	8.10	5.61	0.18	243	6.41	0.33	0.46	0.89	0.26
VT73	131	141	2.11	4.08	852	8.10	5.61	0.18	243	6.41	0.33	0.46	0.89	0.26
VT74	131	141	2.11	4.08	852	8.10	5.61	0.18	243	6.41	0.33	0.46	0.89	0.26
VT75	131	141	2.11	4.08	852	8.10	5.61	0.18	243	6.41	0.33	0.46	0.89	0.26
VT76	131	141	2.11	4.08	852	8.10	5.61	0.18	243	6.41	0.33	0.46	0.89	0.26
VT77	131	141	2.11	4.08	852	8.10	5.61	0.18	243	6.41	0.33	0.46	0.89	0.26
VT78	131	141	2.11	4.08	852	8.10	5.61	0.18	243	6.41	0.33	0.46	0.89	0.26
VT79	131	141	2.11	4.08	852	8.10	5.61	0.18	243	6.41	0.33	0.46	0.89	0.26
VT80	131	141	2.11	4.08	852	8.10	5.61	0.18	243	6.41	0.33	0.46	0.89	0.26
VT81	131	141	2.11	4.08	852	8.10	5.61	0.18	243	6.41	0.33	0.46	0.89	0.26
VT82	131	141	2.11	4.08	852	8.10	5.61	0.18	243	6.41	0.33	0.46	0.89	0.26
VT83	131	141	2.11	4.08	852	8.10	5.61	0.18	243	6.41	0.33	0.46	0.89	0.26
VT84	131	141	2.11	4.08	852	8.10	5.61	0.18	243	6.41	0.33	0.46	0.89	0.26
VT85	131	141	2.11	4.08	852	8.10	5.61	0.18	243	6.41	0.33	0.46	0.89	0.26
VT86	131	141	2.11	4.08	852	8.10	5.61	0.18	243	6.41	0.33	0.46	0.89	0.26
VT87	131	141	2.11	4.08	852	8.10	5.61	0.18	243	6.41	0.33	0.46	0.89	0.26
VT88	131	141	2.11	4.08	852	8.10	5.61	0.18	243	6.41	0.33	0.46	0.89	0.26
VT89	131	141	2.11	4.08	852	8.10	5.61	0.18	243	6.41	0.33	0.46	0.89	0.26
VT90	131	141	2.11	4.08	852	8.10	5.61	0.18	243	6.41	0.33	0.46	0.89	0.26
VT91	131	141	2.11	4.08	852	8.10	5.61	0.18	243	6.41	0.33	0.46	0.89	0.26
VT92	131	141	2.11	4.08	852	8.10	5.61	0.18	243	6.41	0.33	0.46	0.89	0.26
VT93	131	141	2.11	4.08	852	8.10	5.61	0.18	243	6.41	0.33	0.46	0.89	0.26
VT94	131	141	2.11	4.08	852	8.10	5.61	0.18	243	6.41	0.33	0.46	0.89	0.26
VT95	131	141	2.11	4.08	852	8.10	5.61	0.18	243	6.41	0.33	0.46	0.89	0.26
VT96	131	141	2.11	4.08	852	8.10	5.61	0.18	243	6.41	0.33	0.46	0.89	0.26
VT97	131	141	2.11	4.08	852	8.10	5.61	0.18	243	6.41	0.33	0.46	0.89	0.26
VT98	131	141	2.11	4.08	852	8.10	5.61	0.18	243	6.41	0.33	0.46	0.89	0.26
VT99	131	141	2.11	4.08	852	8.10	5.61	0.18	243	6.41	0.33	0.46	0.89	0.26
VT100	131	141	2.11	4.08	852	8.10	5.61	0.18	243	6.41	0.33	0.46	0.89	0.26

Except were stated values given in ppm

TABLE 4.1 (contd.)

Sample	Rb	Sr	Ba	Rb/Sr	Rb/Ba	Th	U	Th/Sr	Y/Nb	Ba/Nb	Th/U	K/U^{a}	K/Th^{a}	K/Rb
XZ61	104	81	1,11	2,80	800	13,11	0,62	0,39	108	7,300	21,75	5,65	0,29	1,44
YZ62	103	311	1,14	0,85	734	3,79	0,69	0,35	182	17,51	5,50	1,82	0,27	2,11
XZ111	110	159	1,98	0,48	1225	9,87	0,93	0,81	445	12,37	10,84	10,58	0,51	1,08
YZ120	83	280	2,30	0,11	1240	1,83	3,21	0,13	541	15,11	10,45	14,19	0,68	1,00
XZ126	61	110	4,10	2,18	1744	1,28	0,58	0,12	1411	42,54	11,20	45,44	0,32	1,41
YZ133	143	138	1,41	1,04	450	11,21	3,29	0,87	60	9,15	3,41	0,48	0,14	0,47
XZ138	106	134	1,20	3,49	1811	7,84	0,61	0,51	774	10,84	12,86	0,18	0,59	0,70
YZ141	64	184	1,41	0,36	1,11	0,28	1,14	0,19	188	21,11	0,25	11,94	10,24	0,004
XZ151	102	134	1,20	0,76	1107	22,13	0,93	0,17	154	28,93	8,21	0,21	0,21	0,59
YZ154	32	131	1,82	0,23	1,11	0,11	0,11	0,01	188	0,00	21,11	27,41	1,23	0,22
XZ160	101	110	1,00	0,92	1,1	0,82	0,11	0,01	1,11	0,11	0,00	0,00	1,07	0,11
YZ161	44	131	1,01	0,11	1,11	0,11	0,11	0,11	127	11,11	0,00	15,11	0,68	10,42
XZ168	80	111	1,00	1,01	1,1	0,11	0,00	0,00	1,11	0,11	0,00	10,00	1,04	1,00
YZ169	71	101	1,00	0,11	1,11	0,11	0,11	0,11	441	57,00	0,00	8,41	0,11	1,64
XZ170	111	111	1,00	1,00	1,11	0,11	0,11	0,11	1,11	0,11	0,00	0,00	0,11	1,12
YZ171	111	111	1,00	0,11	1,11	10,11	0,11	0,11	464	11,00	10,11	28,87	0,25	1,01
XZ172	111	111	1,00	0,11	1,11	0,11	0,11	0,11	1,11	0,11	0,00	0,00	0,19	0,83
YZ173	111	111	1,00	0,11	1,11	0,11	0,11	0,11	1,11	0,11	0,00	0,00	0,11	0,00
XZ174	111	111	1,00	0,11	1,11	0,11	0,11	0,11	1,11	0,11	0,00	0,00	0,11	0,00
YZ175	111	111	1,00	0,11	1,11	0,11	0,11	0,11	1,11	0,11	0,00	0,00	0,11	0,00
XZ176	111	111	1,00	0,11	1,11	0,11	0,11	0,11	1,11	0,11	0,00	0,00	0,11	0,00
YZ177	111	111	1,00	0,11	1,11	0,11	0,11	0,11	1,11	0,11	0,00	0,00	0,11	0,00
XZ178	111	111	1,00	0,11	1,11	0,11	0,11	0,11	1,11	0,11	0,00	0,00	0,11	0,00
YZ179	111	111	1,00	0,11	1,11	0,11	0,11	0,11	1,11	0,11	0,00	0,00	0,11	0,00
XZ180	111	111	1,00	0,11	1,11	0,11	0,11	0,11	1,11	0,11	0,00	0,00	0,11	0,00

Values were rounded before given to 2DP.

^{a} $\times 10^{4}$

TABLE 4.1 Contd.

VI66													
VI6-													
VI62													
VI60													
VI39													
VI9A													
VI8													
VI													
VI3													
VI5													
VI52													
VI5													
VI5-													
VI5													
VI5													
VI5

TABLE 4.1 Contd.

Sample	Rb	Sr	K2	Ba	Ti	Th	V	Rb/Sr	K/Rb	Ba/Sr	Th/U	K/U*		Th/Ba
[illegible]1	[illegible]	[illegible]	3.21	[illegible]	950	[illegible]	0.[illegible]	0.12	[illegible]03	[illegible]	12.82	11.50	0.9[illegible]	[illegible].99
[illegible]439	[illegible]	[illegible]	4.[illegible]	[illegible]	1226	4.[illegible]5	0.[illegible]	0.[illegible]9	48[illegible]	[illegible].[illegible]	38.64	[illegible]45.[illegible]	[illegible].[illegible]	[illegible].48
[illegible]393	[illegible]	[illegible]	[illegible].[illegible]9	[illegible].[illegible]7	[illegible]	[illegible].[illegible]	0.[illegible]	0.[illegible]0	[illegible]05	[illegible].[illegible]	[illegible].[illegible]8	8.[illegible]	[illegible].[illegible]2	[illegible].[illegible]
[illegible]1-60	[illegible]	[illegible]	1.[illegible]1	[illegible].[illegible]6	[illegible]	[illegible].[illegible]4	0.[illegible]	0.[illegible]1	[illegible]13	[illegible].[illegible]4	[illegible].[illegible]6	[illegible].[illegible]2	1.[illegible]4	[illegible].[illegible]9
[illegible]-[illegible]2	[illegible]	[illegible]	1.[illegible]8	[illegible].[illegible]6	[illegible]	[illegible]3[illegible]	0.[illegible]3	[illegible].[illegible]0	[illegible]98[illegible]	[illegible].[illegible]8	2.[illegible]2	[illegible].[illegible]8	[illegible].[illegible]6	[illegible].[illegible]1
[illegible].[illegible]5	[illegible]3[illegible]	[illegible]	[illegible]—	[illegible]	[illegible]	[illegible].[illegible]7	0.[illegible]1	[illegible].[illegible]9	—	[illegible].[illegible]1	8.[illegible]3	-	-	-
[illegible]3[illegible]3	[illegible]2	[illegible]6[illegible]	[illegible].[illegible]2	[illegible].[illegible]0	[illegible]81	[illegible].[illegible]5[illegible]	0.[illegible]2[illegible]	[illegible].[illegible]3[illegible]	[illegible]9[illegible]	[illegible]06[illegible]	[illegible].[illegible]1	[illegible].[illegible]8[illegible]	[illegible].[illegible]9	[illegible].[illegible]4[illegible]
[illegible]3[illegible]2[illegible]	[illegible]3[illegible]	[illegible].[illegible]3	[illegible].[illegible]8[illegible]	[illegible].[illegible]1[illegible]	[illegible]3[illegible]	[illegible].[illegible]5[illegible]	0.[illegible]3[illegible]	[illegible].[illegible]2[illegible]	[illegible]9[illegible]	[illegible].[illegible]2[illegible]	[illegible].[illegible]3[illegible]	[illegible].[illegible]5[illegible]	[illegible].[illegible]29	[illegible].[illegible]3[illegible]
[illegible]81	[illegible]9[illegible]	[illegible].[illegible]3	[illegible].[illegible]3[illegible]	[illegible]886	[illegible].[illegible]3	[illegible].[illegible]2[illegible]	[illegible].[illegible]3[illegible]	[illegible].[illegible]3[illegible]	[illegible]81[illegible]	[illegible].[illegible]2[illegible]	18.18	17.[illegible]	[illegible].[illegible]2[illegible]	[illegible].[illegible]2[illegible]
[illegible]82	[illegible]7[illegible]	[illegible]4[illegible]	[illegible].[illegible]3[illegible]	[illegible].[illegible]4[illegible]	9[illegible]0	[illegible].[illegible]3[illegible]	[illegible].[illegible]3[illegible]	[illegible].[illegible]3[illegible]	[illegible]7[illegible]	[illegible].[illegible]2[illegible]	[illegible].[illegible]4[illegible]	14.[illegible]2[illegible]	[illegible].99	[illegible].88
[illegible]83	[illegible]0[illegible]	[illegible].[illegible]3	[illegible].[illegible]3[illegible]	[illegible].[illegible]3[illegible]	[illegible]9[illegible]	[illegible].[illegible]3[illegible]	[illegible].[illegible]3[illegible]	[illegible].[illegible]3[illegible]	[illegible]1[illegible]9	[illegible].[illegible]2[illegible]	[illegible].[illegible]3[illegible]	15.[illegible]	[illegible].[illegible]5[illegible]	[illegible].[illegible]86
[illegible]84	[illegible]8[illegible]	[illegible]3[illegible]	[illegible].[illegible]2[illegible]	[illegible].[illegible]3[illegible]	[illegible]9[illegible]	[illegible].[illegible]3[illegible]	[illegible].[illegible]3[illegible]	[illegible].[illegible]3[illegible]	[illegible]1[illegible]	[illegible].[illegible]3[illegible]	[illegible].[illegible]4[illegible]	[illegible]4[illegible]	[illegible].[illegible]4	[illegible].[illegible]9
[illegible]85	[illegible]1[illegible]	[illegible]2[illegible]	[illegible].[illegible]1[illegible]	[illegible].[illegible]2[illegible]	[illegible]8[illegible]	[illegible].[illegible]3[illegible]	[illegible].[illegible]3[illegible]	[illegible].[illegible]3[illegible]	[illegible]49	[illegible].[illegible]3[illegible]	[illegible].[illegible]3[illegible]	[illegible].[illegible]5[illegible]	[illegible].[illegible]4	[illegible].[illegible]3[illegible]
[illegible]86	[illegible]7[illegible]	[illegible]1[illegible]	[illegible].[illegible]3[illegible]	[illegible].[illegible]3[illegible]	[illegible]8[illegible]	[illegible].[illegible]3[illegible]	[illegible].[illegible]3[illegible]	[illegible].[illegible]3[illegible]	[illegible]96	[illegible].[illegible]3[illegible]	[illegible].[illegible]3[illegible]	8.9[illegible]	[illegible].[illegible]8	[illegible].92
[illegible]87	[illegible]1[illegible]	[illegible]2[illegible]	[illegible].[illegible]3[illegible]	[illegible].[illegible]3[illegible]	[illegible]9[illegible]	[illegible].[illegible]3[illegible]	[illegible].[illegible]3[illegible]	[illegible].[illegible]3[illegible]	[illegible]9[illegible]	[illegible].[illegible]3[illegible]	[illegible].[illegible]3[illegible]	[illegible].[illegible]3[illegible]	[illegible].[illegible]3[illegible]	[illegible].[illegible]8
[illegible]88	[illegible]1[illegible]	[illegible]2[illegible]	[illegible].[illegible]3[illegible]	[illegible].[illegible]3[illegible]	[illegible]9[illegible]	[illegible].[illegible]3[illegible]	[illegible].[illegible]3[illegible]	[illegible].[illegible]3[illegible]	[illegible]9[illegible]	[illegible].[illegible]3[illegible]	[illegible].[illegible]3[illegible]	[illegible].[illegible]3[illegible]	[illegible].[illegible]3[illegible]	[illegible].[illegible]68
[illegible]89	[illegible]1[illegible]	[illegible]1[illegible]	[illegible].[illegible]3[illegible]	[illegible].[illegible]3[illegible]	[illegible]9[illegible]	[illegible].[illegible]3[illegible]	[illegible].[illegible]3[illegible]	[illegible].[illegible]3[illegible]	[illegible]9[illegible]	[illegible].[illegible]3[illegible]	[illegible].[illegible]3[illegible]	7.[illegible]	[illegible].[illegible]3[illegible]	[illegible].[illegible]8
[illegible]90	[illegible]2[illegible]	[illegible]1[illegible]	[illegible].[illegible]3[illegible]	[illegible].[illegible]3[illegible]	[illegible]9[illegible]	9.[illegible]6	[illegible].[illegible]3[illegible]	[illegible].[illegible]3[illegible]	[illegible]1[illegible]	[illegible].[illegible]3[illegible]	[illegible].[illegible]3[illegible]	4.7[illegible]	[illegible].[illegible]3[illegible]	0.98
[illegible]91	[illegible]1[illegible]	[illegible]2[illegible]	[illegible].[illegible]3[illegible]	[illegible].[illegible]3[illegible]	8.[illegible]	11.09	0.[illegible]3	[illegible].[illegible]3[illegible]	[illegible]68	[illegible].[illegible]3[illegible]	[illegible].[illegible]3[illegible]	6.[illegible]8	0.[illegible]3	1.12
[illegible]91[illegible]	[illegible]6[illegible]	[illegible]1[illegible]	[illegible].[illegible]3[illegible]	[illegible].[illegible]3[illegible]	[illegible]1[illegible]	[illegible].[illegible]3[illegible]	[illegible].[illegible]3[illegible]	[illegible].[illegible]3[illegible]	[illegible]8[illegible]	[illegible].[illegible]3[illegible]	[illegible].[illegible]3[illegible]	9.76	[illegible].2[illegible]	[illegible].[illegible]4
[illegible]92[illegible]	[illegible]3[illegible]	[illegible]2[illegible]	[illegible].00	[illegible].[illegible]3[illegible]	6[illegible]9	[illegible].54	0.[illegible]1	0.[illegible]8	[illegible]3[illegible]	[illegible].[illegible]3[illegible]	[illegible].[illegible]3[illegible]	[illegible]6.[illegible]	7.[illegible]	[illegible].27
[illegible]92[illegible]	[illegible]9[illegible]	[illegible]430	[illegible].91	[illegible].[illegible]3[illegible]	[illegible]8[illegible]	[illegible].[illegible]3[illegible]	0.[illegible]3[illegible]	[illegible].[illegible]3[illegible]	19[illegible]	[illegible].[illegible]3[illegible]	1.8[illegible]	[illegible].[illegible]3[illegible]	7.8[illegible]	1.[illegible]8
[illegible]93[illegible]	[illegible]1[illegible]	[illegible]10	0.90	[illegible].89	[illegible].29	[illegible].[illegible]4	[illegible].[illegible]1	0.[illegible]2	[illegible].[illegible]3[illegible]	[illegible].[illegible]3[illegible]	8.[illegible]6	2.6[illegible]	0.[illegible]1	0.[illegible]3
[illegible]94[illegible]	[illegible]3[illegible]	[illegible]71	3.59	2.77	[illegible]2[illegible]	[illegible]6.86	[illegible].[illegible]8[illegible]	[illegible].[illegible]3[illegible]	[illegible]93[illegible]	[illegible].[illegible]3[illegible]	9.19	1.[illegible]8	0.[illegible]1	[illegible].[illegible]3[illegible]
[illegible]95[illegible]	[illegible]1[illegible]	[illegible]1[illegible]	0.29	1.9[illegible]	[illegible]1[illegible]	[illegible].[illegible]3[illegible]	0.[illegible]8	[illegible].[illegible]3[illegible]	86[illegible]	[illegible].[illegible]3[illegible]	[illegible].[illegible]3[illegible]	[illegible].6[illegible]	0.9[illegible]	[illegible].[illegible]1[illegible]
[illegible]96[illegible]	[illegible]8[illegible]	[illegible]2[illegible]	[illegible].[illegible]1[illegible]	[illegible].[illegible]4	88[illegible]	—	—	[illegible].[illegible]20	469	[illegible].[illegible]3[illegible]	—	—	—	[illegible].[illegible]3[illegible]
[illegible]97[illegible]	[illegible]1[illegible]	[illegible]2[illegible]	[illegible].[illegible]3[illegible]	[illegible].[illegible]3[illegible]	9[illegible]1	[illegible].[illegible]1	0.[illegible]1	0.30	4[illegible]6	[illegible].[illegible]2[illegible]	[illegible].[illegible]3[illegible]	[illegible].38	0.40	[illegible].[illegible]8
[illegible]98[illegible]	[illegible]1[illegible]	[illegible]1[illegible]	[illegible].81	[illegible].[illegible]3[illegible]	24[illegible]	[illegible].[illegible]3[illegible]	0.59	1.[illegible]1	[illegible]49	[illegible].[illegible]3[illegible]	[illegible].[illegible]3[illegible]	8.[illegible]4	0.[illegible]3	[illegible].[illegible]3[illegible]

Except where stated values given in ppm

* x [illegible]$^{-4}$

TABLE 4.7 CONTD.

Sample	Be	Sc	Ni	Cu	Zn	Ga	As (ppm)	Rb/Sr	Ba/Sr	Th/U	Zr/Hf^{*}	Nb/Ta	Ta/Yb
KR31	1.21	19.1	3.44	1.08	98.4	111.8	17.43	11.49	0.11	1.14	38.20	8.84	0.17	1.24
KR34	1.11	4.00	1.08	1.14	4.0	11.20	4.21	0.47	0.4	0.11	33.60	17.24	0.10	0.07
KR35	1.00	1.11	0.27	0.14	0.1	18.30	1.14	1.31	0.14	0.11	34.10	7.31	0.15	0.04
KR36	1.11	1.17	0.44	0.13	0.16	28.11	1.24	0.81	0.11	1.40	42.14	5.00	0.12	0.03
KR37	1.07	0.1	0.05	0.19	0.1	16.12	0.9	0.44	0.01	0.10	9.10	2.71	0.13	0.04
KR38	1.1	0.01	0.11	0.11	0.1	0.11	0.9	0.04	0.11	0.07	8.44	0.91	0.11	0.03
KR39	1.04	0.04	0.07	0.11	0.07	0.11	0.04	0.1	0.01	0.01	0.11	0.01	0.11	0.04
KR40	1.1	0.1	0.11	0.11	0.1	0.11	0.11	0.01	0.01	0.01	0.11	0.01	0.11	0.11
KR41	1.11	0.11	0.11	0.11	0.11	0.11	0.11	0.11	0.11	0.11	0.11	0.11	0.11	0.11
KR42	1.11	0.11	0.11	0.11	0.11	0.11	0.11	0.11	0.11	0.11	0.11	0.11	0.11	0.11
KR43	1.11	0.11	0.11	0.11	0.11	0.11	0.11	0.11	0.11	0.11	0.11	0.11	0.11	0.11
KR44	1.11	0.11	0.11	0.11	0.11	0.11	0.11	0.11	0.11	0.11	0.11	0.11	0.11	0.11
KR45	1.11	0.11	0.11	0.11	0.11	0.11	0.11	0.11	0.11	0.11	0.11	0.11	0.11	0.11
KR46	1.11	0.11	0.11	0.11	0.11	0.11	0.11	0.11	0.11	0.11	0.11	0.11	0.11	0.11
KR47	1.11	0.11	0.11	0.11	0.11	0.11	0.11	0.11	0.11	0.11	0.11	0.11	0.11	0.11
KR48	1.11	0.11	0.11	0.11	0.11	0.11	0.11	0.11	0.11	0.11	0.11	0.11	0.11	0.11
KR49	1.11	0.11	0.11	0.11	0.11	0.11	0.11	0.11	0.11	0.11	0.11	0.11	0.11	0.11
KR50	1.11	0.11	0.11	0.11	0.11	0.11	0.11	0.11	0.11	0.11	0.11	0.11	0.11	0.11
KR51	1.11	0.11	0.11	0.11	0.11	0.11	0.11	0.11	0.11	0.11	0.11	0.11	0.11	0.11
KR52	1.11	0.11	0.11	0.11	0.11	0.11	0.11	0.11	0.11	0.11	0.11	0.11	0.11	0.11
KR53	1.11	0.11	0.11	0.11	0.11	0.11	0.11	0.11	0.11	0.11	0.11	0.11	0.11	0.11
KR54	1.11	0.11	0.11	0.11	0.11	0.11	0.11	0.11	0.11	0.11	0.11	0.11	0.11	0.11
KR55	1.11	0.11	0.11	0.11	0.11	0.11	0.11	0.11	0.11	0.11	0.11	0.11	0.11	0.11
KR56	1.11	0.11	0.11	0.11	0.11	0.11	0.11	0.11	0.11	0.11	0.11	0.11	0.11	0.11
KR57	1.11	0.11	0.11	0.11	0.11	0.11	0.11	0.11	0.11	0.11	0.11	0.11	0.11	0.11

Values were crustal values given in ppm

* $\times 10^{-4}$

TABLE 4.2 Major and Select Trace Elements : Traverse 1

	VT24	VT211	VT62	VT121	VT431	VT430	VT419	VT428	VT380	VT393	VT142	VT144
SiO_2*		75.56	74.47	74.92	72.40	74.19	74.66	67.51	74.10	74.79	73.84	73.10
Al_2O_3		13.27	14.01	14.08	14.26	14.00	14.29	18.95	15.22	13.48	14.45	14.03
Fe_2O_3		0.50	0.03	0.30	0.84	0.27	0.06	0.20	n.d.	0.33	n.d.	0.14
FeO		1.03	1.06	0.81	1.08	1.08	0.47	0.63	0.32	0.90	1.08	0.45
MgO		0.04	0.37	0.16	0.54	0.17	0.12	0.01	0.04	0.18	0.31	0.10
CaO		0.71	1.18	1.66	1.45	1.27	0.82	0.66	0.74	1.02	0.98	0.31
Na_2O		3.61	3.84	4.35	4.34	4.14	3.82	6.84	5.22	4.29	4.15	3.27
K_2O		5.39	4.00	3.77	3.59	3.78	5.09	5.19	4.39	3.75	4.35	7.42
Ti_2O		0.07	0.20	0.10	0.36	0.17	0.07	0.76	0.03	0.15	0.09	0.02
H_2O^+		0.46	0.55	0.51	0.37	0.39	0.50	1.37	0.22	0.59	0.41	0.36
Sb**	n.d.	n.d.	n.d.	n.d.	n.d.	n.d.	n.d.	n.d.	n.d.	n.d.	n.d.	n.d.
Tc	4.0	2.8	7.5	2.7	7.3	4.0	2.3	9.1	3.2	6.3	n.d.	5.0
Zr	157	55	155	84	201	157	47	23	34	109	117	38

* Values given in %

** Values given in ppm

TABLE 4.2 Contd.

	VT57	KK12	KK13	VT173	KK14	KK15	KK16	KK1	VT55	KK2	KK3	KK4
SiO_2*	74.98	72.71	72.70	74.58	74.20	68.68	75.13	67.86	73.40	75.07	73.04	72.33
Al_2O_3	13.54	14.46	15.28	13.48	14.37	14.21	13.59	15.74	14.24	14.01	14.88	14.01
Fe_2O_3	0.33	0.38	n.d.	n.d.	n.d.	1.00	n.d.	1.11	0.16	0.05	0.05	0.20
FeO	1.01	1.30	0.43	0.90	0.45	3.26	0.83	3.14	1.24	0.65	0.91	1.75
MnO	0.11	0.20	0.15	0.25	0.01	1.05	0.16	0.81	0.87	0.29	0.69	0.67
CaO	0.92	1.20	1.31	0.73	0.95	3.49	1.21	2.28	1.15	1.07	1.61	1.70
Na_2O	3.69	4.34	4.77	2.94	4.78	5.82	3.69	4.55	4.06	3.31	3.45	4.55
K_2O	4.47	4.09	4.15	5.92	4.16	1.04	4.13	3.80	4.97	4.40	3.25	3.46
TiO_2	0.13	0.26	0.06	0.10	0.13	0.57	0.08	1.02	0.16	0.09	0.16	0.09
H_2O^+	0.52	0.49	0.43	0.38	0.35	0.48	0.47	0.67	0.51	0.26	0.53	0.57
Nb**	n.d.	5.9	n.d.	1.5	n.d.	8.6	1.1	14.9	n.d.	n.d.	n.d.	3.9
Y**	3.4	6.5	2.1	3.5	3.1	17.9	3.2	10.1	3.9	2.3	4.0	6.4
Zr**	175	181	18	125	28	211	42	365	109	37	134	135

* Values given in %

** Values given in ppm

TABLE 4.2 Contd.

	KK5	KK6	VT53	KK7	KK8	VT52	KK9	KK10	KK11	KK20	KK21	VT67
SiO_2*	72.74	72.38	71.54	72.10	72.47	73.11	68.96	72.29	73.06	72.35	73.71	74.49
Al_2O_3	15.83	14.62	14.23	14.37	14.28	14.41	15.45	14.40	14.21	13.55	14.06	13.75
Fe_2O_3	0.06	0.14	0.17	0.07	0.01	n.d.	1.01	0.79	n.d.	0.16	0.02	n.d.
FeO	1.04	1.48	1.31	1.43	1.54	1.48	3.04	0.78	1.20	1.58	1.19	1.16
MgO	0.27	0.38	1.27	0.49	0.37	0.35	1.24	0.34	0.36	1.05	0.43	0.37
CaO	1.32	1.49	1.42	1.36	1.38	1.22	3.05	1.65	1.37	0.55	0.88	1.18
Na_2O	4.05	4.55	4.55	4.69	4.43	4.78	4.64	4.39	4.78	3.29	4.19	3.84
K_2O	3.90	3.46	3.81	3.75	3.75	3.40	2.08	3.25	3.09	5.89	4.07	4.00
TiO_2	0.11	0.24	0.19	0.20	0.29	0.26	0.57	0.30	0.20	0.23	0.19	0.22
H_2O^+	0.49	0.54	0.63	0.66	0.74	0.73	0.97	0.79	0.68	0.68	0.73	0.65
Nb**	n.d.	7.1	5.0	8.6	11.0	8.0	8.7	8.3	5.3	2.0	3.5	3.0
Yt	5.3	8.1	7.6	14.3	21.2	22.4	10.7	10.9	7.4	7.9	7.3	9.9
Zr	134	110	113	181	172	151	299	188	117		97	102

* Values given in %

** Values given in ppm

TABLE 4.3

Major and Select Trace Elements : Traverse 2

	VT64	VT523	VT524	VT68	VT128	VT402	VT460	VT127	VT132	KK53	KK54	KK40	KK41
SiO_2*	74.09	37.38	66.30	71.09	69.60	52.33	66.37	73.00	69.15	73.32	74.98	71.48	70.96
Al_2O_3	14.03	4.86	14.82	14.58	14.26	14.88	15.61	14.11	15.36	14.92	14.05	15.46	14.96
Fe_2O_3	0.23	28.19	0.92	0.12	0.89	4.27	1.44	0.18	1.22	0.08	0.19	0.14	0.19
FeO	0.96	22.22	4.96	1.45	2.10	6.95	2.44	0.79	1.55	1.04	0.61	1.52	1.65
MgO	0.30	2.86	3.50	0.83	0.81	5.30	1.98	0.91	0.66	0.37	0.15	0.56	1.18
CaO	1.03	1.29	1.67	1.66	1.58	9.07	3.46	0.26	2.20	1.31	0.75	3.03	2.37
Na_2O	3.91	0.03	2.98	3.47	3.70	4.06	4.77	3.67	4.28	4.17	3.42	4.85	4.49
K_2O	4.59	0.31	2.21	4.72	4.83	0.83	1.69	5.28	3.79	4.18	5.32	1.33	2.64
TiO_2	0.12	0.21	0.29	0.21	0.61	0.93	0.56	0.07	0.35	0.13	0.04	0.29	0.35
H_2O^+	0.41	0.75	0.82	0.48	0.57	0.60	0.61	0.53	0.60	0.50	0.30	0.46	0.52
Sb**	2.8	11.9	8.7	7.3	33.2	7.3	12.1	2.5	5.3	1.5	3.0	3.7	1.5
Yt	7.1	18.3	28.8	5.6	19.0	20.4	14.7	5.3	4.7	2.5	1.7	2.8	2.1
Zr	161	43	128	174	485	79	169	100	217	126	104	175	153

* Values given in %

** Values given in ppm

TABLE 4.3 Contd.

	KK42	KK43	KK44	KK45	KK46	KK47	KK48	KK49	KK50	KK56	KK55	KK57	KK51	KK52
SiO_2*	74.35	66.85	71.55	73.40	68.12	67.38	74.06	73.09	70.73	70.94	71.85	74.37	71.48	72.16
Al_2O_3	14.06	16.87	14.78	14.95	15.73	16.07	14.76	14.63	15.23	14.07	14.51	13.87	14.94	14.73
Fe_2O_3	0.12	0.72	0.26	0.09	0.85	0.99	0.15	0.04	0.16	0.43	0.46	0.24	0.22	0.64
FeO	0.81	2.12	1.28	1.15	1.68	1.94	0.54	1.17	1.58	1.66	1.24	0.87	1.44	0.99
MgO	0.14	1.34	1.07	0.41	1.31	0.89	0.19	0.05	1.30	0.81	0.87	0.24	0.49	1.02
CaO	0.99	3.50	1.59	1.38	2.25	2.38	1.12	1.40	1.48	1.10	1.15	0.65	0.99	0.94
Na_2O	3.45	4.67	4.10	4.48	4.19	4.78	4.34	4.98	4.74	3.95	4.06	3.69	4.64	3.87
K_2O	5.28	2.93	4.01	3.45	3.62	3.25	4.02	3.18	3.23	5.13	4.87	5.09	4.61	4.50
TiO_2	0.10	0.32	0.24	0.18	0.50	0.61	0.18	0.16	0.27	0.28	0.16	0.11	0.23	0.31
H_2O^+	0.36	0.63	0.48	0.54	0.67	0.69	0.43	0.54	0.65	0.65	0.63	0.49	0.83	0.63
Nb**	1.1	5.6	5.3	4.0	5.1	4.8	2.0	4.9	14.9	8.8	7.9	4.6	5.4	15.5
Y	n.d.	6.6	6.6	4.2	6.7	7.2	6.1	5.7	12.3	15.7	12.1	2.7	6.9	17.7
Zr	96	239	113	125	252	243	53	124	156	312	190	68	143	243

* Values given in %

** Values given in ppm

TABLE 4.4 Major and Select Trace Elements : Traverse 1

	VT45	VT44	VT43	KK24	KK28	KK29	KK25	KK26	KK27	VT41	KK30	KK31	KK32	VT6
SiO_2*	74.69	-	73.47	-	74.04	-	72.84	72.01	75.04	75.38	72.94	72.26	73.42	-
Al_2O_3	13.45	-	14.73	-	13.76	-	13.69	14.56	13.55	14.44	13.56	14.76	14.44	-
Fe_2O_3	n.d.	-	n.d.	-	0.08	-	0.42	0.06	n.d.	n.d.	0.10	0.38	n.d.	-
FeO	0.44	-	1.19	-	1.26	-	1.60	1.71	1.00	0.84	1.45	1.18	0.97	-
MgO	0.01	-	0.40	-	0.27	-	0.38	0.50	0.28	0.44	0.32	0.47	0.28	-
CaO	0.17	-	1.41	-	0.83	-	0.71	1.34	1.16	0.99	0.95	0.97	1.28	-
Na_2O	2.99	-	4.85	-	3.73	-	3.03	4.21	4.19	3.49	3.68	3.81	4.33	-
K_2O	7.62	-	2.92	-	4.63	-	5.15	3.65	3.59	3.94	4.76	4.98	3.77	
TiO_2	0.04	-	0.15	-	0.18	-	0.14	0.28	0.09	0.11	0.24	0.20	0.15	
H_2O^+	0.18	0.37	0.50	0.40	0.45	0.45	0.59	0.57	0.46	0.49	0.60	0.43	0.38	0.41
Nb**	0.5	7.8	17.2	12.3	19.6	36.2	16.1	22.9	27.2	46.4	27.0	25.0	13.9	2.1
Yt	4.8	13.3	10.0	6.3	20.9	38.2	21.9	26.4	36.7	54.6	25.1	26.9	29.4	7.8
Zr	28	171	119	100	175	349	333	265	73	109	223	182	108	55

* Values given in %

** Values given in ppm

5 RADIOELEMENT PROFILE AND HEAT PRODUCTION

5.1 Introduction

Most of the existing knowledge on the variation of the radioelement content with depth comes from two indirect approaches.

Firstly, Lambert and Heier (1968, 1969) and Lambert (1971) found low concentrations of the radioelements in high pressure granulites compared to "normal" granites, which led to the conclusion that the crust in a Precambrian shield can be approximated by a radioactive-rich granitic layer overlying depleted granulite facies rock. Inferred profiles of the distribution of the radioelements with depth (Fig. 5.1) are presented by Lambert (1971). The distribution profiles are based on a statistical comparison of the radioelement concentrations from high pressure granulites of the Musgrave Range in south west Australia, to the abundances in more "normal" surface rocks of the South West Australian shield. The mean Archaean crustal abundances for the radioelements calculated from these profiles are estimated at 1.5% K, 1.1 ppm U and 4.5 ppm Th.

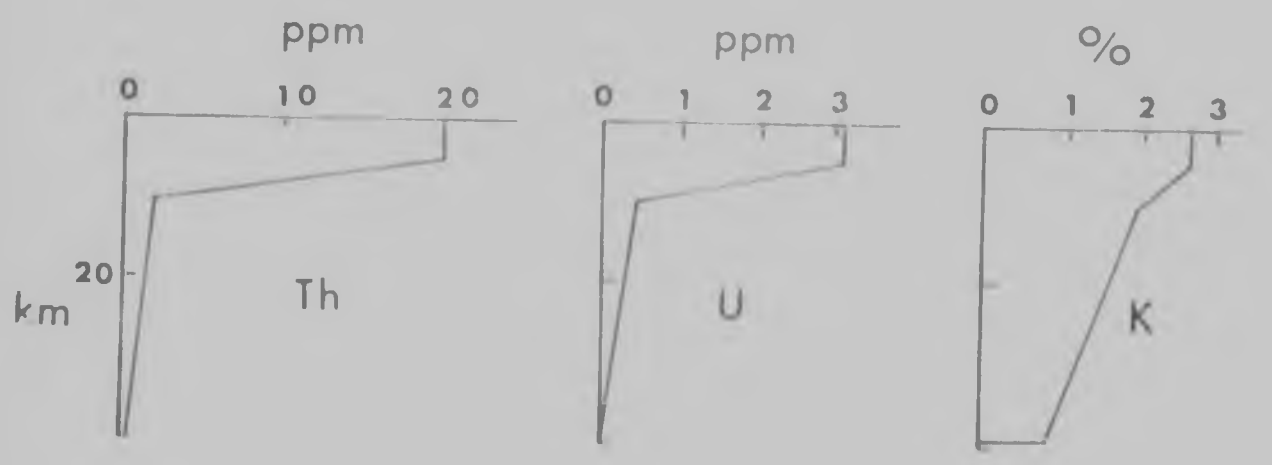


Fig. 5.1 Inferred radioelement profiles with depth (after Lambert 1971)

The second approach is based on the linear relationship, between the heat flow measured at the surface (Q), and the radioactive heat production of surface rocks (A)(Birch et al., 1968).

$$Q = q + bA \qquad (1)$$

The intercept value of the straight line (q) is the reduced heat flow from the base of the radioactive layer and (b) the slope of the line has dimensions of depth.

This made it possible to calculate models for radioelement concentration as a function of depth in the crust. It was found that a variety of models (for the depletion with depth) satisfied the linear relationship found by Birch, of which the step function, linear and exponential models are mathematically simplest (Lachenbruch, 1970). The step function of Roy et al., (1968) assumes that the continental crust is made up of a pile of one or more discrete layers with (A) constant to the depth given by the slope of the straight line. The heat flow from beneath the radioactive layer (q) remains constant throughout the region and the variable radioactivity of the upper crust generates the variable heat flow observed at the surface. This implies that the same erosional level is attained over large regions. Lachenbruch (1968, 1970) shows that an exponential dependence of heat production on depth, according to the relation:

$$A_z = A_o e^{-z/D}$$

(where A_o is the surface heat production, A_z is the heat production at a depth z, and $-\frac{1}{D}$ is the slope of the straight line formed by plotting $\ln A_z$ against Z) is needed for the correlation to hold for different erosional levels.

These indirect approaches must ultimately be superseded by direct measurements of radioelement concentrations in crustal profiles or borehold cores which extend deep into the continental crust. Published examples of direct measurements of radioelement concentration gradients in borehole cores, Lachenbruch and Bunker (1971), and from an exposed vertical

section of the Pennine basement in Austria, Hawkesworth (1974), suggest an exponential decrease in heat production with depth. The results however, were ambiguous, and it was not possible to distinguish an exponential model from, for example, a linear diminution of heat production with depth (Lachenbruch and Bunker, 1971; Hawkesworth, 1974). By comparing measured heat generation with estimated depths of emplacement for the Idaho batholith, Swanberg (1972) concludes that the data is incompatible with a constant depth heat source model, and that heat production appears to decrease exponentially with depth. A linear depth dependance model, however, is not ruled out by Swanberg.

5.2 Results from the Vredefort crustal profile

The profile of heat production with depth at Vredefort (Table 5.1), is calculated from the average radioelement profiles obtained in Chapter 4, (Table 4.5). The conversion factors for radioelement concentration to heat production are given in Table 5.2, after Birch (1954).*

TABLE 5.2 (after Birch 1954)

Element	Heat generation cal/cm^{3}sec x 10^{-13} per unit conc. of radioelement
Total U	0.232 x ℓ
Th	0.0634 x ℓ
K	0.086 x ℓ
	ℓ = density of rock: gm/cm^3

The variations in radioelement concentrations and heat production are shown in Figure 5.2. Heat production falls off regularly with depth over the upper 7 km of the Vredefort profile, and clearly the data are not consistent with a step function model.

*Footnote
Calculation on heat generation due to radioactive decay of the radioelements, where mass is converted to energy have not changed significantly over the last [illegible] years. (D. Mingay, Dept. of Nuclear Physics, Witwatersrand University, pers. comm.).

New parameters have been revised for publication by N.H. Gale.

Table 5.1 Averaged radioelement concentrations and heat production for the Vredefort basement (excl. S-W quad.).

Km	U (ppm)	Th (ppm)	K (%)	U (A)	Th (A)	K (A)	Combined (A)
1	0.88	15.50	3.60	0.55	2.60	0.82	3.97
2	0.88	13.62	3.68	0.55	2.29	0.78	3.62
3	0.65	11.53	3.32	0.41	1.93	0.75	3.09
4	0.59	10.16	3.19	0.37	1.71	0.72	2.80
5	0.41	9.05	3.10	0.26	1.52	0.73	2.51
6	0.29	8.24	3.20	0.18	1.38	0.75	2.31
7	0.22	7.42	3.28	0.14	1.23	0.74	2.13
8	0.23	7.18	3.32	0.14	1.21	0.76	2.11
9	0.54	8.36	3.29	0.34	1.57	0.75	2.66
10	0.58	9.12	3.57	0.36	1.53	0.79	2.66
11	0.52	8.80	3.41	0.32	1.48	0.77	2.57
12	0.32	7.80	3.60	0.20	1.31	0.82	2.33
13	0.33	6.56	3.18	0.20	1.10	0.72	2.03
14	0.29	7.31	3.86	0.18	1.23	0.87	2.28

A Cal./cm.^{3}sec. x 10^{-13}

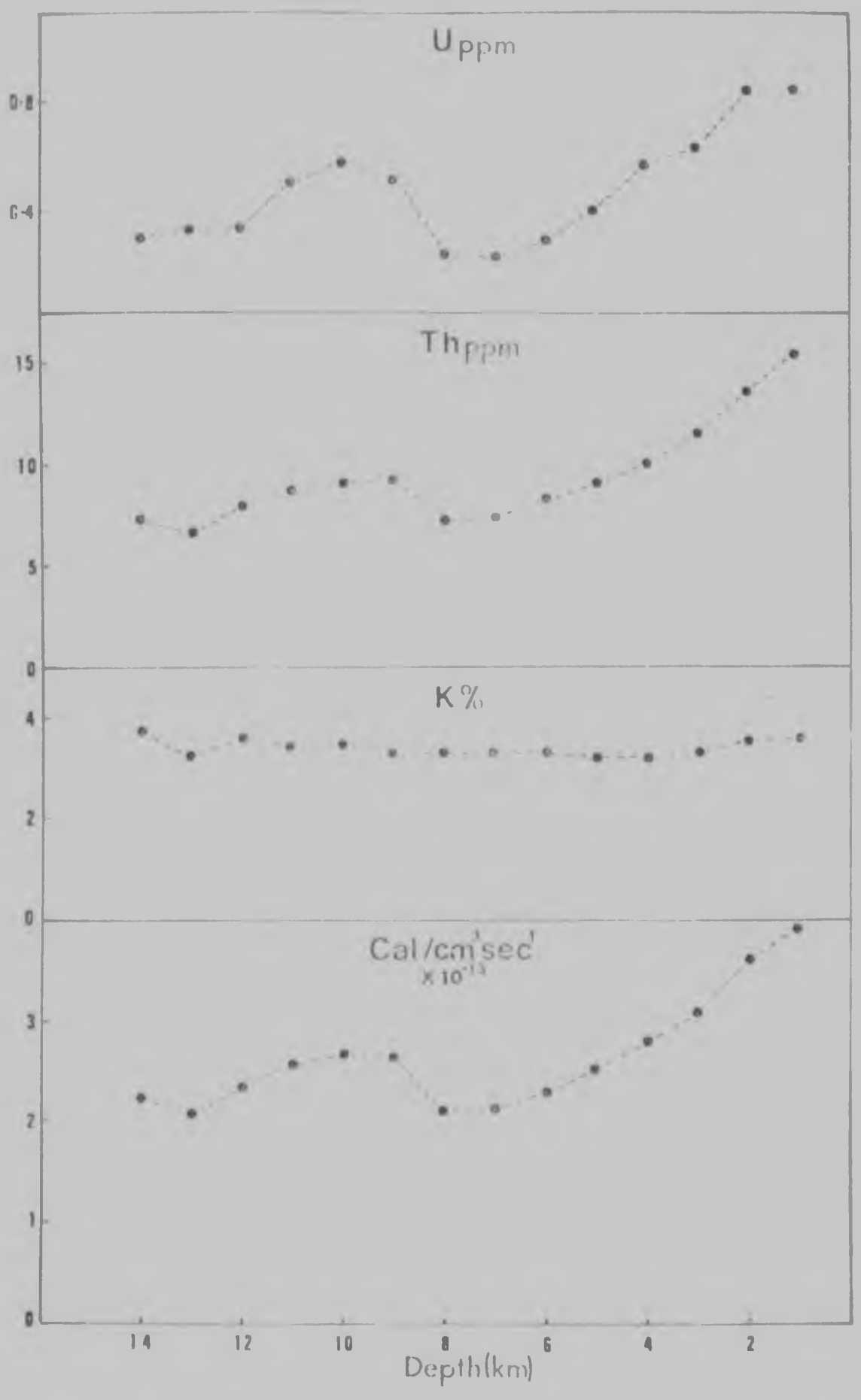


FIGURE 5.2 Average radioelement and heat production profiles for the Vredefort basement (excl. S-W quad.)

Whether or not an exponential decrease provides the best fit, for the Vredefort data has been tested by fitting a regression line to the data points for the upper 8 km of the profile for both a linear and an exponential function with depth (Figure 5.3). The degrees of fit, defined by the correlation co-efficient (r) are then compared. (r) can be calculated directly from the equation

$$r^2 = \frac{\left(\Sigma xy - \frac{\Sigma x \Sigma y}{n}\right)^2}{\left(\Sigma x^2 - \frac{(\Sigma x)^2}{n}\right)\left(\Sigma y^2 - \frac{(\Sigma y)^2}{n}\right)}$$

In general, if r = 1 all points (x_n, y_n) lie on the coincident line of regression and there is perfect correlation between x and y. Values of r around 0.5 indicate a fair amount of correlation whereas for r < 0.5 the correlation is weak. When r = 0 there is no correlation at all (Mack, 1966).

The correlation coefficients for the exponential and the linear functions are:

r = 0.989 (Exponential function)

r = 0.969 (Linear function)

A more meaningful comparison between the two curves is given by the "proportion of the variance unexplained" $(1 - r^2)$ which is 0.02 and 0.06 respectively (This procedure was recommended by D.M. Hawkins, Dept. of Applied Maths, University of the Witwatersrand, pers. comm.).

The slope of the best fit straight line (Fig. 5.3), which reflects the gradient or rate of fall off of heat production gives D = 9.3 ± 0.4 km. This value is very close to results obtained from heat flow measurements in the Baltic Shield (8,5 km) and Canadian Shield (7,5 km) respectively (Rao and Jessop, 1975).

Beneath the radioactive layer in the lower 7 km of the Vredefort profile, there are remarkable features that have not previously been

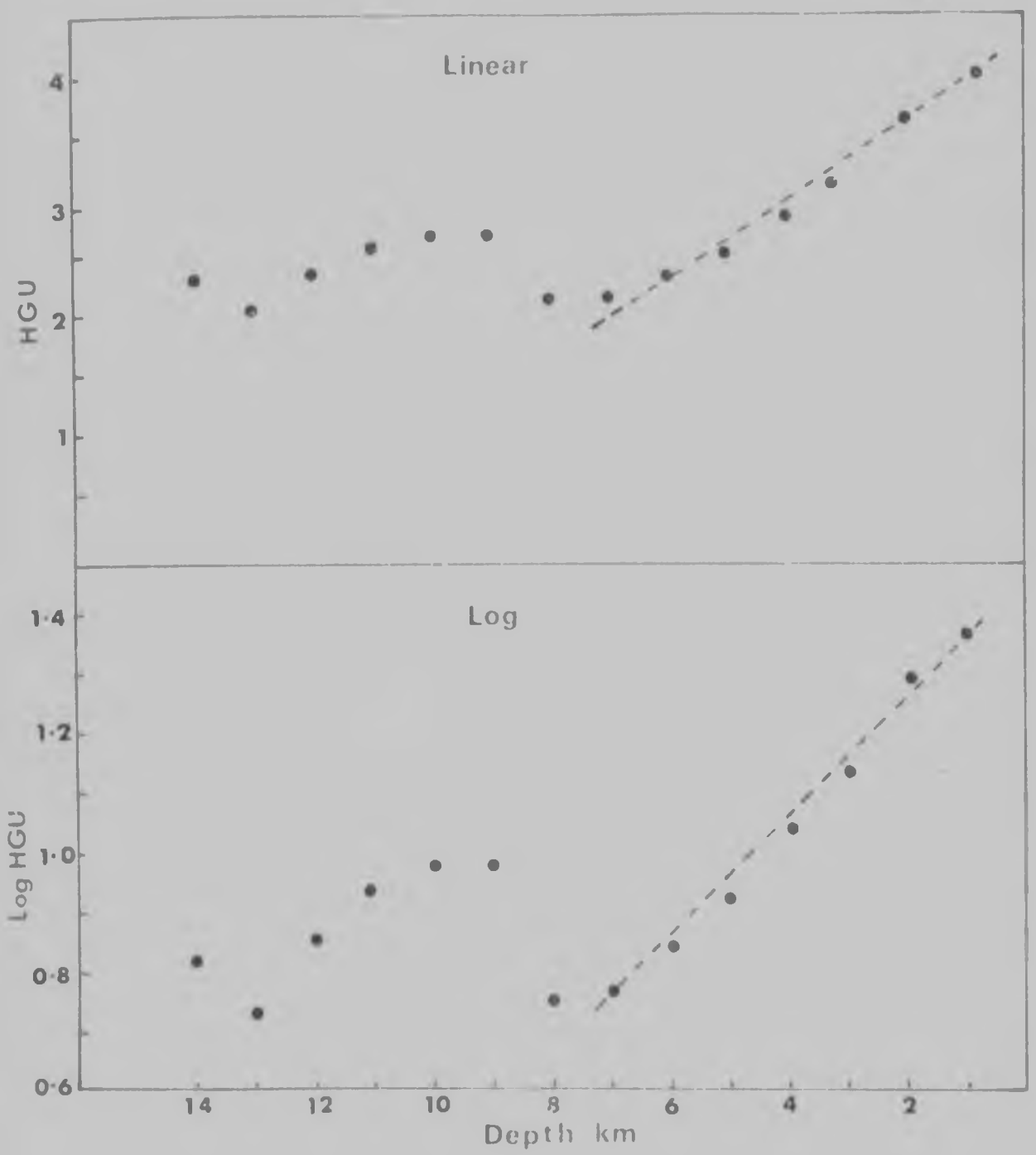


FIGURE 5.3 Comparison of the degree of fit between a linear and an exponential radioelement distribution funtion with depth in the Vredefort basement (excl. S-W quad.)

predicted by the models of Lambert and Heier and co-workers, or by the correlation between heat flow and heat production. Firstly, the average concentration of the radioelements in the lower 7 km of the Vredefort profile (U = 0.38 ppm, Th = 8.0 ppm and K = 3.43%) are not consistent with the values obtained by workers in the granulite terrains of central Australia and northern Norway (see Table 5.3, after Lambert and Heier, 1967 and Heier and Thoreson, 1970). Although U is in good agreement, both Th and K are relatively high.

TABLE 5.3 Average concentration of U, Th and K from granulites of the Musgrave range (South West Australia) and from North Norway

	Th ppm	U ppm	K%
Musgrave range[1]	2.1	0.4	2.0
North Norway[2]	5.1	0.5	2.5
Lower 7 km of Vredefort profile	8.0	0.38	3.43

(1) after Lambert and Heier (1967)

(2) after Heier and Thoreson (1970)

5.3 Th/U, K/U and K/Th profiles

The radial variation of Th/U, K/U and K/Th ratios from Vredefort averaged over all available data, are shown graphically in Figure 5.4. Qualitatively the variations for all three parameters are similar, and also show similarities with the K/Rb (Rb-K) profile discussed in the last chapter. The ratios increase from the margins inwards. This increase continues regularly inwards for 8 km, at which point there is a marked decrease in the three ratios. The "troughs" for the radioelement ratios in the lower half of the profiles are characteristic of certain trace and major element trends in the Vredefort basement. (The averaged K/Rb ratios, however, do not show any significant variations in the lower half of the profile) They effectively span an annular zone corresponding

predicted by the models of Lambert and Heier and co-workers, or by the correlation between heat flow and heat production. Firstly, the average concentration of the radioelements in the lower 7 km of the Vredefort profile (U = 0.38 ppm, Th = 8.0 ppm and K = 3.43%) are not consistent with the values obtained by workers in the granulite terrains of central Australia and northern Norway (see Table 5.3, after Lambert and Heier, 1967 and Heier and Thoreson, 1970). Although U is in good agreement, both Th and K are relatively high.

TABLE 5.3 Average concentration of U, Th and K from granulites of the Musgrave range (South West Australia) and from North Norway

	Th ppm	U ppm	K%
Musgrave range[1]	2.1	0.4	2.0
North Norway[2]	5.1	0.5	2.5
Lower 7 km of Vredefort profile	8.0	0.38	3.43

(1) after Lambert and Heier (1967)

(2) after Heier and Thoreson (1970)

5.3 Th/U, K/U and K/Th profiles

The radial variation of Th/U, K/U and K/Th ratios from Vredefort averaged over all available data, are shown graphically in Figure 5.4. Qualitatively the variations for all three parameters are similar, and also show similarities with the K/Rb (Figure 4.11) profile discussed in the last chapter. The ratios increase from the margins inwards. This increase continues regularly inwards for 8 km, at which point there is a marked decrease in the three ratios. The "troughs" for the radioelement ratios in the lower half of the profiles are characteristic of certain trace and major element trends in the Vredefort basement. (The averaged K/Rb ratios, however, do not show any significant variations in the lower half of the profile) They effectively span an annular zone corresponding

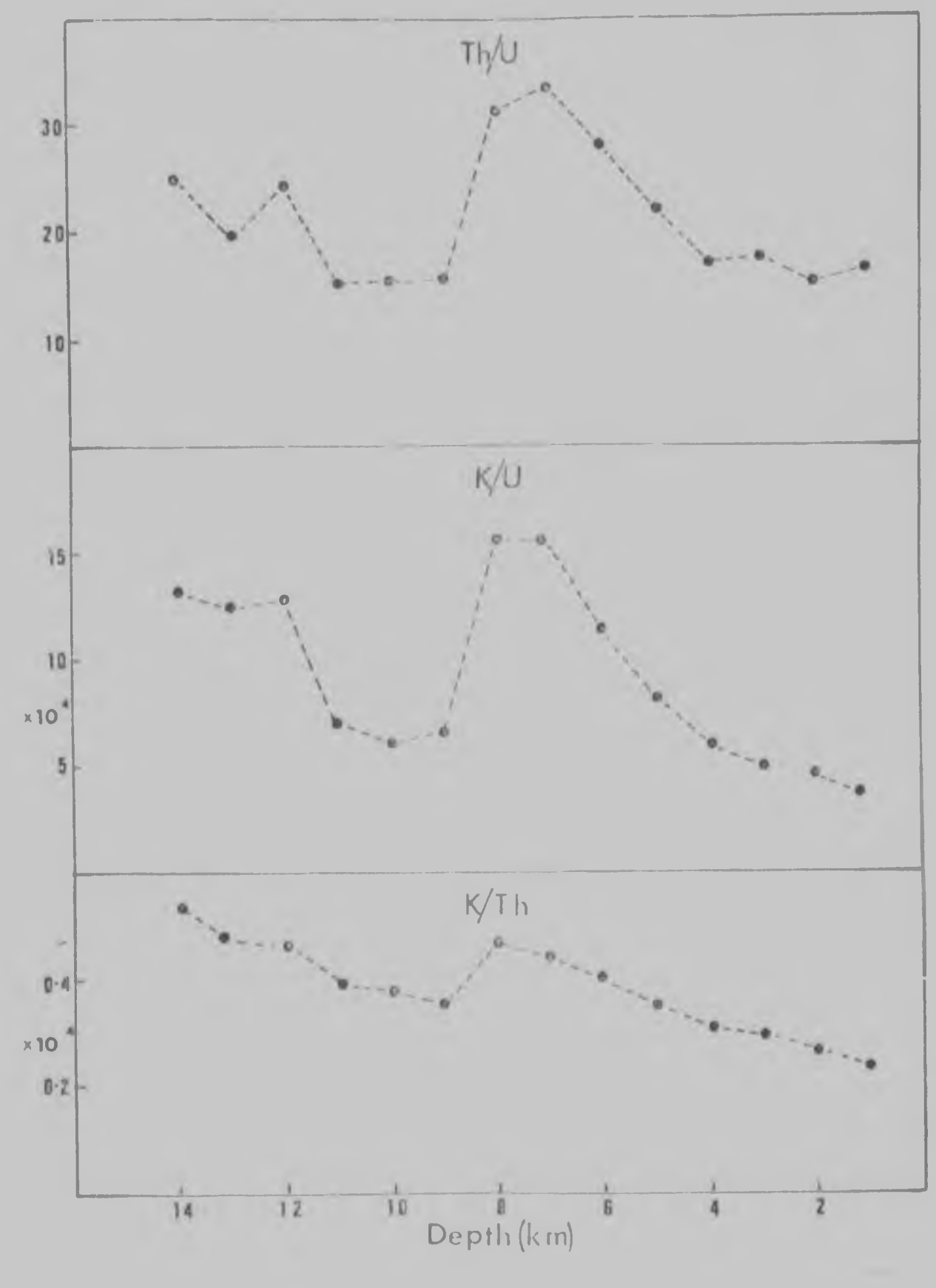


FIGURE 5.4 Averaged Th/U, K/U and K/Th profiles for the Vredefort basement (excl. S W quad.)

to the Steynskraal metamorphic zone. However, in the case of the Th/U, K/U and K/Th ratios, the anomaly includes a limited zone of Outer Granite Gneiss occurring on the outer margin of the SMZ (at about 9 to 10 km from the collar); these gneisses have relatively high U and Th concentrations.

The magnitude of the change in the three ratios is as follows:

ratio	range of averaged values	factor of change	actual range
Th/U	16 to 34	~ 2	0.44 to 100
K/U	3.8 to 16 ($\times 10^{-4}$)	~ 5	0.1 to 48 (10^{-4})
K/Th	0.28 to 0.53 ($\times 10^{-4}$)	~ 2	0.02 to 7.8 (10^{-4})

5.4 Discussion

Apart from the mafic granulites, it is only the outer margin, and then again mainly the south west where the values of Th/U, K/U and K/Th approach the average values obtained by other workers (Table 5.4).

TABLE 5.4 Average Th/U, K/U and K/Th ratios for Precambrian shield rocks

Th/U(1)	K/U x 10^{-4} (2)(3)	K/Th x 10^{-4} (3)
3 to 4	1.1	0.4

(1) accepted crustal average (Rogers and Adams, 1969).

(2) suggested terrestrial value (Wasserburg et al., 1964).

(3) average for the Canadian shield (Shaw, 1968).

In the felsic rocks from the interior of the dome, the Th/U ratios are an order of magnitude greater than the values given in Table 5.4. K/U ratios are greater by a factor of 15 whereas K/Th only differ by a factor of 2. Although they display low absolute abundances of Th, U and K, some of the mafic rocks from the SMZ have K/U, Th/U and K/Th ratios (Table 5.5) which more closely approximate the values given in Table 5.4.

TABLE 5.5 U, Th and K for the mafic granulites from the Vredefort basement

	U	Th	K	Th/U	K/U	K/Th
KK15	.34	2.76	.9	8.06	2.7	.33
KK17	.15	.28	.26	1.86	1.7	.93
VT523	.21	1.54	.14	7.33	0.7	.09
VT524	.72	9.25	2.65	12.85	3.7	.29
VT460	.25	.94	1.83	3.76	7.1	1.96
VT462	.13	.34	1.28	2.62	9.8	3.75

These observations suggest that firstly, although both U and Th are depleted relative to K in the greater proportion of the felsic rocks of the Vredefort basement, removal of U has occurred to a far greater extent than Th. Secondly, 'normal' Th/U, K/U and K/Th ratios in the mafic rocks of the SMZ indicate that Th and U have not been depleted relative to K, and further that U has not been depleted relative to Th. Similar observations have been made by Lambert and Heier (1967), who show that in the granulites from central Australia (Table 5.6) U and Th are depleted relative to K in the felsic rocks of the pyroxene granulite subfacies, whereas Th and U are not depleted relative to K in the mafic rocks of the pyroxene granulite subfacies.

TABLE 5.6 Comparison of K/Th and K/U ratios between pyroxene granulite and amphibolite subfacies rocks from the South West Australian shield (after Lambert and Heier, 1967).

Felsic rocks of the pyroxene granulite subfacies: U and Th depleted relative to K.

	$K/Th \times 10^4$	$K/U \times 10^4$
Amphibolites	.16	1.66
Granulites	1.25	6.67

Mafic rocks of the pyroxene granulite subfacies: U and Th are not depleted relative to K.

	$K/Th \times 10^4$	$K/U \times 10^4$
Amphibolites	.24	1.0
Granulites	.25	1.25

Specific mineral assemblages have a strong control on the behaviour of the radioelements during regional metamorphism in the Vredefort basement. Prior to granulite facies metamorphism U and Th in the mafic rocks must have been largely located within the refractory mafic mineral structures, which were able to retain these elements during high grade regional metamorphism. The location of these elements in the surrounding quartzo-feldspathic rocks must have been different, since the effects of regional metamorphism in these rocks was to deplete U strongly relative to Th, giving rise to abnormally high Th/U ratios. Similarly both Th and U are depleted relative to K. Potassium in fact shows very little variation throughout the profile and from this it is concluded that the K which occurs as an integral part of the feldspar structure, is not affected by regional metamorphism except possibly in the mafic rocks when it occurs in hydrous mineral phases.

A further point worthy of comment is that concentrations of Th and U are relatively high, at about 10 km from the margin (Figure 5.2), i.e. in felsic rocks cutting in and around the outer limits of the SMZ. Apart from U and Th and, in some cases, Rb concentrations (e.g. VT 127 and [illegible]), have a major element chemistry which is indistinguishable from other felsic rocks of the OGG, and it is thus assumed that the radioelements (now at higher concentrations) occur in interstitial sites. A possible reason for this relatively enriched zone is given in a later chapter, after the Th-U-Pb isotopic data has been discussed.

6 HEAT FLOW / HEAT PRODUCTION IN THE VREDEFORT AND FAR WEST WITWATERSRAND AREAS

6.1 Introduction

Since the discovery of the linear relationship between heat flow and radioactive heat production, and the introduction of the concept of heat flow provinces, workers in this field have been able to make reasonable estimates of the contribution to surface heat flow from the radioactive decay of elements in the upper crust, and the depth to which the relatively radioactive layer extends.

An important focus in such studies is the heat flow q (from beneath the relatively radioactive layer) which consists of two components: one from the lower crust, and a component from the mantle. Further knowledge on the abundances of the radioelements in the lower crust is essential for providing a means of estimating accurately the heat flow from the mantle.

The numerous deep boreholes drilled in the exploration for gold in the Witwatersrand basin have made it possible to obtain reasonably reliable heat flow data in the area, Carltonville south western Transvaal. These boreholes also present the opportunity of sampling a thick section of stratified rocks of the Transvaal, Ventersdorp and Witwatersrand Groups which overlie the basement granite, for the purpose of radio-element analyses. The summed heat production in these stratified rocks, together with the Vredefort basement heat production, is now compared to heat flow values measured in the Witwatersrand synclinorium boreholes.

The Vredefort structure occurs some 50 km to the south of the borehole localities in which heat flow measurements were obtained (Figure 2.1). At the outset one must assess whether the Vredefort basement profile is likely to be representative of the craton in which the Vredefort structure is located.

Footnote: Throughout this chapter the units of heat flow; 10^{-6} cal./cm^{2}sec., will be replaced by the abbreviation HFU, and the units of heat generation 10^{-13} cal/cm^{3}sec, by HGU.

6.2 Geological evidence

The Vredefort profile was obtained at a strikingly unusual domical structure near the centre of the Witwatersrand basin, forcing a query as to whether the dome developed specifically at Vredefort due to a local singularity in the petrography and chemistry of the Archaean continental crust.

The uppermost portion of the Vredefort basement immediately below the sedimentary Witwatersrand Group, would therefore be compared with the granitic terrain north of Johannesburg, and with the basement west of Carletonville (Figure 2.1). Although the exposed Vredefort basement rocks vary considerably in colour and texture, they consist essentially of varying amounts of quartz, pink microcline, plagioclase, biotite and minor amounts of apatite. Sphene, zircon and magnetite occur as accessory minerals (Nel, 1927; Willemse, 1937). Willemse (1937) observed a close resemblance between these rocks and the basement rocks of the Pretoria-Johannesburg basement dome, in both petrographical and chemical composition. The granites of the western Transvaal, typically quartz orthoclase plagioclase biotite granites, lying unconformably below the Dominion Reef and Witwatersrand Group. The general geological and petrological constitution of these three basement zones are therefore quite similar. Also, the isotope data reported by Clauson (1976) and Hart in this study, for the outer Vredefort basement, show similar ages to those found near Johannesburg and Klerksdorp (Allsopp, 1961/1963) and demonstrate that there was no significant change in Rb-Sr geochemistry in the Vredefort basement during the past 2850 million years. Any singularity in the Vredefort crust, particularly in the radioelement distribution, must therefore have formed in the period preceding 2850 million years ago.

Radioelement concentrations in granitic rocks exposed in the ancient basement terrain of the eastern Transvaal and Swaziland (Hart, unpublished)

and the average concentration for the upper crust of the south west Australian shield reported by Lambert(1971) are compared with the uppermost 3 km of crust in the Vredefort profile (Table 6.1).

TAPLE 6.1 Comparison of U, Th and K concentration from the southwest Australian shield, the upper Vredefort basement and the basement rocks of the eastern Transvaal and Swaziland.

	U(ppm)	Th(ppm)	K(%)
Average concentrations of southwest Australian Archaean shield.	1	20	3.0
Average upper granitic crust of Vredefort profile (outer 3 km) including S-W quadrant.	1.9	14.6	3.57
Granitic rocks exposed in Eastern Transvaal and Swaziland.	3.3	18.2	3.5

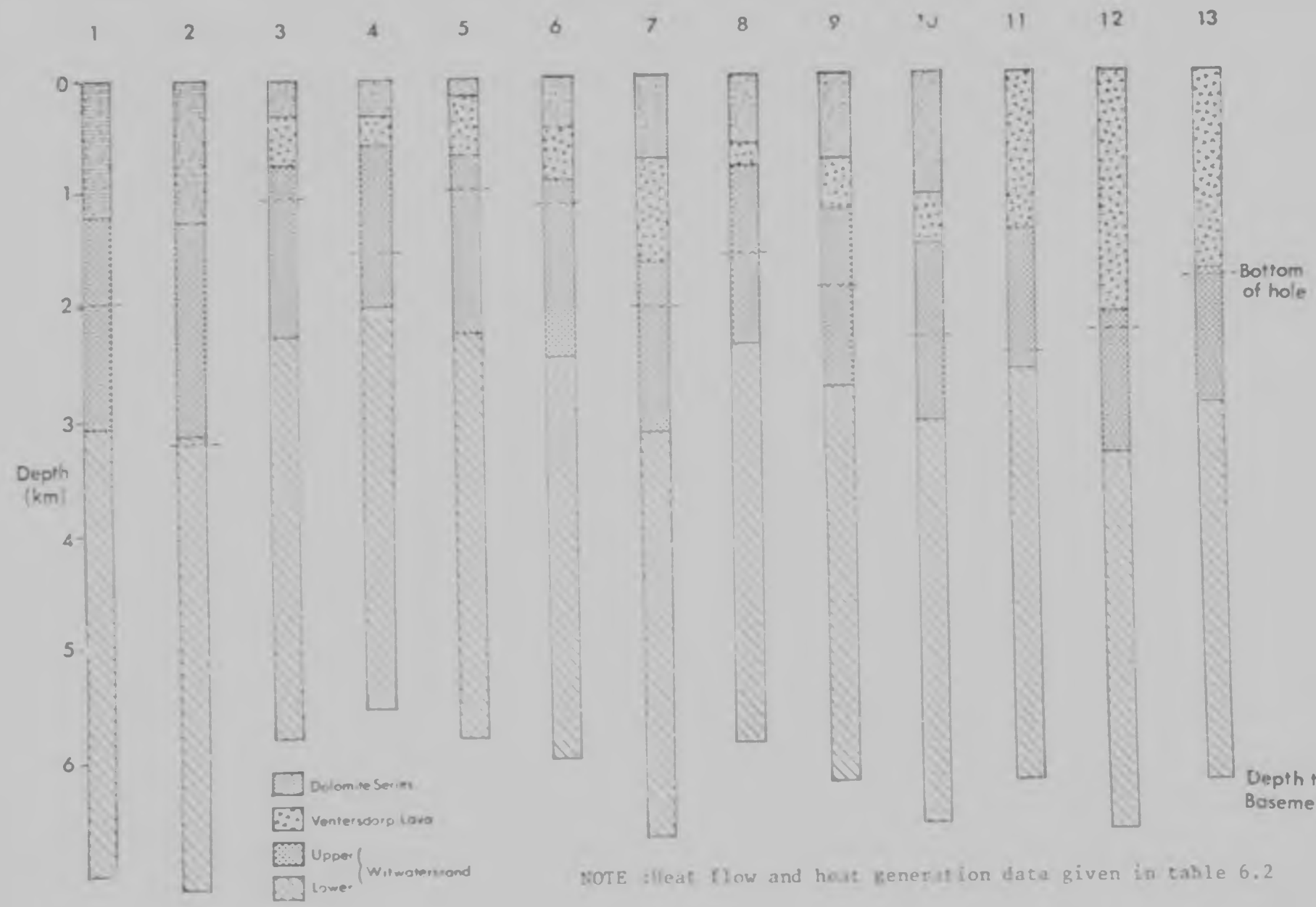
The outermost, more radioactive portion of the Vredefort basement is evidently quite typical of the outer portions of the continental crust in the eastern Transvaal, Swaziland and the southwest Australian Archaean shield. The radioelement distribution in at least this upper portion of the crust is therefore quite likely to extend to the basement beneath the boreholes N-W of Vredefort. If there is an important singularity in crustal constitution at Vredefort, it must be confined to the deeper portion of the crust.

6.3 Heat flow measurements

The possibility of using the deep gold exploration boreholes in the Witwatersrand Basin for reliable heat flow measurements was first investigated by Bullard (1939). Further data were obtained by Carte (1954) and Carte and van Rooyen (1969). Figure 2.1 shows the locations of the boreholes from which heat flow data has been obtained in relation to the Vredefort structure, and the boreholes from which heat production data has been obtained.

The depth to which each borehole has been drilled is indicated in Figure 6.1. The depth to basement has been extrapolated by using

FIGURE 6.1 Boreholes from which heat flow data has been obtained



NOTE :Heat flow and heat generation data given in table 6.2

isopach maps of the Witwatersrand Basin published by Brock and Pretorius (1964). Table 6.2 lists the heat flow values from these boreholes.

The heat flow values in the Ventersdorp lavas, which show a variation of ± 0.16 around a mean of 1.00 HFU, are significantly lower than the values obtained in the Witwatersrand quartzites, which vary by 0.06 either side of 1.22 HFU.

Two factors might account for this consistent difference between the two stratigraphic formations:

(i) The quartzites are deeper than the lavas, and consequently the heat flow is less influenced by surface topographical effects, or recent changes in the earth's climatic conditions. Generally, however, such effects would not be expected to account for a systematic difference of about 20% (Richardson, personal communication).

(ii) The mean value for the conductivity used to calculate heat flow is either too high for the quartzites, or too low for the lavas.

Since the conductivity measurements obtained by both Bullard (1939) and Carte (1954) generally agree, and both obtain the same systematic difference in their heat flow values, it is difficult to choose a correct heat flow value.

For this study, an average of two mean values of 1.00 HFU for the lavas and 1.22 HFU for the sediments, that is a heat flow value of 1.1 HFU has been adopted.

6.4 Sampling a section through the stratified rocks of the Witwatersrand Basin.

About 6 km of core, from boreholes drilled in mining exploration near Carltonville, (Figure 2.1) were systematically sampled. The borehole cores make up a 'cover profile' penetrating most of the sediments and lavas of the Witwatersrand, Ventersdorp and Transvaal Groups which overlie the basement granite rocks.

TABLE 6.2 Heat Flow Measurements in the Transvaal and Orange Free State

Borehole	Ventersdorp Lava	Witwatersrand Quartzite	Difference	Contribution to Surface heat Flow
1 Dornkloof	-	1.20	-	0.17
2 Gerhardminnebron	-	1.28	-	0.19
3 ST 11	0.91	-	-	0.15
4 ST 14	0.89	-	-	0.15
5 ST9	0.98	1.16	0.18	0.16
6 HB3	1.15	1.25	0.10	0.17
7 HB15	1.01	1.22	0.21	0.17
8 HB14	0.90	1.19	0.29	0.15
9 HB8	1.12	-	-	0.17
10 BU1	1.08	1.23	0.15	0.17
11 R57	0.86	-	-	0.16
12 Jacoba No.3	0.95	-	-	0.17
13 Dornhoutrivier	0.97	-	-	0.16
Mean	0.99 ± 0.16	1.22 ± 0.06	0.19	0.16

3 to 11 Measurements by Carte (1954)

1,2 and 12,13 Measurements by Bullard (1939)

Heat Flow Measurements expressed in cal. cm^{-2} sec^{-1} x 10^{-6}

Representative core samples were taken at regular 20 metre intervals. The samples, once crushed, were then grouped, each group made up of about 8 samples, all within the same lithological unit. Thus, 40 composite samples representing 6 km of stratified rock were obtained. The radioactive element content of the composite samples are given in Table 6.3.

From these data the average radioelement concentration and average heat production within each major lithological unit of the Witwatersrand, Ventersdorp and Transvaal groups have been obtained (Table 6.4). The average radioactive element concentration in each group of rocks is presumably dependent on the source area, nature and chemistry of the rock types, and depositional environment.

The gold- and uranium-bearing conglomerates were omitted from the core samples analysed. Although enriched in uranium these conglomerate beds are very thin compared to the total thickness of sediments, and their contribution to the surface heat flow is small (~ 5%). (This estimate is based on radioactive element concentrations in the conglomerates given in mining company reports, and the literature.)

6.5 Heat generation in the stratified rocks

The thickness of each lithological unit for each borehole listed in Table 6.5, together with the average heat production for each lithological unit listed in Table 6.4, have been used to calculate the total contribution to surface heat flow within the various columns of rocks represented by each borehole in Figure 6.1 respectively. The values obtained vary from 0.15 to 0.19 HFU (Table 6.5), with an average value of 0.16 HFU. The heat generated by radioactivity in and near the conglomerate horizons has been estimated at about 0.04 HFU*. Thus the total contribution to surface heat flow from the stratified rocks amounts to 0.20 HFU.

The radioelement measurements on the stratified rocks were made by N.H. Gale of Oxford University.

* The conglomerate beds of the Witwatersrand [illegible] concentration of [illegible] ppm (F.C. Cousins, S.A. Atomic Energy Board; personal communication). If 2 metres of footwall and hangingwall are included in the total thickness then the heat flow from this horizon is ~ 0.04 H.F.U.

TABLE 6.3 Radioelement concentrations for the stratified rocks of the Witwatersrand Basin

		U	Th	K%
Ongeluk Lavas of Pretoria Series	UD 1	4.76	25.28	1.03
	2	3.61	18.24	1.23
	3	4.30	26.13	1.10
Pretoria Series	4	4.60	31.51	2.50
	5	2.61	16.63	0.97
	6	7.68	39.42	2.13
	7	4.72	31.40	3.58
Dolomite Series	8	0.19		0.09
	9	0.24	9.90	0.29
	10	1.09	10.00	1.88
	11	2.12	0.38	0.15
	12	0.10	6.79	0.09
	13	0.09	0.70	0.09
	14	0.35	2.24	1.33
Lavas of Ventersdorp Group	15	0.70	3.76	2.34
	16	0.85	4.76	1.32
	17	0.91	5.24	1.28
	18	0.76	5.16	1.10
	19	0.95	7.29	1.20
Strata of Upper Witwatersrand Supergroup	DK 1	1.16	9.85	2.25
	2	1.27	13.51	1.96
	3	0.93	6.43	2.22
	4	1.64	4.74	2.05
	5	1.73	7.49	1.45
	6	1.57	7.51	2.01
	7	1.50	7.67	2.21
	8	1.74	7.67	2.21
	9	0.75		0.74
	K 10	2.67	10.22	2.48
	11	10.68	34.06	1.44
Strata of Lower Witwatersrand Supergroup	E 1	1.16	4.28	1.31
	2	1.22	6.73	1.30
	3	1.54	8.47	1.78
	4	1.00	5.00	1.52
	5	0.90	5.59	0.95
	6	1.13	6.94	1.42
	S 1	1.10	8.37	1.11
	2	1.38	7.29	1.50
	3	2.24	13.11	2.32

TABLE 6.4 Average radioelement concentrations and heat productions (expressed in cal cm^{-3} sec^{-1} x 10^{-13}) for the stratified rocks of the Witwatersrand basin

	U (ppm)	Th (ppm)	K (%)	Combined average heat production
Ongeluck lava				
Conc.	4.02	23.22	1.12	
Heat production (HGU)	1.49	3.95	0.26	6.7
Pretoria series				
Conc.	4.90	29.74	2.30	
Heat production (HGU)	3.04	5.06	0.53	8.6
Dolomite series				
Conc.	0.60	5.00	0.56	
Heat production (HGU)	0.37	0.85	0.13	1.2
Ventersdorp lavas				
Conc.	0.83	5.24	1.45	
Heat production (HGU)	0.51	0.89	0.33	1.7
Upper Witwatersrand				
Conc.	2.33	10.92	1.91	
Heat production (HGU)	1.44	1.86	0.33	3.8
Lower Witwatersrand				
Conc.	1.30	7.31	1.47	
Heat production (HGU)	0.81	1.24	0.34	2.4

Table 6.5 The Thickness of the Lithological Units for the Boreholes in fig. 6.1 (km)

Borehole	Dolomite Series	Ventersdorp Lava	Upper Witwatersrand	Lower Witwatersrand
1 Dornkloof	1.2	-	1.9	3.4
2 Gerhardminnebron	1.2	-	2.0	4.1
3 ST11	0.2	0.4	1.6	3.6
4 ST14	0.2	0.3	1.5	3.6
5 ST9	0.2	0.5	1.7	3.6
6 HB3	0.5	0.5	1.7	3.6
7 HB15	0.7	1.0	1.6	3.6
8 HB14	0.5	0.2	1.6	3.5
9 HB8	0.7	0.4	1.7	3.6
10 BU1	1.0	0.4	1.7	3.6
11 K57	-	1.5	1.3	3.7
12 Jacoba No. 3	-	2.2	1.3	3.3
13 Dornhoutriver	-	1.8	1.3	3.3

6.6 Heat generation in the Vredefort basement granite

The heat generation for each radioelement, and the total heat generation in each successive kilometre is listed in Table 6.6. It is interesting to note that throughout the profile Th is the major producer of radiogenic heat. In the upper 3 km U generates more heat than K, however, this relation is reversed throughout the remaining 11 km of the profile.

In the upper 7 km of the Vredefort basement profile the contribution to surface heat flow due to the radioactive elements is 0.32 HFU whereas the lower 7 km of crust contributes 0.18 HFU to surface heat flow.

6.7 Total measured contribution to surface heat flow

The exposed crust and its heat generation can be portioned as follows:

		Average Heat generation (HGU)	Contribution to heat flow (HFU)
6 km	Stratified rocks	3	0.20
7 km	Upper portion of Vredefort basement profile	4.6	0.32
7 km	Lower portion of Vredefort basement profile	2.5	0.18
20 km			0.70

Thus the total measured contribution of the stratified rocks and "observed" basement to the heat flow in this area is 0.70 HFU.

6.8 Heat production in the lower crust

The total measured heat production given above, accounts for 20 km of upper and middle crustal material. Obtaining the heat production in the lowermost crust is more speculative. However, use can be made of geophysical studies as well as the radioelement concentrations in the rocks which occur on surface in the central regions of the Vredefort dome. Seismic refraction measurements in the western and southern Transvaal (Gane et al., 1956) revealed a crustal thickness of 36 km.

Table 6.6 Averaged radioelement concentrations and heat production for the Vredefort basement (incl. S-W quad.)

No.	U (ppm)	Th (ppm)	K (%)	U (A)	Th (A)	K (A)	combined (A)
1	2.39	17.86	3.57	1.49	3.17	0.81	5.47
2	3.38	17.41	3.54	2.11	2.92	0.80	5.83
3	3.60	17.19	3.51	2.25	2.88	0.80	5.93
4	2.79	15.95	3.53	1.74	2.68	0.80	5.22
5	1.24	13.18	3.58	0.77	2.21	0.81	3.79
6	1.20	12.38	3.68	0.75	2.01	0.83	3.59
7	0.22	7.42	3.26	0.14	1.25	0.74	2.13
8	0.23	7.19	3.34	0.14	1.21	0.76	2.11
9	0.54	9.36	3.29	0.34	1.57	0.75	2.66
10	0.58	9.12	3.50	0.36	1.53	0.79	2.66
11	0.50	8.80	3.41	0.32	1.48	0.77	2.57
12	0.32	7.80	3.60	0.20	1.31	0.82	2.33
13	0.33	6.56	3.18	0.20	1.10	0.72	2.02
14	0.29	7.31	3.98	0.18	1.23	0.90	2.31

A : Cal./cm.^{3}sec. x 10^{-13}

This leaves 16 km of crustal material that has to be accounted for.

Mafic Archaean rocks are sporadically exposed in the central regions of the Vredefort dome, and extend from the SMZ inwards. However, apart from the SMZ where the overall quality of the exposures of mafic and felsic rock is good, weathering and the thin Phanerozoic cover make it difficult to establish the proportion of mafic to felsic rocks, and the extent to which the abundance of mafic inclusions increases towards the centre.

The 30 mgal central positive gravity anomaly at Vredefort (Maree, 1944; Stepto, unp. in preparation) demonstrates that there is a large volume of rock with a higher density than granite beneath the exposures of the most central region. This denser rock either intrudes the Inlandsee leucogranofels, or it represents a very steeply domed portion of a denser lower crust, underlying the Inlandsee leucogranofels.

Two hypothetical models for the lower 16 km of basement have been compiled. Lower Crust A (LCA) consists entirely of mafic rocks in the granulite facies, represented by three of the most centrally exposed mafic granulites in the Vredefort structure (specimen no's. 49, 352 and 377). In the Lower Crust B (LCB) model, only the lowermost 6 km (immediately above the Mohorovicic discontinuity) consists of such mafic granulite. Above it is 10 km of rock with equal proportions of ILG and mafic granulite. LCB accords better with gravity data and is preferred.

Table 6.7 summarises the heat production for these two models for the lower 16 km of crust. The radioelement concentrations for mafic granulites has been obtained by averaging the concentration of the mafic rocks exposed in the most central depth zones (0.08 ppm U, 0.54 ppm Th and 0.59% K).

TABLE 6.7 Models for the heat production for the lower 16 km of the crust.

Model	Thickness	Constitution	Heat production HGU	Contribution to heat flow
LCA	16 km	Mafic granulite	0.27	0.04
LCB	(10 km	(50% ILG	2.4	0,12)
	(	(50% Mafic granulite	0.27	0.01) 0.15
	(			)
	(6 km	Mafic granulite	0.27	0.02)

The total contribution to surface heat flow as a result of heat production due to the radioelements in the continental crust (southern Transvaal) is thus calculated at between 0.74 and 0.75 HFU. In the lowermost part of the crust, potassium is the most significant contributor of radiogenic heat.

6.9 Estimate of heat flow at the Mohorovicic discontinuity

Noting the surface heat flow value of 1.1 HFU adopted earlier in this study for the Carletonville area, and the LCA and LCB approximations for the lower crust, the heat flow across the Mohorovicic discontinuity below Carletonville is calculated as 0.85 HFU (LCA) and 0.95 HFU (LCB) respectively. The error estimation on each of these values is at least ± 0,1 HFU, due to the systematic differences observed in borehole heat flow measurements.

These values should be compared with the estimate of Sclater and Francheteau (1970) who constructed a simple model of a three layered lithosphere on top of a primitive upper mantle, in a shield area with assumed heat flow of 1,0 to 1,05 HFU:

TABLE 6.8 Heat production model for a three layered lithosphere.

	Thickness (km)	Contribution to surface heat flow (HFU)
Upper radioactive layer	6	0.25
Lower crust	32	0.20
Dunite peridote lithosphere	100	0.05
Total	138	0.50

In their model, a heat flow of 0,55 or 0,60 HFU moves through the base of the crust. Slack (1974) calculated a corresponding flux of 0,68 HFU for the North American craton and shield areas.

6.10 Consequences of low mantle heat flow

The base of the lithosphere is one of the most important geophysical boundaries of the earth. It is often assumed to coincide with the top of the low velocity zone.* Sclater (1972) assumed that the low velocity zone is probably a partial melt and that the temperature gradient in the underlying upper mantle is adiabatic. He, therefore concluded, that the low velocity zone can be considered isothermal, whether below an ocean basin or a continent. The low heat flow from the mantle beneath the continents (0.5 HFU in his paper) was compared to the mantle value of 0,9 to 1,0 HFU for the deep ocean basins. Sclater calculated that the lithosphere under the continents was twice as thick as that for old ocean basins.

Quantitively, however, Sclater's model suffered because of inadequate information on the radioelement concentrations throughout the crust. The new information on the heat production in the Transvaal crust (presented in this study) serves to update this model.

The mean heat flow from beneath the lithosphere of the Kaap Vaal craton has been calculated at 0,30 HFU. This value is approximately one-third of the heat flow under the ocean basins.

Assuming that the mean thermal conductivity of the continental lithospheric mantle is the same as that beneath the old ocean basins, then the mantle heat flow that reaches the M-discontinuity must be

*Footnote
For the ocean basins, this depth is readily calculated from seismic surface wave observations. For the continents and particularly the shield areas, the low velocities are proven only for the shear wave data. Even in these profiles of S wave velocity vs. depth, the top of the layer is not well defined.

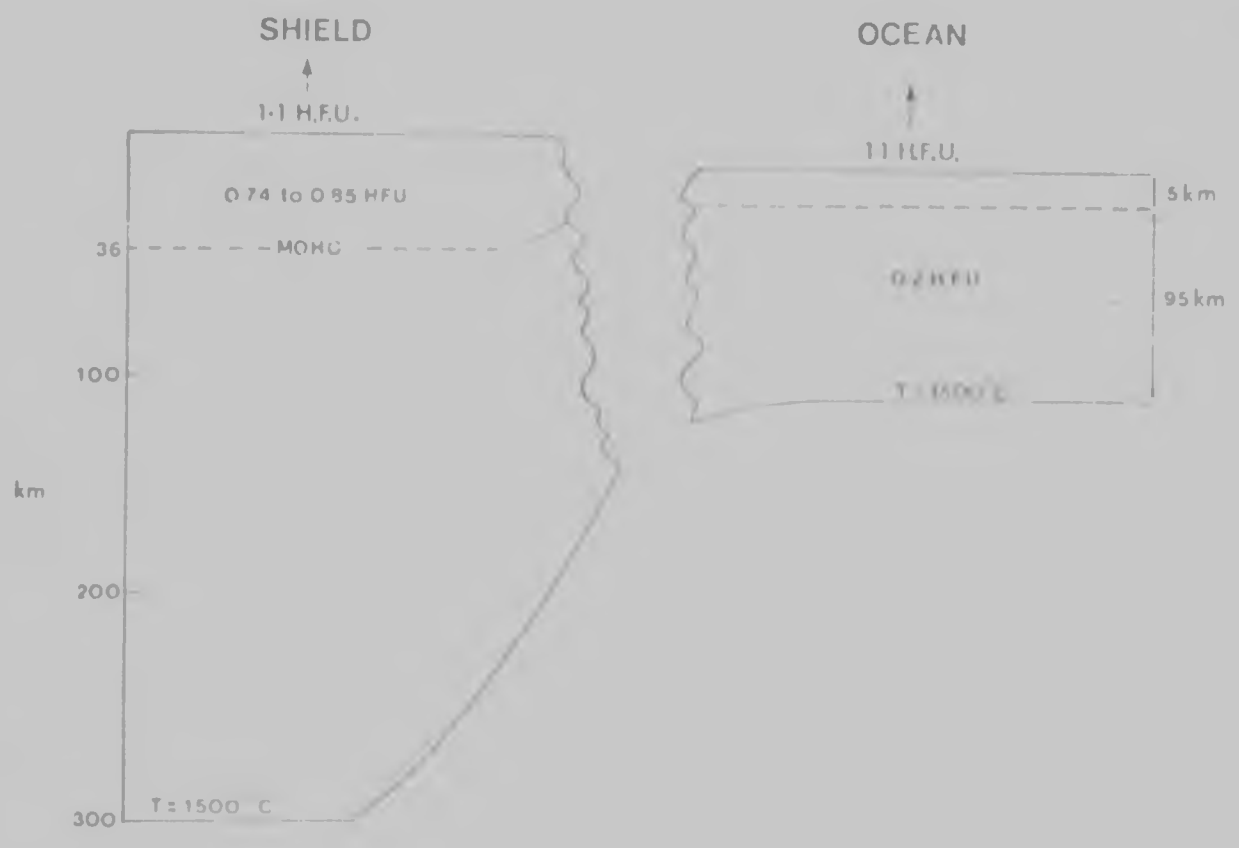


FIGURE 6.2 Ocean and continental lithosphere (modified after Sclater 1972).

proportional to the gradient, and therefore inversely proportional to the lithosphere thickness.

Thus in order to maintain an equality between oceanic and continental heat flow, the lithosphere beneath the continental shields must be at least three times as thick as under the old basins (Fig.62). On the basis of this argument, the depth to the low velocity zone is calculated at 300 km.

6.11 Conclusions

(1) The heat production from the exposed profile in the Vredefort basement, together with the stratified rocks of the Carletonville area (upper 20 km) is considerably greater than previous estimates of the heat production in the crust.

(2) The heat production in the lower 16 km of crust is partly conjecture. However, assuming the preferred model LCB, then the total contribution to surface heat flow for a 36 km continental crust is 0.85 HFU. The heat flow from beneath the mantle has been calculated at between 0.35 (Model LCA) and 0.25 (Model LCB) in the Carletonville area.

(3) Using this mantle heat flow value the thickness of the lithosphere below the southern African shield has been calculated at approximately 300 km, following the method of Sclater (1972).

(4) The Vredefort data together with the stratified rocks from the Witwatersrand basin permit a new budget of U, Th and K concentrations in the Archaean continental crust. Hart et al. (ms. in preparation) show that new estimates of the total mass of each individual radio-element in the terrestrial crust weaken the criticisms of the chondrite model (for the earth's primitive constitution) made by Birch (1965) and Gast (1968).

7 GEOCHRONOLOGY OF THE VREDEFORT [illegible]

7.1 Introduction

The geochronology of the basement granite of the Vredefort structure was first investigated by Slawson (1976). A Rb-Sr whole rock isochron yielding an age of 2850 ± 60 m.y. ($\lambda = 1.39 \times 10^{-11}$ years^{-1}) and an initial Sr ratio (i.e. Sr^{87}/Sr^{86}) of 0.7064 ± 0.0009 (1σ) was obtained. Primarily the objective of Slawson's study was to investigate the Rb-Sr isotopic systematics, and to test the hypothesis of Poldervaart (1962) of a possible age difference between the centre and the extreme margin of the granite core resulting from the updoming of the Vredefort granite. Poldervaart (1962) suggested that Rb-Sr age discrepancies may in turn "yield information on the age of the major upthrust of the core".

The Rb-Sr isochron obtained by Slawson, however, suggested that over the area sampled, the geochemical gradients within the Vredefort basement, at least for Rb and Sr, were established during the early stages of crustal evolution and have remained undisturbed by the updoming and overturning of the Vredefort granite.

Without exception all 13 samples plotted on the Rb-Sr whole rock isochron by Slawson (1976) were felsic in composition. Nine samples were collected from the outer granite gneiss, three (VT 5, 24 and 66) from the Inlandsee leucogranofels, and one sample (VT 28) is intermediate between the two rock suites. The initial test whether the data points on Slawson's isochron are truly represented by granitic basement with a common Sr isotopic system was made by recalculating Slawson's data omitting the latter four samples. An older age of 3025 ± 110 m.y. (1σ) and a lower initial ratio of .698 ± .004 was obtained (using $\lambda = 1.41 \times 10^{-11}$ years^{-1}) as compared with the 2820 ± 60 m.y. ($\lambda = 1.41 \times 10^{-11}$ years^{-1}) and an initial ratio of .7064 for the 13 point isochron obtained by Slawson. The data points for the ILG samples define an isochron plot which has a shallower slope but a higher initial Sr

ratio than the OGG isochron plot. Thus the four relatively unradiogenic ILG samples have the effect of reducing the age while increasing the initial Sr ratio of the OGG isochron calculation.

A more detailed knowledge of the geology (Stepto ms. in preparation) and geochemistry (this study), and the greater precision of the mass spectrometer now available, afforded the opportunity to re-examine the geochronology with a view to establishing age relationships between the different rock groups recognized in the field. Furthermore, in the light of the 'crustal edge' model, such additional knowledge may in turn yield information of the effect of depth in the crust on isotopic systematics.

Although this study deals mainly with the Sr isotopic evolution of the Archaean basement rock types, a Rb-Sr whole rock isochron for the younger intrusive biotite granite occurring in the central portion of the dome is also presented. The data for this intrusive body have a strong bearing on the theory of crustal evolution of the lower crust and provide additional knowledge on the tectonic formation of the Vredefort structure.

The Th-U-Pb geochronology results which are used in the discussion that follows are reported in a paper by Welke et al., (ms. in preparation). The U and Pb isotopic analyses on the Vredefort basement rocks were carried out by H. Welke and the Th analyses were executed by the author by the delayed neutron activation method (see Appendix C). The paper has been written jointly by H. Welke, R.J. Hart and L.O. Nicolaysen.

7.2 Results

The linear plots given below were obtained by fitting regression lines to the data points for the individual rock suites (localities shown in Fig. 7.1), using the method of York (1966). This technique is discussed in greater detail in Appendix A. The regression analyses

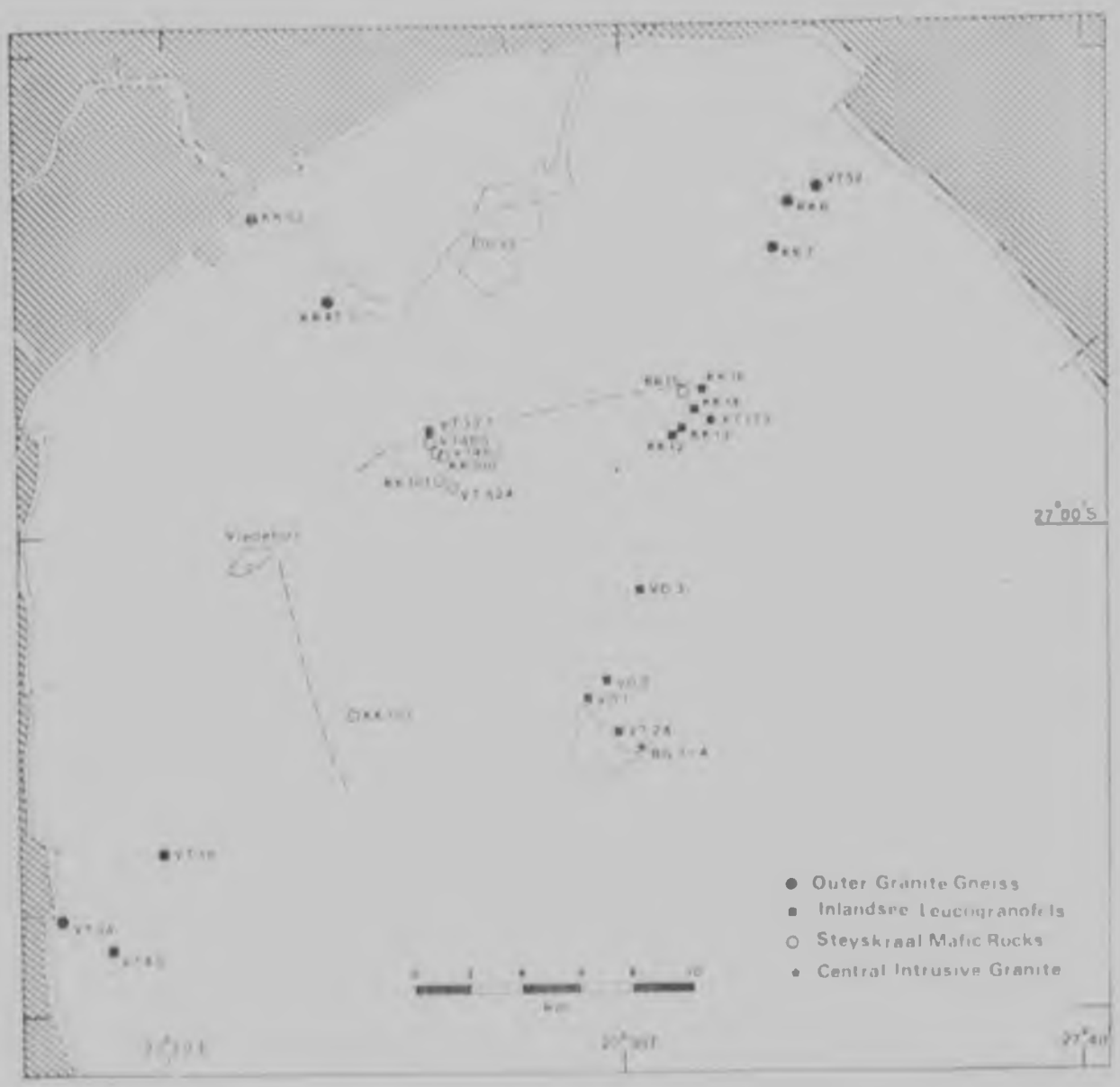


Fig. 7.1 Sample location

were tested following the theory of Brooks et al. (1972) which allows for the critical distinction between an isochron and an errorchron. In this study this distinction is based on a comparison of the mean sum of the residuals (M-Sum, York, 1969) to the F ratios for a given number of samples and degrees of freedom at the 95% confidence level. If the M-Sum is less than the F ratio, then the data points define an isochron. Details of this procedure are given in Appendix A. All the ages reported are calculated using a Rb^{87} decay constant of 1.41 x 10^{-11} $years^{-1}$.

(a) Metabasites and metadiorites of the Steynsdraal Metamorphic zone

Seven mafic xenolithic rafts from the SMZ have been studied by the Rb-Sr whole rock method and the results are listed in Table 7.1. Although the mafic xenoliths include rocks of sedimentary and igneous origin, which are not necessarily contemporaneous, geological evidence clearly indicates that they are all older than the felsic rocks of the ILG (Stepto personal communication). The data points for the SMZ metamorphosed mafic gneisses and metadiorites in fact show (Fig. 7.2) small but significant scatter, and the regression line defines an errorchron (M-Sum 7.3; F ratio = 2.7) giving an age of 3656 ± 320 m.y. (1σ) and an initial Sr ratio of 0.[illegible] ± 0.0004 (1σ).

Two of the samples studied (KK 15 and KK 103) have been described by Stepto (ms. in preparation) as charnockitic gneisses. Although older than the ILG they intrude the metabasite sequence. If KK 15 and KK 103 are excluded from the isochron plot, the five remaining data points then define an isochron (M-Sum [illegible].0; F ratio < 3.1). The age defined by the isochron is 3478 ± 130 m.y. (1σ) and the initial Sr ratio is 0.7006 ± 0.0002 (1σ). The age given by the 5 point isochron is not significantly different from the age given by the 7 point errorchron.

TABLE 7.1 Rb - Sr Isotopic Data for the Steynskraal Metasediments and Metabasites

SAMPLE	Rb^{87}	Sr^{86}	Rb^{87}/Sr^{86} (a)	Sr^{87}/Sr^{86}
VT642	2.889	25.59	0.0965	0.70504
VT524	17.79	21.04	0.8359	0.74404
VT460	9.620	42.73	0.2211	0.71146
KK15	2.265	39.31	0.0576	0.70482
KK100	0.408	14.29	0.0286	0.70218
KK101	9.021	8.886	1.0032	0.75257
KK103	5.519	4.358	0.1319	0.70874

(a) Atomic ratios

TABLE 7.2 Rb - Sr Isotopic Data for the Inlandsee Leucogranofels

SAMPLE	Rb^{87}	Sr^{86}	Rb^{87}/Sr^{86} (a)	Sr^{87}/Sr^{86}
VD1	30.38	33.16	0.9056	0.7412*
VD2	26.29	40.38	0.6436	0.7298
VD3	19.48	8.74	2.203	0.7947
VT24	26.20	25.99	0.9965	0.7455*
VT127	40.88	16.30	2.480	0.8049
VT173	29.56	17.10	1.708	0.7739
KK12	22.78	54.69	0.4117	0.7215
KK13	25.10	30.18	0.8221	0.7373
KK14	28.30	22.24	1.259	0.7552
KK16	20.97	26.05	0.7957	0.7377

* Sr^{87}/Sr^{86} ratios determined on spiked solutions

(a) Atomic ratio

TABLE 7.3 Rb - Sr Isotopic Data for the Outer Granite Gneiss

SAMPLE	Rb^{87}	Sr^{86}	Rb^{87}/Sr^{86}(a)	Sr^{87}/Sr^{86}
KK6	23.16	31.00	0.7385	0.73396
KK7	31.38	22.69	1.367	0.76197
KK47	16.12	7[illegible].28	0.220[illegible]	0.71140
KK53	17.51	33.70	0.51[illegible]6	0.72427
VT34	78.10	10.24	7.539	1.0230
VT36	56.88	11.50	4.889	0.9[illegible]64
VT40	80.08	13.32	5.9[illegible]	0.9639
VT52	49.24	19.[illegible]6	2.488	0.8102

(a) Atomic ratios

TABLE 7.4 Rb - Sr Isotopic Data for the Central [illegible]

SAMPLE	Rb^{87}	Sr^{86}	Rb^{87}/Sr^{86}(a)	Sr^{87}/Sr^{86}
BG1	41.91	31.56	1.313	0.74621
BG2	50.27	31.83	1.561	0.75360
BG3	45.81	34.18	1.325	0.74737
BG4	58.76	23.89	2.431	0.77785

(a) Atomic ratios

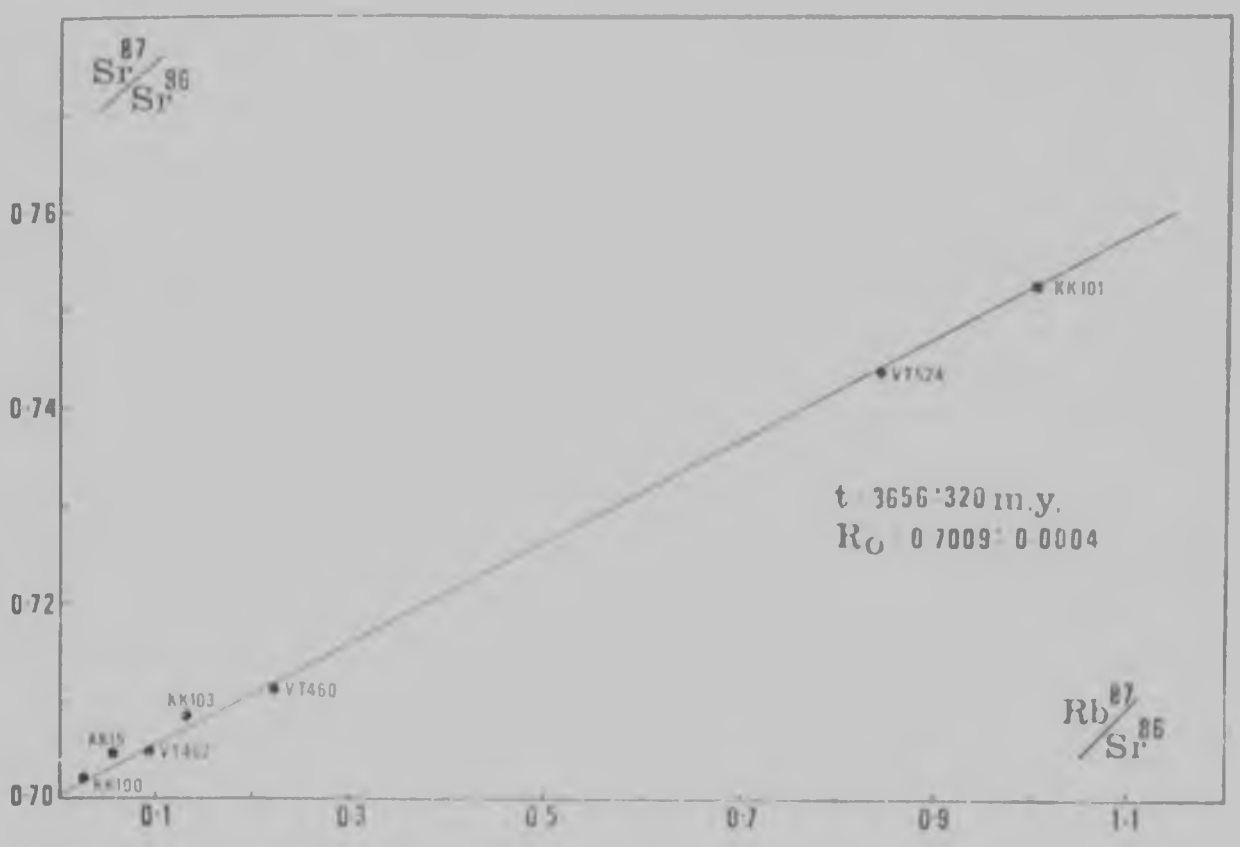


FIGURE 7.2 Rb-Sr isochron diagram for the SMZ

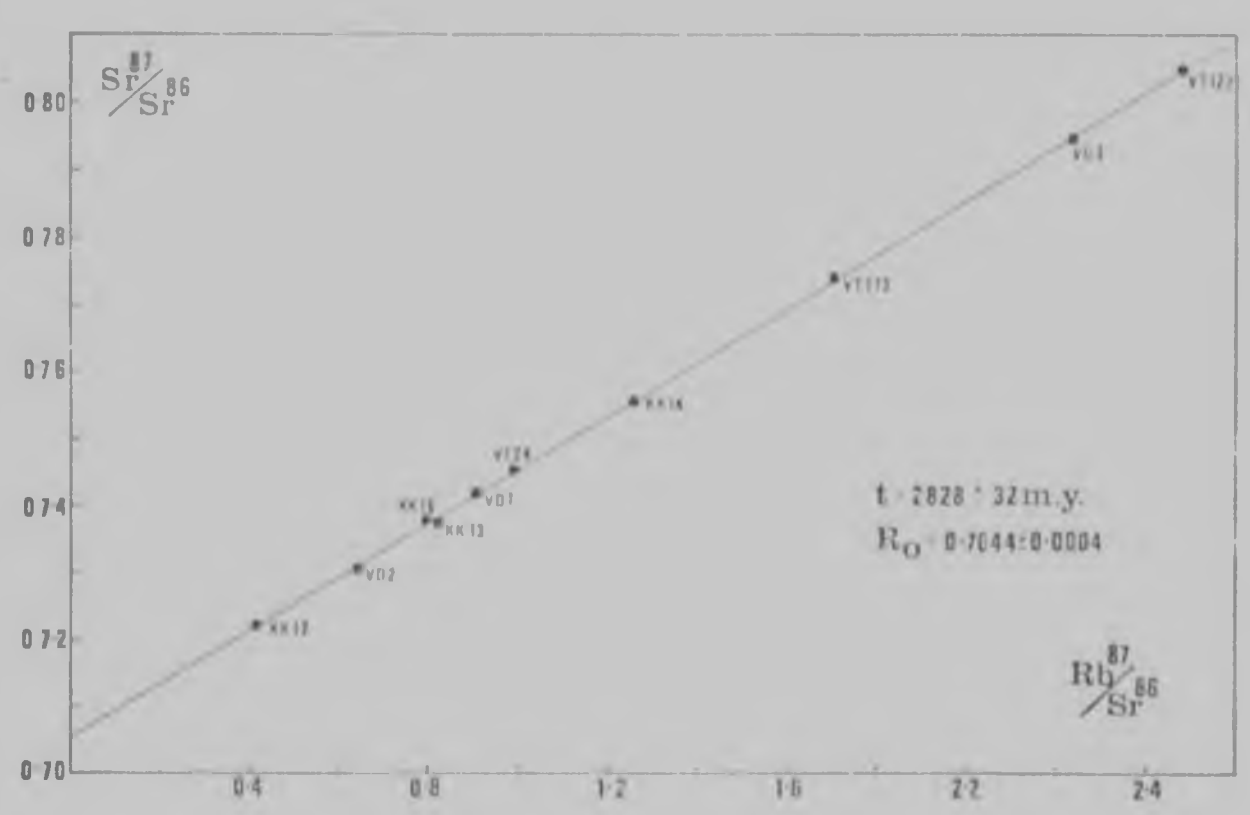


FIGURE 7.3 Rb-Sr isochron diagram for the ILG

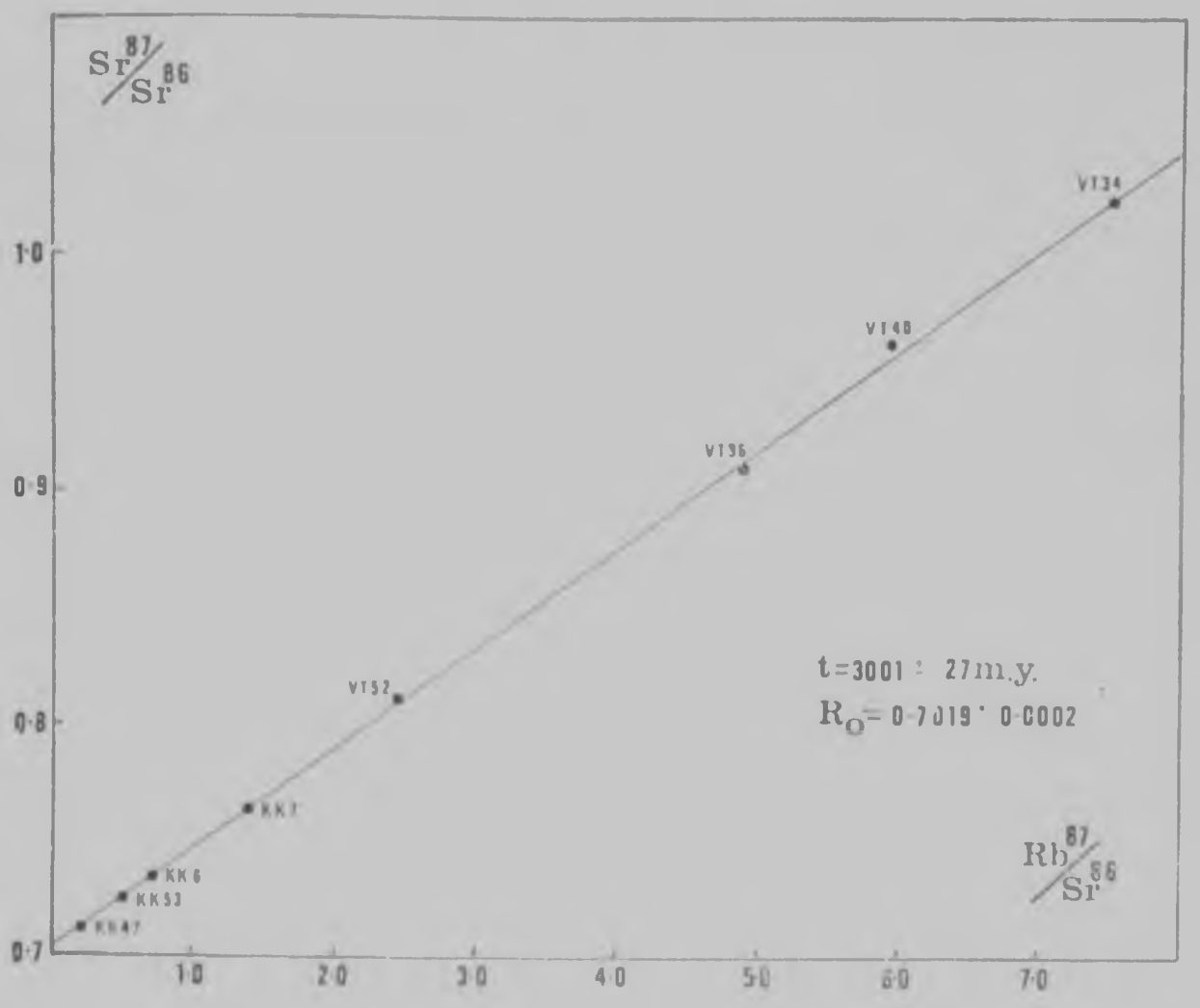


FIGURE 7.4 Rb-Sr isochron diagram for the OGG

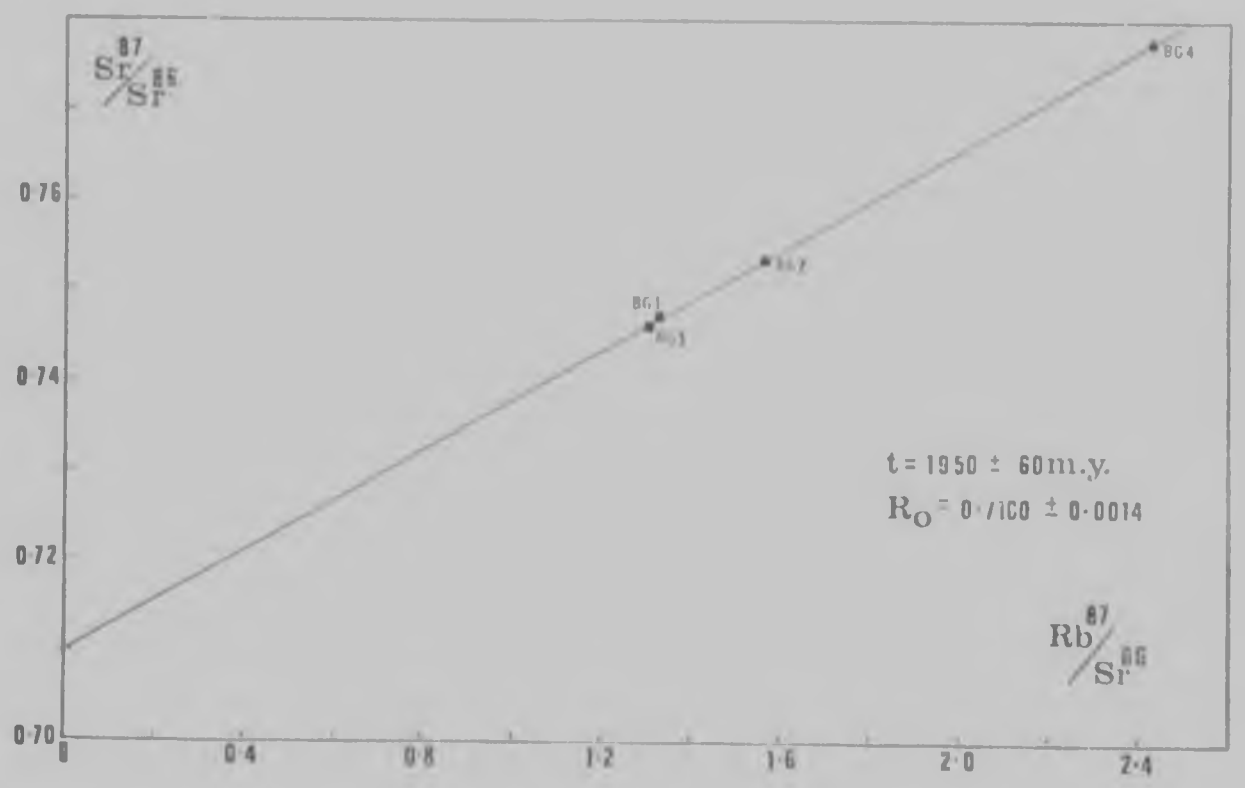


FIGURE 7.5 Rb-Sr isochron diagram for the CIG

(b) Inlandsis leucogranofels

Analytical data for the ILG are given in Table 7.2 and are plotted on an isochron diagram (Fig. 7.3). Ten points were fitted to a regression line that defines an isochron (M-Sum = 1.22; F ratio = 2.4), yielding an age of 2828 ± 32 m.y. (1σ) and an initial Sr ratio of 0.7044 ± 0.0004 (1σ).

(c) Outer granite gneiss

Rb-Sr whole rock analyses were made on 8 samples of the OGG. The analytical data are given in Table 7.3. A regression fit gives an age of 3001 ± 27 m.y. (1σ) and an initial Sr ratio of 0.7019 ± 0.0002 (1σ). The data points (Fig. 7.4) define an isochron (M-Sum = 1.83; F ratio = 2.6).

(d) Central intrusive granite

The central intrusive biotite granite outcrops over an area of only a few square kilometres and only 4 samples of sufficiently different Rb/Sr ratios to give a reasonable spread on an isochron diagram were obtained. Nonetheless the four samples investigated define a good isochron yielding an age of 1950 ± 60 m.y. (1σ) and an initial Sr ratio of 0.7100 ± 0.0014 (1σ) (Fig. 7.5). (M-Sum = 1.1; F ratio = 3.5).

(e) U-Th-Pb geochronology results

The U-Th-Pb results (Welke et al. ms. in preparation) are summarized in Table 7.5

TABLE 7.5 Summary of the Th-Pb, U-Pb and Pb-Pb isotopic data

		Age (m.y.)	Initial ratio
OGG	Th-Pb isochron	3060 ± 50	31.78 ± 0.14
	Pb-Pb secondary isochron	3080 ± 20	12.712 ± 0.045 (206/204)
			14.216 ± 0.021 (207/204)

The U-Pb concordia plot show that some samples have suffered recent U loss : the discordia plot (which defines a straight line) intercepts the concordia curve at 150 and 3090 m.y. respectively.

		Age (m.y.)	Initial ratio
ILG	Th-Pb 'younger' isochron*	3070 ± 110	31.67 ± 0.25
ILG + SMZ	Th-Pb 'older' isochron*	3540 ± 70	32.77 ± 0.04

The U-Pb data on the Pb^{206}/Pb^{204} - U^{238}/Pb^{204} plot, indicate open system behaviour: the majority of the points are scattered and lie well above a 3050 m.y. reference line. Some of the scatter (for four of the samples) is due to recent U loss. A comprehensive interpretive study has been made of all the U-Pb isotopic analyses for the ILG and SMZ rock suites, and a 3 stage evolution model fits the data reasonably well. In this model small changes in μ value were effected 3800 m.y. ago and a major diminution in μ values occurred $\sim$ 2800 m.y. ago.

*Although the data for most of the felsic rocks from the Inlandsee area plot on a Th-Pb isochron giving an age of 3070 ± 110 m.y., the data for some of the felsic rocks fall on a steeper isochron, characterised by the mafic metamorphic suite, and giving an older age of 3540 ± 70 m.y.

7.3 Geological interpretation of whole rock ages and initial ratios

Before discussing the Vredefort isotopic data, the methods of interpretation of whole rock isochron data are briefly reviewed.

Whole rock ages as defined by an isochron relate either to the time of crystallization of a magma, or to the time of a major metamorphic event that effected complete isotopic rehomogenization. Initial ratios are believed to reflect the nature of the source regions. For example a magma derived directly from the mantle would be expected to be characterised by a relatively low Sr initial ratio varying from 0.699 at 4650 m.y. ago to about 0.704 at the present day if a single stage development of the mantle was followed.

Spooner and Fairbairn (1970), and more recently Moorbath (1975), contended that the low primary ratios measured in certain Precambrian gneissic terrains are inherited from the mantle, and that the magmas were transferred into the crust shortly before the time of emplacement. Moorbath concluded that such younger Precambrian granite gneisses, mainly from Scotland and Greenland, could not have been derived as a result of reworking the pre-existing older crustal rocks; this precluded the possibility of long periods of crustal residence prior to the age given by an isochron.

Bridgwater and Collerson (1976) on the other hand argue that such calculations of brief crustal residence times are only valid if the average Rb content of the rock suite today is the same as the average content at the time of initial separation from the mantle. They suggest that a low Sr initial ratio, characteristic of the upper mantle, need not necessarily indicate a short crustal history if a rock suite which previously had a low Rb/Sr ratio gained Rb during the metamorphic processes which effected isotopic rehomogenization.

A further important, but until recently, commonly overlooked aspect of isotopic geology is centred around the possibility of mantle inhomogeneity in Precambrian times. The characteristically low Sr isotopic values for oceanic volcanic rocks are believed to reflect the isotopic composition of the mantle. Mantle derived magmas in continental areas, however, often have high and variable initial Sr ratios (Brooks et al., 1976; Kramers, 1977). With specific reference to southern Africa primary Sr ratios from both acid and mafic phases of five intrusive complexes of different ages are reported by Davies et al. (1970). The initial Sr ratios of the intrusives (Table 7.6) which are possible derivatives of the upper mantle, all lie above the single stage upper mantle growth curve. The majority of the points lie along a line which has been drawn in accordance with a two stage model for the isotopic evolution of the continental crust. Because mantle derived magmas in continental areas have to traverse between 30 and 40 kilometers of sialic crust, the high and variable initial ratios (Table 7.6) may also be interpreted as being due to crustal contamination (Davies et al. 1970).

While the evidence for a two stage mantle development beneath southern Africa is not altogether conclusive, the author does believe that the data in Table 7.6 possibly reflect mantle isotopic heterogeneities. Lead and strontium isotopic patterns from South African cretaceous kimberlites and mantle derived xenoliths are interpreted by Kramers (1977) as providing strong evidence that the upper mantle beneath southern Africa is isotopically heterogeneous on a regional scale.

TABLE 7.6

Intrusive	Age	**Ro(Acid rocks)	**Ro(Mafic rocks)	Rb/Sr (Mafic rocks)
Great Dyke	2541 ± 30		0.7024 ± 0.0008	0.30
Bushveld	1954 ± 30	0.7153 ± 0.0088	0.7065 ± 0.0020	0.005
Losberg	1881 ± 282		0.7064 ± 0.0024	0.20
Trompsburg	1372 ± 142	0.7066 ± 0.0196	0.7043 ± 0.0004	0.005
Ushushwana	2874 ± 30	0.7029 ± 0.0036	0.7031 ± 0.0028	0.04
	2931 ± 38*	0.7009 ± 0.0136*		

*Excluding UC 11

**Ro - initial Sr^{87}/Sr^{86} ratios

After Davies et al. (1970).

7.4 Discussion of results

The Rb-Sr whole rock results fall into three well defined groups which are consistent with the division of the three Archaean rock types on the basis of geochemical and field evidence.

(a) Metabasites and metasediments of the Steynskraal metamorphic zone.

The mafic metamorphic rocks excluding the charnockitic gneisses yield an age of 3478 ± 130 m.y. and an initial Sr ratio of .7006 ± 0.0002. They are amongst the oldest known rocks in southern Africa and the age and initial ratio are comparable to those obtained from the Onverwacht formation of the Swaziland greenstone belt (Jahn and Shin, 1973).

Provided that the average Rb/Sr ratio of the mafic metamorphic rock suite has been preserved, which in the author's view is probable because of refractory nature of the mineral assemblages, then the low initial ratio of 0.7006 which is only slightly higher than the oceanic

mantle for this age, shows that these rocks did not form more than 200 m.y. before ∿ 3500 m.y. ago. It is concluded that the Rb-Sr isochron reflects the age of a group of rocks of both sedimentary and igneous origin, and of different ages, possibly formed over an extended period, and which have subsequently suffered isotopic homogenization ∿ 3500 m.y. ago. Further, the initial Sr ratio of the mafic metamorphic suite is significantly lower than the value suggested for the sub-continental mantle (3500 m.y. ago) by Davies et al., (1970) and provides evidence for mantle isotopic heterogeneities, rather than for two stage mantle development beneath southern Africa.

The Rb-Sr whole age agrees within experimental error with that obtained by the Th-Pb method (Welke et al., ms. in preparation). However, the initial Pb^{208}/Pb^{204} ratio (Table 7.5) is relatively high for rocks of this age and corresponds rather to a model age of 3000 m.y. (Stacey and Kramers, 1975). This implies that the mafic metamorphic suite of rocks had participated in a system with above-normal Th-Pb ratios prior to losing Th and taking on their present composition with normal to sub-normal Th-Pb values 3500 m.y. ago (Welke et al., ms. in preparation).

(b) Inlandsee Leucogranodiels

The initial Sr ratio of 0.7044 ± 0.0004 for the 2826 ± 32 m.y. old ILG lies well above the suboceanic mantle development line. In the light of the previous discussion, there are two possible explanations for the relatively high initial Sr ratio. The first possibility is that the ILG rocks were derived from a sub-continental mantle characterised by relatively high Sr initial ratios, and the second is that the ILG were derived from a mantle similar to that found beneath the oceans (with respect to Sr isotopes) long before 2800 m.y. ago, and subsequently developed in a crustal environment characterised by an average Rb/Sr ratio higher than that of the sub oceanic mantle. The

measured age of ∿ 2800 m.y. then relates to the time of cessation of an anatectic or metamorphic event which effected complete Sr isotopic homogenization. Assuming maintenance of the present day average Rb/Sr ratio of 0.20, the period of crustal residence prior to ∿ 2800 m.y. is given by linear extrapolation of the primary Sr ratio back to the oceanic mantle development line (as indicated in Fig. 7.6). This shows that the parent rocks may have had a crustal residence of ∿ 350 m.y., provided the average Rb/Sr ratio was preserved. If the ILG lost Rb at ∿ 2800 m.y. ago, then the duration of crustal residence prior to ∿ 2800 m.y. ago would be shortened, depending on the extent of the Rb loss. However there is no convincing evidence that the ILG rocks have lost Rb, except that these rocks have unusually high K/Rb ratios, especially for felsic rocks, which could be interpreted as being due to Rb loss.

Faced with these contrasting explanations how, do we then interpret the ∿2800 m.y. age obtained for the ILG? Fortunately, the Th-Pb isotopic data (Welke et al., ms. in preparation) provides a further constraint on the history of these rocks. Although the data for most felsic rocks from the Inlandsee area plot on an isochron giving an age of ∿ 3070 m.y., some of the felsic rocks (KK 14, VD 3, VD 5 and VT 211) fall on a steeper isochron, containing all the mafic metamorphic suite, and giving an age of ∿ 3540 m.y. (Table 7.5). On the basis of the high Sr initial ratio together with the Th-Pb isotopic data the ∿ 2800 m.y. Rb-Sr age is thus interpreted as a "metamorphic" age, whereby Sr isotopes were homogenized. A corollary of the Rb-Sr ∿ 2800 m.y. metamorphic age compared to the Th-Pb age is that in certain instances the Th-Pb isotopic system may remain unaffected by metamorphic conditions which otherwise result in Sr isotopic homogenization. In turn the extreme scatter of the data points on the Pb^{206}/Pb^{204} vs U^{238}/Pb^{204} diagram for some felsic rocks suggest that U is the most vulnerable of the radioelements to metamorphic influences.

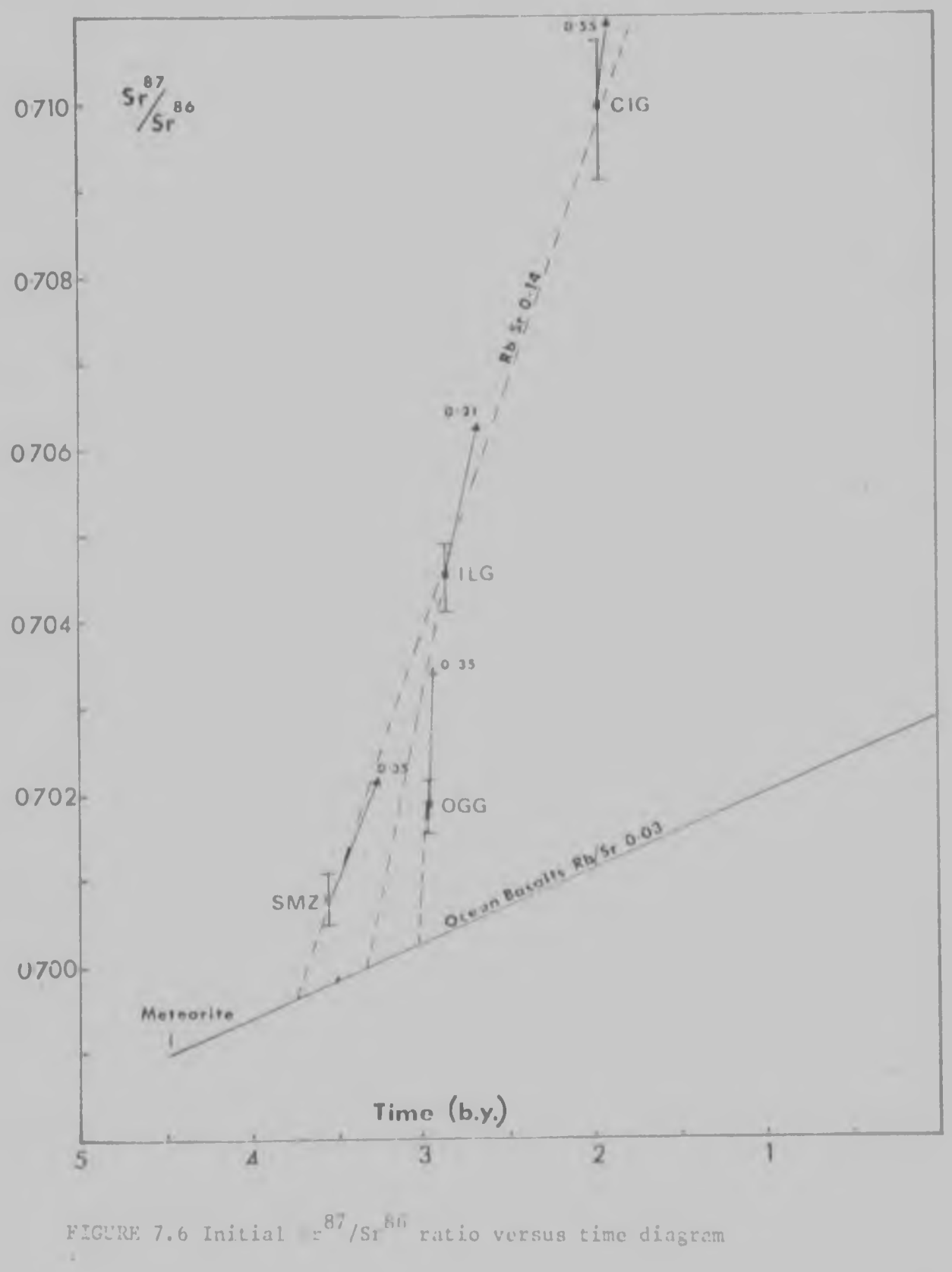


FIGURE 7.6 Initial Sr^{87}/Sr^{86} ratio versus time diagram

One of the most interesting features of the Rb-Sr geochronology of the lower Vredefort crust is the fact that the metamorphosed mafic inclusions, engulfed by granitic rocks which exhibit an age of ∿ 2800 m.y., have retained their older ∿ 3500 m.y. age. This suggests that because of the refractory nature of the mineral assemblages of the metasediments and metabasites, the Rb-Sr chemical system within the mafic metamorphic suite remained unaffected by the metamorphic event. This event nevertheless reset the Rb-Sr chemical system of the surrounding felsic rocks. Furthermore it is suggested that since an older age of ∿3500 m.y. is defined by the mafic inclusions, this rock suite has been characterised by a relatively dry mineral assemblage since 3500 m.y. ago.

(c) Outer granite gneiss

The relatively high present day average Rb/Sr ratio of 0.35, and low initial Sr ratio of ∿ 0.7010 (compared to suboceanic mantle) for the ∿ 3000 m.y. old OGG permits a prior crustal residence time of only ∿ 100 m.y. To account for a crustal residence for the OGG of any significant length (e.g. ∿ 500 m.y.) a pre-existing rock suite which an average Rb-Sr ratio of about 0.1 would be required. Thus on the assumption of retention of the Rb-Sr ratio during the OGG-forming event, it would appear that the OGG rocks were derived from the mantle shortly (less than ∿ 100 m.y.) before ∿ 3000 m.y. ago.

It has already been mentioned, however, that the above analysis is only valid if the average Rb content of the OGG today is the same as the average content at the time of initial separation from the mantle; there are two further criteria with respect to the OGG which must be examined before conclusions as to the origin and evolution of the OGG can be drawn. Firstly, the regional geology of the OGG indicates that these rocks have undergone a complex tectonic and metamorphic history (Chapter 2.2), which cannot easily be reconciled with a crustal history of only 100 m.y. prior to a ∿ 3000 m.y. metamorphic

One of the most interesting features of the Rb-Sr geochronology of the lower Vredefort crust is the fact that the metamorphosed mafic inclusions, engulfed by granitic rocks which exhibit an age of ∿ 2800 m.y., have retained their older ∿ 3500 m.y. age. This suggests that because of the refractory nature of the mineral assemblages of the metasediments and metabasites, the Rb-Sr chemical system within the mafic metamorphic suite remained unaffected by the metamorphic event. This event nevertheless reset the Rb-Sr chemical system of the surrounding felsic rocks. Furthermore it is suggested that since an older age of ∿3500 m.y. is defined by the mafic inclusions, this rock suite has been characterised by a relatively dry mineral assemblage since ∿ 3500 m.y. ago.

(c) Outer granite gneiss

The relatively high present day average Rb/Sr ratio of 0.35, and low initial Sr ratio of ∿ 0.7010 (compared to suboceanic mantle) for the ∿ 3000 m.y. old OGG permits a prior crustal residence time of only ∿ 100 m.y. To account for a crustal residence for the OGG of any significant length (e.g. ∿ 500 m.y.) a pre-existing rock suite which an average Rb-Sr ratio of about 0.1 would be required. Thus on the assumption of retention of the Rb-Sr ratio during the OGG-forming event, it would appear that the OGG rocks were derived from the mantle shortly (less than ∿ 100 m.y.) before ∿ 3000 m.y. ago.

It has already been mentioned, however, that the above analysis is only valid if the average Rb content of the OGG today is the same as the average content at the time of initial separation from the mantle; there are two further criteria with respect to the OGG which must be examined before conclusions as to the origin and evolution of the OGG can be drawn. Firstly, the regional geology of the OGG indicates that these rocks have undergone a complex tectonic and metamorphic history (Chapter 2.2), which cannot easily be reconciled with a crustal history of only 100 m.y. prior to a ∿ 3000 m.y. metamorphic

event. Secondly, although the Th-Pb whole rock isochron date of ∿ 3000 m.y. (Table 7.5) is in good agreement with the corresponding Rb-Sr age, the initial Pb^{208}/Pb^{204} ratio of 31.7 is anomalously low, and corresponds rather to a model age of 3500 m.y. (Stacey and Kramers, 1975). This suggests that the outer granite gneiss has participated in a Th-Pb system of low κμ values during a certain interval of time prior to gaining Th and taking on their present day κμ values ∿ 3000 m.y. ago. At that stage the Th/Pb ratios increased to normal- above normal values (Welke et al., ms. in preparation). It must be mentioned that all of the discussion on Pb^{208}/Pb^{204} initial ratios is dependent on the existence of mantle homogeneity, and mantle heterogeneities would nullify most of this latter argument.

(d) Central intrusive granite

The age and initial Sr ratio of the CIG provides information not only on the time of the Vredefort doming event, but also on the evolution of crustal material under conditions of partial melting.

The point defined by the CIG samples lies on a steep initial Sr ratio versus time development line (Fig. 7.6) common to the Vredefort lower crust (SMZ + ILG) The slope of the line is characterised by a Rb/Sr ratio of 0.14, which closely approximates the crustal average of 0.15 (Armstrong, 1968).

A similar alignment of points on a Sr^{87}/Sr^{86} versus time plot for granitic rocks from the Archaean basement of Swaziland has been interpreted by Davies and Allsopp (1976) as evidence for repeated metamorphism and Sr isotope homogenization within the sialic crust. The high initial Sr ratio, and the fact that (on a Sr^{87}/Sr^{86} versus time diagram) the point for the CIG samples plots on the strontium development line, is compatible with such a model and suggests that this small intrusive granite has a genetic relationship with the surrounding country rocks.

The occurrence of the central intrusive biotite granite in the central regions of the structure provides conclusive evidence for a thermal event in the deeper regions of the Vredefort crust at 1950 m.y. ago. This age could be interpreted as being a minimum age for the time of formation of the Vredefort structure.

7.5 Movement of LIL elements in the Vredefort crust

On the basis of the geological evidence, and [illegible] the anomalously low initial Pb^{208}/Pb^{206} ratio obtained for the [illegible] the Th-Pb whole rock isochron, [illegible] m.y.) characterised by relatively low Rb/Sr and Th/Pb ratios and normal U/Pb ratios, is suggested for the OGG. The time of ascent of the LIL elements into the enriched upper zone of the OGG, [illegible] .W. sector, occurred prior to, or at the time given by the Rb-Sr, U-Pb and Th-Pb whole rock isochron dates of 3000 m.y.

While the lower crust (ILG + SMZ) have suffered episodic loss of uranium and possibly Th, this episode cannot be convincingly correlated with the entry of LIL elements into the upper crust. Welke et al., (pers. in preparation) demonstrate that the melt metasomatic veins, as well as a large proportion of the felsic ILG samples suffered Th loss ∿ 3500 m.y. ago. These rocks could therefore only have served as a Th source for the OGG if the transfer of thorium took place at least 3500 m.y. ago.

The upper regions of the OGG, particularly in the South-West, have a "uranium prehistory" which is sharply complementary to that of the SMZ and ILG. It might be conjectured that the uranium lost by the SMZ and ILG "parent" was gained by the OGG when it took on its present form ∿ 3000 m.y. ago, but the time of uranium loss (∿ 3500 m.y. ago) from the lower crust contradicts this conjecture.

There is no convincing evidence that Rb loss from the lower crust has occurred. However the Rb/Sr isotopic data from the lower crust suggests that: firstly, the mafic metamorphic suite have retained their Rb content since ∿3500 m.y. ago and secondly, that if the ILG had lost Rb, this most probably occurred at around 2800 m.y. ago, although Rb loss from the ILG prior to ∿ 2800 m.y. ago cannot be excluded.

What then is the source of LIL elements in the enriched upper zone of the OGG?

Geochemical evidence suggests that the lower regions of the OGG have lost substantial amounts of U and, to a lesser extent, Th which are thought to have been redistributed via fluid phases during partial melting processes operating within the OGG. As yet, however, there is not enough isotopic evidence to quantitatively test this hypothesis. The source of the Rb in the OGG remains an enigma; the relatively high present day average Rb/Sr ratio (which includes both the upper and the lower OGG) suggests that these rocks have gained Rb on a regional scale in order to account for a crustal residence of ∿ 500 m.y. prior to 3000 m.y. ago.

The present-day location of the uranium lost from the ILG + SMZ at ∿ 2800 m.y. remains an unsolved problem. The author suggests however that there might be some genetic link between the uranium loss in the lower crust, and those samples with anomalously high radioelement concentrations (KK 16 and VT 127) occurring in the outer regions of the SMZ which result in a "hump" at the 9 to 10 km depth zone of the radioelement profile (Fig. 5.2). There is also isotopic evidence for one of these samples (KK16) incurring uranium gain at ∿ 2800 m.y. (Welke et al., ms. in preparation).

8 INTERPRETATION OF RESULTS

8.1 Models for the evolution of the Vredefort crust

The geochemical, geochronological and geological evidence is now examined with the aim of reconstructing the history of the Archaean basement rocks exposed at the Vredefort dome. Two models for the evolution of the Archaean crust providing possible explanations for the data obtained in this study are outlined below. A schematic view of these models is given in Fig. 8.1 and 8.2, and are summarized in Table 8.1.

The early (pre ~ 3.6 b.y.) history for both models is the same (Fig. 8.1A and 8.2A): the crust consisted of a thin (5 to 10 km) sequence of sedimentary supra-crustals and interlayered basic to intermediate volcanics. This thin primordial crust was invaded and largely broken up by sialic material derived from the mantle, during a major period of crust-mantle differentiation close to 3.6 b.y. ago.

In Model I the 3.6 b.y. old proto sialic crust was still relatively thin (15 to 20 km)(Fig. 8.1B) and was characterised by geological and major element features observed in the lower Vredefort crust (ILG) today, except that the rocks had not as yet obtained granulite facies metamorphic conditions; thus the ILG + SMZ precursor had a non-depleted geochemical character with 'normal' contents of U, Th and Rb. The precursor for the upper crust (OGG) represents either juvenile igneous rock derived directly from the mantle shortly before 3.0 b.y. ago, (which is the case shown in Fig. 8.1C and D) or a slab of pre-existing crust mechanically emplaced on top of the lower crust (ILG) precursor. The actual mechanism of emplacement of this upper crust is not specified; it will suffice to say that its emplacement was concommitant with downward movement of the lower crust precursor to the depth required for granulite facies metamorphism, with consequent upward loss of LIL elements.

In Model II most of the sialic crust is differentiated from the mantle early on in the earth's history, and no further significant addition of mantle

TABLE 8.1 Summary of Models

Model I

A. Pre 3.6 b.y. primordial crust.

B. The formation of a relatively thin proto sialic crust ~ 3.6 b.y. ago.

C. and D. Progressive addition of juvenile sialic material from the mantle to the upper sequences of the crust, with the major phase of crust accretion occurring shortly before 3.0 b.y. ago. This juvenile material had a non-depleted character with respect to LIL elements compared to the upper crust today.

E. The upper crust undergoes extensive partial melting and differentiation (especially with respect to LIL element-solid squares) to form the OGG at ~ 3.0 b.y. ago.

F. The addition of material to the upper crust pushed the lower crust (Parent to the LGG) down to depths required for granulite facies metamorphism, with the consequent upward loss of volatiles and uranium close to 2.8 b.y. ago, to form the crust as is seen today. In this model the present day location of the U lost from the lower crust is not specified.

Model II

A. Pre 3.6 b.y. primordial crust.

B. Major emplacement of a thick (35 km) sialic crust ~ 3.6 b.y. ago. At this stage the upper levels of this primitive crust must have had chemical compositions fundamentally different (in terms of LIL elements) to those seen in the upper crust in later geological times. The primordial crust is highly fragmented and spaced out in a thickening crust e.g. the reference frame in Fig. 8.1A suffers a relative downward motion from a depth of 5 to 10 km to a depth of nearly 15 km (Fig. 8.1B).

C. Shortly after 3.6 b.y. ago volatiles together with LIL elements begin to move upwards from the lower crust (Parent to LGG) into the upper crust (Parent to OGG). The increased volatile and radioelement content in the upper crust induces partial melting.

D. Final termination of partial melting in the upper crust at ~ 3.0 b.y. resulting in the formation of the OGG. (The lower crust (LGG) is left relatively depleted in LIL element.) Stage B represents the crust observed today.

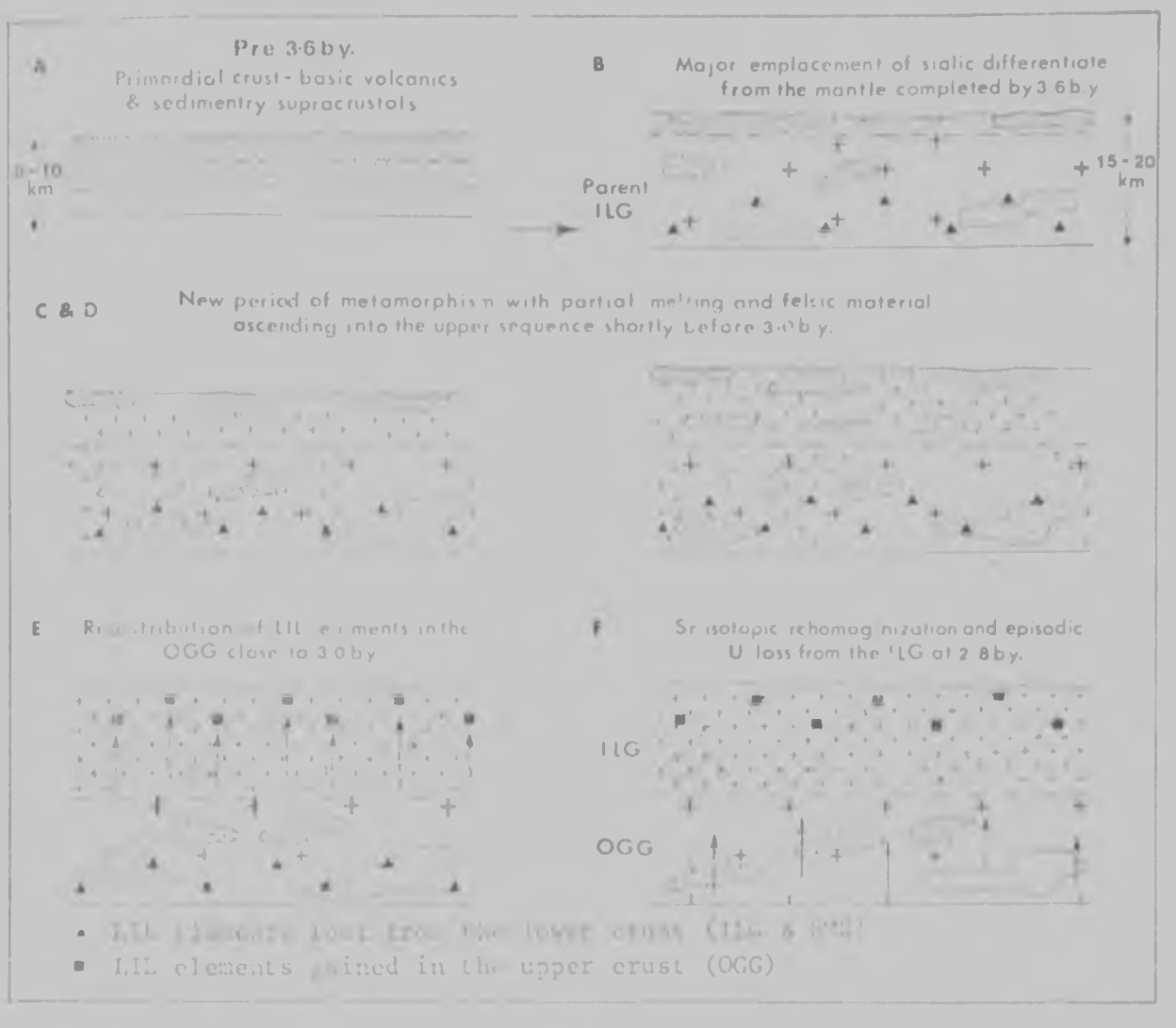


FIGURE 8.1 Model I for the evolution of the Vredefort crust

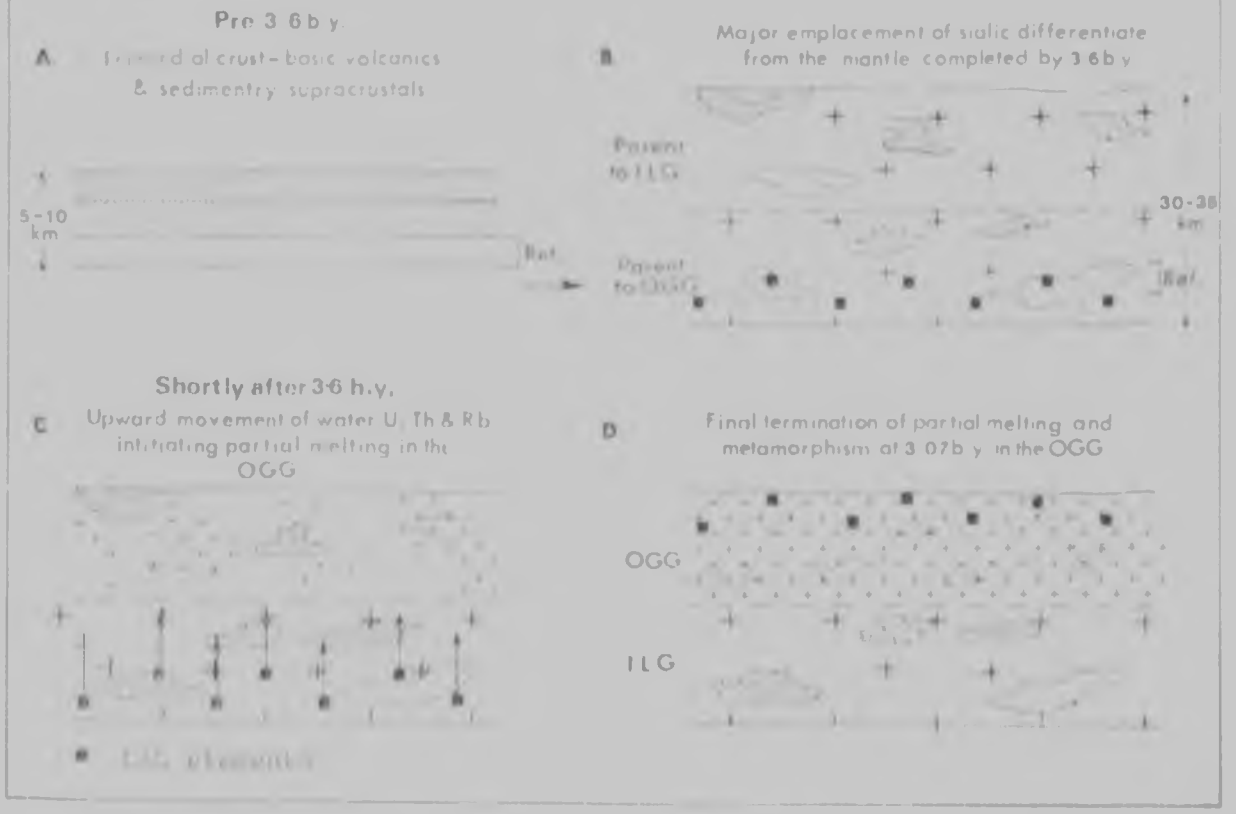


FIGURE 8.2 Model II for the evolution of the Vredefort crust

material to the crust occurs subsequent to the ∿ 3.6 b.y. crust forming event. (A major difference between the two models is that in the former model further addition of sialic material, and crustal thickening, is regarded as essential.) The sialic magma invaded the primordial ~~sialic~~ mafic crust, causing its fragmentation, and resulting in the formation of a 35 km thick continental crust, consisting of fragments of sedimentary supracrustals and mafic volcanics enclosed by a silicious ILG type granite (Fig. 8.1B). At this stage the upper crust must have had chemical compositions fundamentally different (in terms of LIL elements) to those seen in the upper crust in later geologic times. The younger OGG formed largely by anatexis of the upper levels of this primitive crust.

Model II requires that the felsic differentiates of the lower crust were emplaced into a high pressure - high temperature environment where granulite facies metamorphism prevailed. This implies that the geochemical characteristics of granulite facies rocks of the lower Vredefort crust are characteristic of the chemistry of the early protocrust rather than a product of high grade regional metamorphism. This possible explanation for the evolution of granulite facies rocks was first proposed by Heier(1976). The mafic inclusions caught up in the transfer of sialic material into the crust suffered a relative downward motion by virtue of being "spaced out" in a thickening crust, and thus attained granulite facies metamorphism. U, Th and Rb introduced into the lower crust during crust-mantle differentiation were incompatible with their high pressure environment, and started to move upwards along with the hydrous components as the lower crust began to crystallize. The continuous introduction of volatiles into the upper crust induced partial melting, whereby the basic volcanic and sedimentary remnants in the upper crust were extensively remobilized and mixed in with the more felsic components resulting in the complete isotopic homogenization of the upper crust (the OGG). This event culminated ∿ 3.0 b.y. ago.

What is the source of the LIL elements which started to move into the upper crust during the strong reworking? They are presumed to have

originated in episodes of LIL-element expulsion from deeper crustal levels. Model II has (thus far) no obvious explanation for their initial concentration in the lower crust, and their relative depletion in the upper crust.

8.2 Summary and Conclusions.

The findings of this study are now summarized, with the aim of evaluating the proposal of a Vredefort 'crust on edge model' and genetic schemes for the evolution of the Vredefort crust.

Rocks of the granulite facies have been proposed by many previous writers as a major constituent of the lower crust. Accepting the framework of a 'crust on edge model', it is noteworthy that at Vredefort the principal metamorphic facies lie in their expected vertical sequence, with granulite facies rocks occurring in the central regions of the Vredefort dome (Fig. 2.5, Chapter 2).

(a) Geochemistry of the middle Vredefort crust (ILG + SUZ)

In the Vredefort middle crust (exposed basement from 10 km to 15 km below the Orange Grove quartzite) rocks of granitic composition (in granulite facies) predominate. In this part of the Vredefort basement, mafic granulites constitute a lesser proportion than felsic rocks. The character of the mafic granulite relicts indicates that most of them were probably supracrustal strata before reconstruction of the middle crust took place (Fig. 8.1A and 8.2A).

The surrounding quartzo-feldspathic ILG rocks are characterised by a felsic mineral assemblage, and low concentrations of ferromagnesian minerals. The major element chemistry of the ILG shows little variation over the area sampled.

The ILG rocks have unusually high K/U and Th/U ratios and high K/Th, K/Rb and Ba/Rb ratios. These ratios are consistent with the concept of strong depletion of U and to a lesser extent Th and Rb during metamorphism only if the primitive rocks at some time prior to metamorphism had

an overall lithophile element content similar to that of typical felsic upper crustal rocks currently exposed at the earth's surface. "Normal" K/U, Th/U and K/Th ratios in the mafic inclusions, indicating that for these rocks Th and U have not been depleted relative to K, suggest that the mineral assemblages of the rocks had a strong control on the behaviour of Th and U during metamorphism. I conclude that U and Th were located in the rockforming minerals of the mafic rocks, whereas in the surrounding quartzofeldspathic rocks Th and U occupied interstitial sites.

The questions of the time of U (with Th and Rb) loss and subsequent U gain elsewhere in the Vredefort crust is discussed after the isotopic data are summarised.

(b) Geochemistry of the Outer Granite Gneiss

On average the OGG zone shows a slight but nonetheless significant increase in cafemic character with depth. The distribution of the alkali earth elements Ba and Sr shows a strong positive correlation with the major oxides Na_2O and Al_2O_3, which therefore suggests that Ba and Sr contents are controlled by the plagioclase feldspar content. Both Ba and Sr exhibit trends expected from a crust on edge profile, i.e. they are relatively enriched in the lower Vredefort crust and fall off sharply towards the margin. The linear relationship between Ba and Sr (Fig. 4.8) as well as the observed relationships between the refractory elements such as Fe and Zr (Fig. 4.1) are commonly ascribed to partial melting processes (eg. McCarthy, 1976).

The distribution of the lithophile elements over the upper 8 km of the Vredefort crust conforms to an exponential decrease with depth, and shows a roughly inverse correlation to the more refractory elements such as Ba and Sr. Like the ILG, the lower half of the OGG has unusually high K/U and Th/U ratios, as well as high K/Th, K/Rb and Ba/Rb ratios and it is only the outer 5 km of the Vredefort basement granite that has absolute

element abundances and interelement ratios that approach values obtained for near-surface shield rocks in other continents. It is proposed that the lithophile elements in the OGG have been redistributed via fluid phases released during metamorphic and partial melting processes in the upper crust.

The geochemical trends observed in the OGG are consistent with expected trends through a section of the upper and middle crust, and support a partial melting model for the reconstitution of the upper middle crust, at least in this area. I believe that these partial melting processes, and the "granitization" of supracrustal strata, were largely restricted to the upper crust (OGG), possibly due to higher concentration of volatiles, while the lower crust, which remained in a relatively dry environment, was therefore better able to resist partial melting processes (Model II, Fig. 8.2C). The above contention is born out by the fact that in the lower crust, rocks of extremely different compositions (ILG + SMZ) have retained their isotopic identity over the past ~ 3.5 b.y. whereas the OGG was homogenized (at least for the Sr and Pb isotope systems) at 3.0 b.y. ago.

(c) Heat production and the implications for continental heat flow

The distribution of the radioelements and the distribution of heat production with depth over the outer 8 km of the Vredefort crust is consistent with an exponential dependence on depth; it is consistent with the theoretical model of an exponential fall off of heat production with depth proposed by Lachenbruch (1968, 1970). This in turn lends weight to the Vredefort 'crust on edge' model.

The heat production from the exposed profile in the Vredefort basement, together with the stratified rocks of the Carletonville area (upper 20 km) is considerably greater than previous estimates of the heat production in the crust.

Most of the heat production, especially in the lower 7 km of the

Vredefort basement profile, comes from thorium decay. The significantly greater Th concentrations in the middle crust reported in this study, compared to results obtained by other workers, arise possibly from some bias in previous middle crust sampling towards mafic granulite horizons.

The heat production of the lower 16 km of the crust is partly conjectural. However, assuming the preferred heat production model LCB, (Ch.6) then the total contribution to surface heat flow for a 36 km continental crust is 0.85 HFU. The heat flow from beneath the mantle has been calculated at between 0.35 (Model LCA) and 0.25 (Model LCB) in the Carletonville area.

Using this mantle heat flow value the thickness of the lithosphere below the southern African shield has been calculated at approximately 300 km, following the method of Sclater(1972).

(d) Geochronology

The oldest Archaean rocks in the Vredefort basement are the mafic xenoliths which yield Rb-Sr and Th-Pb whole rock ages of ~ 3.5 b.y. The mafic metamorphic suite is thought to represent ancient metasedimentary supracrustals and pyroxene granulites that were caught up and preserved in a highly siliceous material (IIG) differentiated from the mantle shortly after ~ 3.6 b.y. (Fig 8.1b and 8.2b).

The fact that rocks of both sedimentary and igneous origin (from the Steynskraal Metamorphic Zone) have shared a common Rb-Sr isotopic history since ~ 3.5 b.y. ago, suggests that the measured age represents a time of isotopic rehomogenization. The scatter on the Rb-Sr errorchron may indicate that isotopic homogenization was only partially attained. The duration of crustal residence prior to ~ 3.5 b.y. remains an enigma: the low Sr^{87}/Sr^{86} initial ratio suggests that these rocks formed shortly before 3.5 b.y. On the other hand, the relatively high Pb^{208}/Pb^{204} initial ratio suggests that these rocks participated in an extended period of high μ prior to 3.5 b.y. Alternatively, the high μ values may have

been inherited directly from the mantle, which in turn implies considerable heterogeneities within the mantle in 3.5 b.y. times.

The high initial Sr^{87}/Sr^{86} ratio of the ILG suggests that these rocks have had a crustal residence of at least 500 m.y. prior to the measured Rb-Sr whole rock age of .8 b.y. This viewpoint is supported by the observation that some of the felsic rocks lie on a steeper Th-Pb isochron yielding an age of 3.5 b.y. The scatter of the data points for the U-Pb plot provides evidence for substantial uranium loss. The time when most of the U was lost has been calculated at about 2.8 b.y. ago. (Welke et al., ms. in preparation).

The Rb-Sr whole rock age of 3.0 b.y. for the OGG agrees with the ages obtained by the Th-Pb, U-Pb and Pb-Pb whole rock isochrons. The primary ratio for the Rb-Sr isochron is characteristic of the oceanic mantle for 3.0 b.y. times and is consistent with the [illegible] model that the OGG was derived from the mantle shortly before 3.0 b.y. ago (Model I).

The anomalously low Pb^{207}/Pb^{204} initial ratio would then be interpreted as being inherited from the mantle, which implies a heterogeneous mantle prior to 3.0 b.y. The above interpretation of the data however do not reconcile with the field evidence, which indicates that the OGG has participated in a long and complex thermal and tectonic history prior to 3.0 b.y. ago. A 600 m.y. crustal history characterised by relatively low [illegible] values and normal [illegible] prior to 3.0 b.y. ago, followed by a [illegible] event to the high [illegible] values observed today is the preferred interpretation. Thus a general 3.0 b.y. enrichment of LIL elements (particularly in the S.W. sector) is the suggested explanation (Model II).

8.3 Implications for the evolution of the early Precambrian crust

The conclusions of this study have a direct bearing on two of the main problems concerning the evolution of the early Precambrian crust.

been inherited directly from the mantle, which in turn implies considerable heterogeneities within the mantle in 3.5 b.y. times.

The high initial Sr^{87}/Sr^{86} ratio of the ILG suggests that these rocks have had a crustal residence of at least 500 m.y. prior to the measured Rb-Sr whole rock age of ∿ 2.8 b.y. This viewpoint is supported by the observation that some of the felsic rocks lie on a steeper Th-Pb isochron yielding an age of ∿ 3.5 b.y. The scatter of the data points for the U-Pb plot provides evidence for substantial uranium loss. The time when most of the U was lost has been calculated at about 2.8 b.y. ago. (Welke et al., ms. in preparation).

The Rb-Sr whole rock age of ∿ 3.0 b.y. for the OGG agrees with the ages obtained by the U-Pb, Th-Pb and Pb-Pb whole rock isochrons. The primary ratio for the Rb-Sr isochron is characteristic of the oceanic mantle for 3.0 b.y. times and is consistent with the model that the OGG was derived from the mantle shortly before 3.0 b.y. ago (Model I).

The anomalously low Pb^{206}/Pb^{204} initial ratio would then be interpreted as being inherited from the mantle, which implies a heterogeneous mantle prior to 3.0 b.y. The above interpretation of the data however do not agree with the field evidence, which indicates that the OGG has participated in a long and complex thermal and tectonic history prior to ∿ 3.0 b.y. ago. A ∿ 600 m.y. crustal history characterised by relatively low Rb/Sr ratios and μ values and normal μ prior to 3.0 b.y. ago, followed by a striking increase to the Rb/Sr, μ and μ values observed today is the preferred interpretation. Thus a general ∿ 3.0 b.y. enrichment of LIL elements (particularly in the S.W. sector) is the suggested explanation (Model II).

8.3 Implications for the evolution of the early Precambrian crust

The conclusions of this study have a direct bearing on two of the main problems concerning the evolution of the early Precambrian crust.

(i) The strontium and lead isotopic ages and initial ratios bear directly on the question of movement of material between crust and mantle and taken together with the geological evidence, strongly suggest that the sialic crust in southern Africa was derived during a major period of mantle differentiation close to 3.5 b.y. ago (Model II). The observed variations in ages and initial ratios and the geochemical variations (especially in the OGG) are thought to be the result of subsequent large scale reconstitution of the crust due to metamorphic and partial melting processes which occurred close to 3.0 b.y. ago. The preferred Model II provides a satisfactory explanation for a long and complex pre 3.0 b.y. old crustal history for the OGG, for the complementary nature of relative enrichment of U in the upper CGG, and for the relative depletion of U in the lower Vredefort crust (ILG + SMZ). In Model II the accent of the LIL elements, especially U to the enriched upper zone of the OGG was completed close to 3.0 b.y. ago. However, constraints on the time at which the granulites appear to have suffered episodic U loss (2.8 b.y.) present a difficulty in correlating this episode with the entry of LIL elements into the upper regions of the OGG and is a serious limitation to the acceptance of this model.

The isotopic results for the Swaziland Precambrian gneissic rocks (Davies and Allsopp, 1976) are in many ways comparable to the results obtained in this study. Rb-Sr whole rock for the Swaziland granite gneisses in the range from 3400 to 3100 m.y. lie on a steep initial Sr^{87}/Sr^{86} ratio versus time development line that intersects the oceanic mantle development line at 3500 m.y. ago. The rocks from the central part of the Vredefort dome (ILG + SMZ) lie on a similar steep initial Sr^{87}/Sr^{86} ratio versus time development line. The preferred interpretation for the Swaziland rocks is that, locally, the sialic crust did not begin forming much before 3500 m.y. ago and that various gneissic rocks defining this steep development line attained their present state by repeated metamorphism and Sr isotopic homogenization within the early sialic crust. These views are similar to my

interpretation for the development of the felsic rocks in the central region of the Vredefort basement. The isotopic data for the OGG, on the other hand, are in close alignment with the data for the younger granites from the Eastern Transvaal (De Gasparis, 1967; Davies, 1970 and Oosthuysen, 1970). The initial ratios for these rocks all lie to the right of the Sr^{87}/Sr^{86} development line for the Swaziland gneisses (Davies and Allsopp, 1976) and are also outside the basalt field. The interpretation of the isotopic data for the OGG, as well as those of the Eastern Transvaal granitic rocks has already been discussed in depth. Other similarities exist between the uppermost portion of the Vredefort basement, and the younger granites from the Eastern Transvaal. For example, the average composition of the Nelspruit migmatites (Viljoen and Viljoen, 1969b) closely approximates the average chemical composition of the OGG (Table 4.5). A similar degree of correspondence is available when comparing the OGG with the granodiorites, gneisses, minor tonalite and porphyritic granites found in the granitic terrain north of Johannesburg (Anhaeusser, 1976). A close resemblance between the OGG and the felsic rocks of the Johannesburg Dome is also observed in the field.

(ii) The second major problem concerns the nature and composition of the early Archaean crust. Engel (1963) outlines the two main hypotheses on the origin of the earth's primitive crust. The first postulates a thin proto crust of sialic material formed early in the earth's history during rapid mantle crust differentiation, while the other theorizes that primordial differentiation was less complete, and resulted in the development of a 'proto crust' which was more basaltic in composition.

A mass of information has been advanced to support both hypotheses from workers in the other early Precambrian shield areas of Canada, western Australia, central America and the North Atlantic craton. In most Precambrian regions, the oldest rocks are largely high grade gneisses, while the apparent ages of the greenstone belts are invariably younger.

Sutton (1967) suggests the same of the earliest known Precambrian metasediments come from the north-east segment of the Baltic shield in the Kola Peninsula of the U.S.S.R., where a variety of psammitic and peltic rocks were in existence before metamorphism 3600 to 3200 m.y. ago. It was the popular belief that the source rocks from which these sediments were derived might approach 4000 m.y. in age, although no crust older than 3600 m.y. would be encountered because of extensive reworking during this early period of crustal history. More recently a Rb-Sr whole isochron ages of 3750 ± 50 m.y. for the Amitsoq gneisses in West Greenland (Moorbath et al. 1972) 3643 ± 102 m.y. from basement dykes which cut Limpopo mobile belt gneisses in South Africa (Allsopp et al. 1977) and 3622 ± 72 m.y. for the Uivak gneisses from Northern Labrador (Bridgwater and Colerson, 1976) have been obtained, and provide the first direct evidence of a granitic crust prior to 3600 m.y. age.

The ∿ 3400 m.y. Ancient Gneiss Complex, Davies and Allsopp (1976), represent some of the oldest rocks exposed in Southern Africa. No definite age relationship has been established between the Ancient Gneiss Complex and the adjacent greenstone belt (Swaziland Supergroup) because of faulting between the two. Hunter (1972, 1974b) considered the former to be older and to represent a group of supracrustal rocks deposited in an area of rapid erosion, transport and deposition accompanied by the extrusion of mafic and ultramafic magma. One or more periods of intense metamorphism, granitization and tectonism, that predate the Swaziland Supergroup, followed.

In contrast Anhaeusser (1973) contends that the greenstone belts, which are particularly well preserved in the Barberton Mountain Land, are older than the Ancient Gneiss Complex. Anhaeusser (1973) points out that <u>nowhere</u> can it be demonstrated that the lower volcanic assemblages of the greenstone belts overlie granitic crust. Further he notes that the ages of these lower volcanic assemblages are relatively imprecisely

known because of geochronological difficulties encountered in dating rocks of this type. The main facets of southern African early Precambrian crustal evolution are summarized by Anhaeusser (1973) as follows:

(i) The lower ultramafic unit of the Transvaal and Rhodesian greenstone belts is thought to have represented a primordial oceanic-type crust. The age of this thin (± 5 to 7 km) primordial crust is unknown but is considered to be well in excess of 3400 m.y. old.

(ii) The mafic-to-felsic units subsequently demonstrate characteristics analogous to modern-day island arcs.

(iii) Incipient granitic development resulted from partial melting of the primitive lithosphere and gave rise to the early Na-rich porphyry bodies which, in turn, became calc-alkaline in character as island arc-like development continued and the crust thickened (± 12 to 18 km).

(iv) The earliest sedimentary rocks comprised mainly chemical precipitates (banded iron formation, chert, minor carbonates) as well as volcanogenic debris (tuffs, epiclastics).

(v) The primitive granites invaded the primordial crust causing its fragmentation and migmatization.

(vi) Regular intrusion of granitic rocks, diapirism, rheomorphism, anatexis, and metasomatic transformation of greenstone relics. The evolution of the granitic rocks was accompanied by a progressive introduction of elements such as U, Th and Rb, with K in particular, being added in increasing amounts.

(vii) Protocontinental segments evolved in the waning phases of island arc-like development. Crustal thickening continued and protocontinental segments aggregated to produce the third, stable, cratons (~ 20 to 37 km). In Anhaeusser's model, the development of the African subcontinent shows a continued evolution from an oceanic to a continental crustal setting, involving mainly chemical differentiation processes,

the latter leading to the production of thicker, more stable crustal fragments which nucleated to form the crystalline shield.

At Vredefort, the presence of pre 3.5 b.y. old metabasites and metasedimentary supra crustals, preserved under dry granulite facies conditions in the lower crust, provide strong evidence of a mafic proto-crust that has been subsequently enveloped by granitic material differentiated from the mantle. Whether the mafic metamorphic suite of the lower Vredefort crust has a chemical affinity with greenstone belts can only be tested by rigorous geochemical comparisons and this is recommended as a further investigation in the Vredefort basement.

APPENDIX A

Isotope Dilution

A.1 Chemical analyses

The chemical extraction of Rb and Sr was performed in a sealed laboratory, the air being electrostatically filtered. High purity chemical reagents were used in all cases. All pyrex glassware, platinum and teflon beakers were cleaned rigorously by boiling in 6 N HCl and then in deionized water.

The effectiveness in eliminating any serious contamination during the course of the chemical processing is demonstrated by periodically measuring blanks. Blank measurements showed that typical contamination levels from all sources was about 0.01 µgm for Rb, and 0.06 µgm for Sr. Contamination of this order of magnitude introduces negligible error in both Rb and Sr analyses. Homogeneous rock powders (0.5 to 1 gm) were dissolved in HF and $HClO_4$. After silica was removed as SiF_4, and subsequent evaporation to dryness, the residue was dissolved in 6 N HCl. The solution was then homogenized and split into 3 separate aliquots. Two of the aliquots were spiked with Rb^{87} and Sr^{84} tracers respectively for the determination of concentrations by isotope dilution. The Sr^{87}/Sr^{86} ratios were determined directly from an unspiked aliquot. Sr was extracted by cation exchange techniques using Bio-Rad 50 x 8, 200-400 mesh. cross-linked resin and HCl eluant. Rb separation was carried out by decanting the supernatant liquid, after allowing a crystalline precipitate of alkali perchlorate to form. After rinsing, the precipitate was ready for mass spectrometry.

In the case of the mafic granulites the chemical methods were slightly different: because of the exceptionally low Rb concentrations in these rocks it was necessary to dissolve large amounts of sample. Because of this, as well as the unusual mineral composition of mafic granulites, complete dissolution was not always obtained. This pre-

TABLE A.1 Specifications of Mass Spectrometers Used in this Study

	BPI-DTM	MAT-CH4	UPDATED BPI-DTM	VG-MICROMASS
Tube radius and degree of curvature	9"/60°	9"/60°	9"/60°	12"/90°
Accelerating voltage	3.2 Kv	3.0 Kv	5.3 Kv	8.0 Kv
Fine mass selection	Manual peak switching of magnet current		Pre-select Hall probe gauss meter	Pre-select Hall probe gauss meter
Ion beam detector	Faraday cup with 7.3.E			
Source	Solid source thermal ionization			
Filaments	Double	Double	Triple	Triple

sented difficulties in homogenising the solutions before splitting, resulting in poor duplication of results. The problem was overcome by making separate dissolutions for Rb and Sr concentration determinations. However, this introduced a problem of sample powder homogeneity which is difficult to overcome. In most cases the concentrations of Rb and K in the mafic granulites were so low that no $KClO_4$ precipitate formed. In these instances concentrated ammonia solution was added to the sample, which was in solution in dilute HCl. Precipitation of unsoluble hydroxides (largely Fe, Al and Si) occurred and the precipitates removed by centrifuging. The supernatant was dried, excess ammonia salts volatilised, leaving a residue sufficiently enriched in Rb to permit analyses by mass-spectrometry.

The preparation and calibration of spikes are described in detail by Barrett (1974). A similar procedure was followed in preparing spike solutions for both Rb and Sr. A weighted amount of spike was dissolved in pure 2.6 N HCl to give solutions of the desired concentrations. The solution is then calibrated accurately by isotope dilution against a standard prepared from Johnson & Matthey 'specpure' salts.

A.2 Instrumentation

Four different mass spectrometers were used during the course of this work. The specifications are given in Table A.1.

Early in the work the Bernard Price Institute DTM (based on the design by the Department of Terrestrial Magnetism) was used for Rb concentration determinations, while the MAT-CH4 was used exclusively for Sr work to avoid contamination with Rb spike. Later the Bernard Price Institute DTM was updated and was then used to determine both Rb and Sr concentrations. The MAT-CH4 was replaced by a VG-Micromass 30 spectrometer which was used for natural strontium determinations. The mass spectrometer used for a specific analysis is indicated in the data tables.

For both the BPI-DTM and the MAT-CH4, data collection was carried out by means of a chart recorder system. In the case of the MAT-CH4 a Leeds & Northrup recorder was modified to incorporate an expanded scale system that allowed a tenfold increase in precision of Sr isotope ratio measurements. The expanded scale system was employed for all Sr^{87}/Sr^{86} measurements carried out on the MAT-CH4. The data obtained on the VG-Micromass was recorded on a digital output display, and then printed on roll paper. The BPI-DTM was later modified to digital output, coupled with an on-line computer.

Loading procedures on all four machines were similar. Each sample was run on a new filament, Re for Sr and Ta for Rb. Sr samples were loaded on to the filament by dissolving the ion exchange residue in dilute HCl, whereas for Rb the sample was taken up in water.

In the case of the BPI-DTM and the MAT-CH4, the filaments were encased in a metal cartridge provided with a slit through which the beam is emitted. For the VG-Micromass, 3 filaments are mounted on metal struts which are embedded in a glass bead (Figure A.1). The source of the updated BPI-DTM was also modified to this filament mounted on glass beads. (For further modifications see Table A.1).

A.3 Data Reduction

Early in this work all data were recorded on chart paper and ratios and isotope abundances calculated by measuring the peak heights recorded. With the acquisition of a Data General Nova 1210 on-line computer (with 16K memory), all isotopic ratios measured on the updated BPI-DTM were directly processed. The programme is written in the Basic language (Stacey and Hope, 1975) and is sufficiently flexible to be used for multiblock analyses of any spectrum containing from two to five peaks. Separate programmes have been written for the Nova 1210 to process digital data obtained from the VG-Micromass.

Programmes of the least squares method of York (1966) for computing the best fit isochron for a data set have also been written. Using this method the slope and intercept of the isochron was determined. Thereafter the age, taking $\lambda = 1.4 \times 10^{-11}$ years^{-1} (BPI practice to conform with new uranium decay constants (Jaffey et al., 1971) were calculated.

In calculating a Sr isochron age, the best fit straight line is fitted to a set of points which are not exactly colinear. The method used (York, 1966) takes into account random errors in both the X and Y coordinates. The regression technique of York (1966) derives its errors in the calculated slope and intercept strictly from the distribution of the data points, which is considered to be more realistic than the regression technique of Nicholls (1969) where the errors are derived from the correlated experimental errors of the data (Allsopp pers. comm.).

The regression calculations must make allowances for pre-determined experimental errors in x and y. The estimate of the experimental errors of Rb^{87}/Sr^{86} and Sr^{87}/Sr^{86} are derived from a consideration of the range in variation in the duplicated values. For twenty duplicate analyses, the range [illegible]. However, the isochron errors resulting from the regression analyses are given at 1σ levels, therefore the experimental errors assigned as weighting factors to the ordinate and the abscissa must also be introduced at the confidence interval of 1σ magnitude. Therefore two-thirds of the value quoted as the range or deviation of the mean for Rb^{87}/Sr^{86} and Sr^{87}/Sr^{86} has been used in the regression analyses.

The regression analyses were tested using the technique of Brooks et al. (1972) which allows for the critical distinction between an isochron (no excess scatter about the fitted line) and an errorchron (excess or geological error).

The distinction between an isochron and an errorchron is based on a comparison of the mean sums of the residuals (M Sum) to the table of F-

ratios for a given number of samples and degrees of freedom. The M Sum is defined as:

$$\text{M Sum} = \left[\frac{X_i(w(X_i)\ (x_i - X_i)^2 + w(Y_i)\ (y_i - Y_i)^2}{(n - z)} \right]^{\frac{1}{2}}$$

where X_i, Y_i are the observations, x_i, y_i are the values adjusted to lie on the straight line and $w(X_i)$, $w(Y_i)$ are the weights of the various observations.

A.4 Analytical Precision and Accuracy

The precision of the actual measurements is determined by repeating a number of measurements on a single sample. The precision of a given determination is dependent on analytical uncertainties, contamination in the chemistry and fractionation in the spectrometry. Sampling errors were eliminated by taking representative fractions which were thoroughly homogenised prior to removing fractions for analysis. Pure reagents and rigorous cleaning techniques eliminate any blank effects through contamination in the chemical processing. Fractionation due to sample solution being inhomogeneous prior to splitting, and the steps taken to eliminate this problem, have already been discussed.

The greatest source of error arises in the mass spectrometry and is introduced if Rb^{87} is present when measuring Sr^{87}/Sr^{86} ratios. The Rb^{87} contribution to Sr^{87} was generally not more than 1% and could be corrected for. Sr^{87} does not interfere in measuring Rb^{87}, since Rb is ionized at a much lower temperature than Sr.

Fractionation effects can introduce systematic error, though of random magnitude when measuring isotopic ratios. Fractionation between isotopes of a particular element occurs because lighter isotopes are preferentially ionized when heated. Fractionation for Sr isotopic measurements can be corrected for since the ratio of Sr^{88}/Sr^{86} in nature is constant, the assumed value being 8.375. No correction can be applied to the measured Rb isotope ratio as it only has two isotopes, and Rb fractionation effects

are minimised by measuring the Rb ratio under constant conditions.

The range of values of the mean for the Rb^{87}/Sr^{86} ratio determined from duplicated is 1.5% for the felsic rocks studied and 3% for the metabasite and metasedimentary inclusions. The standard deviation of the mean for Sr^{87}/Sr^{86} carried out on the MAT-CH4 is 0.7080 ± 0.0002 (1σ) and for the Vg-Micromass the value is 0.70804 ± 0.0003 (1σ).

The accuracy of the data used is determined by measurements of interlaboratory standards. Both the accuracy and the precision of ratios determined are shown by the reproducibility of the Eimer & Amend Standard $SrCO_3$.

TABLE A.2

Sr Isotopic Composition of Eimer & Amend Standard

	MAT-CH4 This study	VG-Micromass This study	The average of 4 different analysts: compiled by the NBS
Sr^{87}/Sr^{86}	0.7080	0.70804	0.70794

A measure of the precision of the spike used in this study is given by the accuracy in the determinations of Rb and Sr concentrations in the NBS-SRM 70a standard (Table A.3)

TABLE A.3

	Rubidium ppm	Strontium ppm
This study	523.31	65.764
Rec. value	523.90 ± 1.01	65.485 ± 0.320

APPENDIX B

X-ray fluorescence

The analyses of major element concentrations presented in this study were performed by the General Superintendence Co. Ltd. The analyses were carried out in the following manner:-

(1) X-ray fluorescence

SiO_2, Al_2O_3, MgO, CaO, Na_2O, K_2O, TiO_2, P_2O_5, MnO

(2) Volumetric

FeO

(3) Gravimetric

H_2O^-, H_2O^+ and CO_2

All trace elements were analysed on the Phillips PW1410 X-ray spectrometer using the pressed pellet method (Norrish and Chappel, 1967). Running conditions are listed in Table B.1.

The analyses of Yt, Nb, Zr, Rb and Sr follow the method proposed by Cherry et al. (1970). Mass absorption corrections were made by using the Mo Compton method (Reynolds, 1967). Interference of Rb on Y, Sr on Zr and Y on Nb were corrected for, by measuring the relative size of these interference peaks on SiO_2 standards for Rb, Sr and Y respectively. Average correction factors were then calculated. Background was corrected for by making background measurements on either side of each peak, and extrapolating beneath the peak.

For Ba, K and Mn, no mass absorption correction was made as the standards and the unknowns were all granitic in composition, with similar Compton peaks. Three background measurements were made for Ba to account for changing slopes in this region of the Cr tube. The background on either side of the potassium (K) and manganese (Mn) peaks were relatively flat, and thus only one background measurement was needed.

TABLE B.1 X - Ray Fluorescence Running Conditions

Element	Crystal	Kv	Ma	Counter	Collimator	Angle(2)	Counting Time(sec)
Nb	LIF 220	65	40	scintillation	fine	30.48	80
Zr	"	"	"	"	"	32.13	"
Yt	"	"	"	"	"	[illegible]	"
Sr	"	"	"	"	"	25.88	"
Rb	"	"	"	"	"	26.62	"
K	PET	50	50	flow	"	5 .74	10
Na	gypsum	50	50	flow	coarse	54.80	200
Ba	LIF 200	50	50	flow	coarse	118.34	120

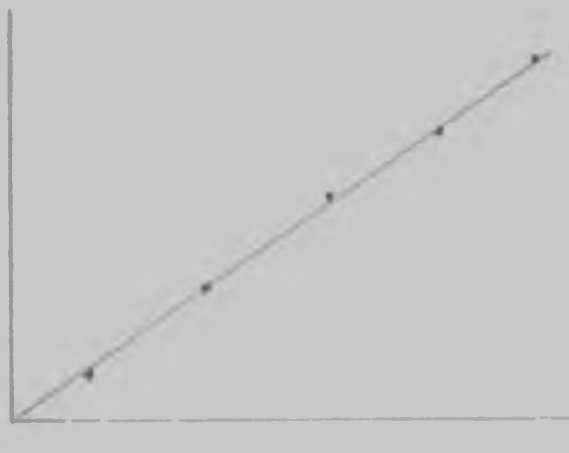
Collimator sizes are:- fine = 150 microns and coarse = 550 microns.

B.1 Data reduction: precision and accuracy

Data for all elements was processed in essentially the same manner by means of an IBM 360/50 computer. Where necessary dead-time, interference and Compton peak corrections were made. The net intensity of a peak is computed by correcting for background.

Net intensity = measured intensity - background under peak

The concentration of an unknown element for a particular sample is determined from a working curve, which is computed by plotting standard concentration vs. intensity.



The errors incurred are dependent on how accurately the concentrations in the standards are known and the error in the measurement of net peak intensity. The number of standards used greatly influence the statically determined errors. In this work four standards were used to determine the calibration curve. Concentration of standards are given in Table B.2.

A measure of the precision and accuracy of the method used are shown by the reproducibility of standards and by the values obtained when treating NBS interlaboratory standards as unknown (Table B.2 and B.3).

TABLE B.2 Recommended values for some Trace Element of Standards used in this study

	Rb (ppm)	Sr (ppm)	Yt (ppm)	Nb (ppm)	Zr (ppm)	Ba (ppm)	K_2O (%)	Na_2O (%)
GSP-1	252.0	235.0	24.5	24.7	537	1300	5.48	2.88
GA	-	-	-	-	-	845	4.03	3.55
GH	-	-	-	-	-	-	4.50	3.80
GH	-	-	-	-	-	-	4.78	3.80
BCR	48.2	328.	37.	15.	191	675	-	-
W	22.0	190.	21.7	6.9	94	-	-	-
G	-	-	-	-	-	475		

Values obtained for Standard GSP-1 in this Study

	Rb	Sr	Yt	Nb	Zr	Ba	K_2O	Na_2O
Rec. value	252.0	235.0	24.5	24.7	537	1300	5.48	2.88
This Study	246.0	234.0	25.5	24.6	570	1348	5.46	2.78
% Diff.	2.4	0.43	3.90	0.40	6.10	3.70	0.36	3.50

TABLE B.3 A Measure of the Precision by the X-Ray Fluoresence Method

	Rb (ppm)	Sr (ppm)	Yt (ppm)	Nb (ppm)	Zr (ppm)	Ba (ppm)	K (%)	Na (%)
	98	108	80	24	371	2742	5.50	2.73
	97	108	80	23	342	2742	5.30	2.82
	99	109	81	24	355	2752	5.40	2.82
	101	107	79	23	367	2737	5.48	2.77
	98	108	79	24	342	2725	5.51	2.13
	102	106	81	24	357	2733	5.46	2.85
	97	111	83	24	349	2737	5.38	2.99
	99	109	80	23	365	2723	5.47	2.99
	99	107	79	23	343	2743	5.50	2.88
Mean	99	108	80	24	354	2744	5.46	2.78
Std. dev.	1.49	1.36	1.22	0.49	10.61	17.23	0.09	0.25
% dev.	1.51	1.29	1.53	2.04	2.99	0.63	1.65	8.99

APPENDIX C

Delayed Neutron Activation

The procedure for inducing and counting delayed neutrons using the DIDO reactor at Harwell follows that set out by Gale (1967).

If a nuclide having Z > 90 undergoes fission, some of the fission product nuclides decay by negaton emission to highly excited states of daughter nuclei, which in their turn decay by emission of a neutron. These neutrons are emitted almost instantaneously after the precursor nuclide has emitted a negaton, and consequently their apparent half lives for practical purposes coincide with that of their precursor nuclide. These neutrons are known as delayed neutrons.

In order to induce fission, it is necessary to bombard the nuclides with neutrons. Fission of the nuclides of uranium, thorium, neptunium and plutonium varies with neutron energy and this dependence on neutron energy enables one to discriminate against some nuclides whilst fission products are counted. The counts obtained are proportional to the concentration of fissionable material in the sample.

Two determinations were made for each sample, one in a thermal flux, for the determination of U, and one in a fast flux, the slow neutrons component being screened out by cadmium shielding for Th determinations. The thermal and fast fluxes available in this facility are 1.2×10^{13} and 2.2×10^{10} cm^{-2} sec^{-1} respectively.

C.1 Comparison of analytical methods for Uranium and Thorium

Most analytical methods for thorium and uranium suffer from interferences, which necessitate destructive chemical treatment of the sample so as to allow the separation of the thorium and uranium prior to quantative determination, Table C.1 (modified) after Gale (1967) presents a comparison of the major analytical methods available.

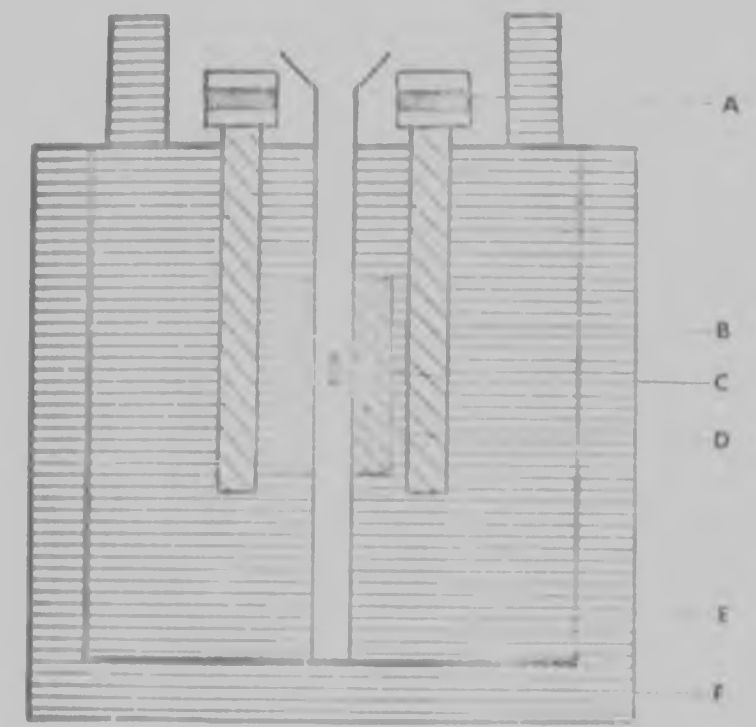
TABLE C.1

Method	Time for single analysis(h)	Approximate range of applicability (μg)	Typical error (%)
Neutron activation - radiochemical separation	5	10^{-4} - 10^{4}	± 5 to 2
Isotope dilution	5	0.1 upwards	± 10 to 2
Fluoroscopy	3	10^{-4} - 1	± 50 to 5
X-ray fluorescence	1 to 3	10 upwards	± 50 to 5
Volumetric	3	1 - 5 x 10^{5}	± 5 to 0.5
Emission spectroscopy	2	100 upwards	± 20 to 5
α- particle to- radiography	5 to 50	1 - 10^{4}	± 15 to 3
Colorimetry	5	10 - 10^{4}	± 5 to 1
γ-ray radiometric methods	15	25 - 10^{4}	± 15
α- particle counting	50	50 - 5 x 10^{3}	± 15

From this Table, it is apparent that most of the methods are either time consuming or far too insensitive and inaccurate for uranium and thorium determinations at low levels of concentration (10 ppm). The delayed neutron activation technique offers a rapid and precise method of determination of uranium and thorium at low levels in rock powder samples. For a typical granite,for example, containing 10 ppm Th and 3 ppm U, a single determination for both Th and U occupies about six minutes.

C.2 Procedure

3 to 4 gm of sample were weighed out into polyethylene snap-top ampoules The ampoules which are sealed by heating, are then transferred into the reactor in tufnol containers ("rabbits"), by means of a pneumatic transfer tube. In the case of the Th measurements, a different transfer system is used, which links up to the fast flux in the reactor. For Th measurements the rabbits are lined



A R.F. SHIELD

B BF_3 NEUTRON DETECTOR TUBE

C SAMPLE IN COUNTING POSITION

D LEAD CYLINDER

E CADIUM SHIELD

F BORATED PARAFFIN WAX

FIGURE C.1 DELAYED NEUTRON DETECTOR APPARATUS

with 0.03" cadmium sheeting to screen out the slow neutrons.

An automatic timer is started on arrival of the sample at the irradiation position inside the reactor. The sample is irradiated for a pre-selected time of 60 seconds and then automatically removed from the reactor to the sending station. The sample is then rapidly removed from the rabbit and dropped into the counter. After a delay time of 30 seconds (taken from the time the sample started on the return journey from the irradiation position) the counter starts counting for a pre-selected time of 60 seconds.

The rabbit is not included in the count because of the possibility of contamination in the form of uranium and oxygen in the tufnol, and contamination picked up in the transfer tube.

The delayed neutron emission for the irradiated sample is measured on a system of BF_3 counter tubes geometrically arranged to give maximum sensitivity.

C. 3 Interference

The BF_3 counters have a small but finite efficiency for the detection of γ-rays. Irradiation of ^{28}Al causes a very high γ-ray flux. By inserting a lead cylinder to shield the BF_3 tubes from γ-rays, it is then possible to adjust the discriminator so as to reject all the γ-rays that may be produced from the irradiation of Al in 3 gm of rock sample. The pulse due to neutrons is hardly discriminated against.

Np and Pu are present in geological material in minute quantities and therefore do not present an interference problem. Thus, detection of delayed neutrons following exposure of a sample to thermal neutron is characteristic of U^{235} whilst fast neutrons will fission U^{238} and Th^{232}. The interference of U^{238} on Th however can be corrected for, if the amount of uranium in the sample is known.

The only other form of interference may be due to ^{9}Li and ^{17}N which have very short half-lives. Thus interference from this source of delayed neutrons becomes negligible if there is an appropriate delay before counting begins.

C.4 Data reduction, precision and accuracy

The concentrations of U and Th were determined by a comparison of the counts obtained on the unknowns to accurately determined gravimetric preparations of U and Th. All determinations were done in duplicate.

Uranium

The sensitivity for U is about a factor of 100 greater than for Th. For uranium the results were calculated using the equation

$$U = \frac{C}{K}$$

where C is the number of counts and K is the calibration constant.

In the suite of rocks studied in this work the lowest U value recorded was 0.02 ppm. Counts for 60 seconds at this level are 11 (for 3 gm of rock) with a background count of 10. The lowest sensitivity over the period in which analyses were carried out was [illegible] counts/μg. Thus the detection limit for U would be about [illegible] ppm for 3 gm of rock, where the background is 10 counts. However the sensitivity at times has been as high as 1000 counts/μg, increasing the sensitivity by a factor of 2.

A measure of precision has been obtained by repeated analyses on select samples, whereas the accuracy has been determined by comparing the results obtained in this work with isotope dilution results obtained for samples over the concentration range of 0.02 ppm to 30 ppm. Periodic analyses on NBS standards were also carried out (Table C.2)

Thorium

The sensitivity for thorium varied between 3.8 and 4.6 counts/μg, and thus for a background of 10 and 3 g of rock, the detection limit is about 1 ppm.

The thorium results were calculated using the formula

$$Th = \frac{1}{S} \left((S - B)_{Th} \right) \Big/ \text{wt. of sample}$$

A correction for background was also made.

r, the cadmium ratio for thorium was taken as 1

k is the calibration constant for Th

K is the unshielded calibration constant for uranium in the fast flux

R, the cadmium ratio for uranium was taken as 19.00. This value is the mean of 5 measurements (standard deviation = 0.20)

A measure of the accuracy and precision of the Th measurements is given in Table C.3.

TABLE C.2 Accuracy and Precision of Delayed Neutron Activation Method : Uranium

Sample	G2	VT40	VT41
	1.98	27.35	20.37
	1.90	26.86	19.37
	1.92	27.18	19.20
	1.86	28.13	19.75
	1.93	[illegible]	19.68
Mean	1.92	27.50	19.67
Std. dev	0.044	0.537	0.445

Standard	This Study	Recommended Value	% Difference
GSP-1	[illegible]	2.68	8.06
G2	1.92	2.07	7.81
BCR	1.63	1.80	10.43

Sample	This Study	Isotope Dilution	% Difference
VT40	27.52	[illegible]	0.10
VT41	19.87	20.100	1.16
KK4	0.24	[illegible]	2.50
KK6	0.35	[illegible]	12.00
KK8	1.38	1.419	2.83

Note: 1. Recommended values for NBS Standards from Flannagan (1969)

2. Values given are the average of duplicate analyses

3. Uranium concentrations in ppm.

TABLE C.3 Accuracy and Precision of Delayed Neutron Activation Methiod : Thorium

Sample	GSP-1	VT40	VT41
	117.59	41.09	23.33
	124.75	38.05	25.74
	115.55	41.81	26.07
	136.18	45.99	19.73
	118.65	49.47	19.42
Mean	122.62	43.28	22.86
Std. dev.	8.30	4.47	3.18

Standard	This Study	Recommended value	% Difference
GSP-1	122.62	116.40	5.07

Sample	This Study	Isotope Dilution	% Difference
KK15	2.74	3.15	14.98
VT460	0.94	0.75	26.66
VT505	7.77	8.11	4.38

Note: 1. Recommended value for GSP-1 from Gale (1967)

2. Values given are the average of duplicate analyses

3. Thorium concentrations in ppm

APPENDIX D

Analysis of water by heating and condensation

The water content of a rock (H_2O^+) is the water expelled from a sample at a temperature greater than 105 - 110°C and excludes the water (H_2O^-) driven off below this range. The H_2O^+ is bound up in the crystal lattice of the minerals that make up the rock, whereas the H_2O^- is found absorbed to grain boundary surfaces. Thus in any water content measurement the sample must first be oven dried at ~ 110°C to drive off the H_2O^-.

Procedure

Temperatures of about 1000°C are needed to expel all the H_2O^+ from the hydrous minerals. However, as a rule it is advantageous to mix the rock powder with a flux, which serves to break down the hydrous mineral structures. The flux also serves to retain other volatiles, and provides a supply of oxygen to prevent reduction of water to hydrogen during the ignition (Maxwell, 1968). Lead chromate was found to be a suitable flux.

The samples, which are in the form of finely ground powders, are accurately weighed out, and mixed with flux in a porcelain, platinum or silica boat. About 2 gms of rock are used. The rock sample in the boat is then heated in a silica tube for about 10 minutes while a current of dry nitrogen is drawn over it. Each sample must be heated for the same period of time, and at the same temperature. The water is absorbed in a suitable agent such as anhydrous magnesium perchlorate. The drying agent used to dry the nitrogen should be the same as that used to absorb the sample water. It is important to separate the H_2O^+ from other volatiles such as CO_2. The CO_2 is absorbed by the use of ascarite.

Details of the apparatus used are shown in Figure D.1.

All measurements were performed in duplicate and agreement to within 15% was obtained for 96% of the samples.

A Sulphuric acid for drying nitrogen

B Ascarite for drying nitrogen

C Anhydrous magnesium perchlorate for drying nitrogen

D Oven (100°C)

E Sample contained in silica boat

F Heating element 100°C

G Water absorbed in anhydrous magnesium perchlorate

H CO_2 absorbed in ascarite

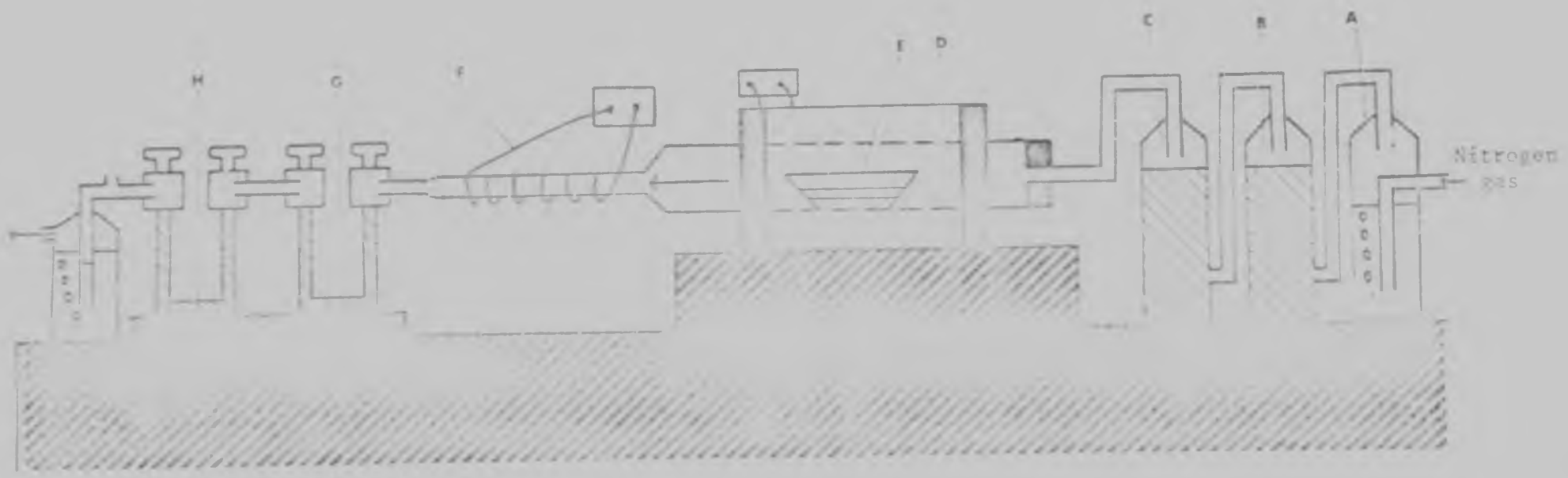


FIGURE D-1 APPARATUS FOR WATER ANALYSIS

APPENDIX E

Petrography of some selected samples which were analysed by the isotope dilution method (Locality Fig. 1.2)

Note: Description of the main metamorphic suite (SMZ), after Stepto, Ms. in preparation.

Sample Number

(A) Mafic inclusions of [illegible]

VT462
VT460
KK100

Fine to medium grained melanocratic mafic granulites; andesine is the dominant mineral, and forms 35 to [illegible]% of these rocks. The grains are generally stubby, and are either equant polygonal or irregularly bounded. The clinopyroxene (diopside) is [illegible] to greenish in colour, and is slightly pleochroic. Diopside comprises 10 to 30% of these rocks. The grains are either equant or to a lesser extent short and prismatic, either with polygonal or irregular boundaries. Hypersthene comprises 5 to [illegible]% of these rocks, and is present in the form of small (< 0.4 mm) equant polyhedra or irregularly bounded short prismatic sections. Biotite is present in minor amounts, in the form of thin laths usually orientated parallel to the foliation direction. Accessory quartz occurs interstitially, or as rounded grains within the plagioclase. Hornblende is also sporadically developed, and invariably it is corroded and retrograded to biotite.

VT524
KK101

Fine to coarse grained holocrystalline and porphyroblastic, thinly banded garnet paragneiss; the prominent banding in these rocks is produced by alternating melanocratic and leucocratic

layers of varying thickness and grain size. Bands are usually 1 to 2 cm wide, but can increase to 10 cm. These rocks consist essentially of garnet, quartz and feldspar. The feldspar is largely an untwinned plagioclase, with minor amounts of K-feldspar, both ranging up to 2.5 cm in size. Grains vary from fairly equant polyhedra to euhedra. Quartz, which forms 15 to 40% of the rocks, is present as large anhedral grains, up to 6 mm long in exceptional cases, but usually of the order of 2 mm. The quartz shows varying degrees of recrystallization, all within the same section, and many complete grains have been changed to fine grained aggregates. The garnet and its alteration products comprise 20 to 50% of the sections. They are usually pink or neutral to purplish in colour. The smaller grains are idioblastic to subidioblastic, but become increasingly more anhedral with size (up to 6 mm). The smaller grains often form small clusters. The garnets have suffered varying degrees of alteration which have produced spectacular corona structures. In some cases, the garnets have been completely altered. The alteration products include ortho- and clinopyroxene, spinnel and cordierite. Accessory biotite occurs in short ragged laths and flakes, concentrated in irregular bands, which often partially envelope garnets. Minor amounts of hypersthene occurs mainly as irregular anhydral grains up to 0.5 mm in size always closely associated with garnets. Opaque minerals which are equant to irregular in shape, occur as inclusions in garnet and also in a secondary form along its cleavages.

KK15
KK103

Bluish grey medium grained xenoblastic hypersthene gneiss; The texture varies from a weakly banded, and in some cases

almost massive appearance, to a strongly banded gneiss near the margins of the bodies. These rocks consist essentially of plagioclase quartz hypersthene and biotite. Plagioclase (oligioclase) is the dominant mineral, and occurs in equant to irregular interlocking grains up to 1.8 mm in size. Incipient recrystallization on fractures; cleavages and grain boundaries, as well as microfaulting, strain shadows and bending of twin lamellae are common features. These rocks are characterised by up to 16% hypersthene which occurs in small stubby prismatic and clusters of prismatic grains, which are often rounded and corroded. The quartz has been partly recrystallised and often occurs as small grains included in the plagioclase or interstitial to it. Clinopyroxene is sometimes present, but in many cases it has largely been retrogressed to hornblende. Biotite is present as short irregular laths and flakes often associated with the pyroxenes. Accessories are apatite and zircon are the only opaque minerals.

(B) Inlandsee leucogranofels

VT211
VT24
VT127
VT144
VT173
VD1
VD2
VD3
KK12
KK13
KK14
KK16

The Inlandsee leucogranofels notably vary considerably in colour and texture but in all cases show a marked lack of mafic minerals. Cream, grey, pinkish and reddish are the predominant colours. In most cases, the Inlandsee leucogranofels exhibit a strong planar tectonic fabric, usually due to flattened lenticular aggregates of quartz. This is particularly prominant in the very centre of the dome, e.g. VT211, VD1, VD2, VD3 but decreases outwards. This feature is due to the partial or complete recrystallisation of quartz and the development of

glomerogranular textures. The quartz is completely recrystallised into aggregates of equant 5 or 6 sided polyhydra. The larger grains form the core and the smaller ones the margins of such aggregates. Feldspars may often be only partially recrystallised, with perthite, being more resistant than plagioclase. In addition to quartz and feldspar which forms 99% of the rocks, brown biotite, microcline, orthopyroxene and zircon may be present in very small amounts.

(C) Outer granite gneiss

VT34
VT36
VT40
VT52
KK6
KK7
KK47
KK37

The essential differences between the Inlandsee Leucogranofels and the outer granite gneiss is that firstly, the latter are not tonitic or secondly, these rocks contain between 3 and 10% biotite and in rare exceptional cases up to 30% biotite. The texture in these rocks varies considerably from mostly banded gneissose alternating of alternating biotite rich and leucocratic layers, through to rocks of granitic texture which may be texturally massive, and quartz feldspar granite pegmatites. VT34, VT36 and VT40 are of this latter type. The majority of the outcrops, however, consist of equigranular medium grained gneissic rocks with a hypidiomorphic granular texture consisting of quartz, plagioclase, orthoclase, perthite, biotite and minor amounts of sphene, apatite and zircon. VT52, KK6, KK7, KK47 and KK53 are of this type.

(D) Central Intrusive biotite granite

BG1
BG2
BG3
BG4

A single outcrop (5m x 5m) of a massive medium grained biotite granite north of the west end of the Inlandsee. The K feldspar occurs in the form of anhedral plates of patch

perthite, and lesser amounts of microcline up to 4 mm in size. Small well twinned hedra of albite, often with zoned extinction are locally concentrated but occur throughout these rocks. The biotite, which is of a brown variety, has a columnar habit and is unoriented. The quartz is free of all strain effects.

REFERENCES

Allsopp, H.L. (1961) Rb-Sr age measurements on total rock and separated mineral fractions from the old granite of the Central Transvaal. J. of Geophys. Res. 3, 1499-1507.

Allsopp, H.L. (1964) Rubidium/Strontium ages from the Western Transvaal. Nature, 204, 361-363.

Allsopp, H.L., Ulrych, T.J., and Nicolaysen, L.O. (1968) Dating some significant events in the history of the [illegible] and system by the Rb-Sr isochron method. Canad. J. Earth Sci. 5, [illegible]-619.

Anhaeusser, C.R. (1973) Early Precambrian crust of southern Africa in a discussion on the evolution of the Precambrian crust (edited J. Sutton and B.F. Windley) Phil. Trans. Roy. Soc. Lond. A, 359-368.

Armstrong, R.L. (1968) A model for the evolution of strontium and lead isotopes in a dynamic earth. Rev. Geophys. 6, 160-166.

Barrett, D.R. (1974) Initial Sr-isotope data and ancillary geochemical studies on kimberlite and [illegible] intrusions. Unpublished Ph.D.

Barton, J.M., Jr., Fripp, R.E.P. and [illegible]n, B. (1977) Rb/Sr ages and geological setting of [illegible]nt dyke in the [illegible] River area, Limpop mobile belt, South Africa. Nature, 267, [illegible]-40.

Birch, F. (1954) Heat from radioactivity : in Nuclear geology (editor H. Faul) p. 148, John Wiley and [illegible] - New York.

Birch, F., Roy, R.F., and Decker, E.R. (1968) Heat flow and thermal history in New England and New York ; In Studies of Appalachain Geology (editor E-An Zen, W.S. White, J.B. Hadley and J.B. Thomson, Jr.), p. 437, Interscience, New York.

Bishopp, D.W. (1941) The geodynamics of the Vredefort dome. Trans. Geol. Soc. S. Afr. 44, 1-18.

Bisschoff, A.A. (1961) The pseudotachylite of the Vredefort dome. Trans. Geol. Soc. S. Afr. 64,

Bisschoff, A.A. (1969) The petrology of the igneous and metamorphic rocks of the Vredefort Dome and adjoining parts of the Potchefstroom syncline. Unpublished D.Sc. thesis to the University of Pretoria - Pretoria.

Borchers, R.B. (1961) The exploration of the Witwatersrand system and its extensions. Trans. 7th Commonwealth Mining and Metallurgical Congress 2, 489-512.

Bor-Ming Jahn and Chi-Yu Shih, (1974) On the age of the Onverwacht group, Swaziland sequence, South Africa. Geochim. Cosmochim. Acta, 38, 873-885.

Bray, J.M. (1942) [illegible] in igneous rocks from Jamestown Colorado. Bull. Geol. Soc. Am. 53, pp 765.

Bridgwater, D. and Collerson, K.D. (1976) The major petrological and geochemical characters of the 3600 m.y. Uivak gneisses from Labrador. Contrib. Mineral. Petrol. 54, 63-84.

Brock, B.B., and Pretorius, D.A. (1964) Rand basin sedimentation and tectonics; In the geology of some ore deposits in Southern Africa (editor S.H. Haughton) Vol. I Geol. Soc. S. Afr. 549-599.

Brooks, L., Hart, S.R., and Wendt, I. (1972) Realistic use of two error regression treatments as applied to rubidium strontium data. Rev. Geophys. Space Phys. 10, 551-557.

Brooks, L., James, D.E. and Hart, S.R. (1976) Ancient lithosphere : Its role in young continental volcanism. Science, 193, 1086-1094.

Bullard, E.C. (1939) Heat flow in South Africa. Proc. Roy. Soc. A, 173, 474-502.

Burger, A.J., Nicolaysen, L.O., and de Villiers, J.W.L. (1961) Lead isotopic compositions of galenas from the Witwatersrand and Orange Free State gold fields, and their relation to the Witwatersrand and Dominion Reef Uranites. Geochim. Cosmochim. Acts, 26, 25-59.

Carte, A.E. (1954) Heat flow in the Transvaal and Orange Free State. Proc. Phys. Soc., B, 67, 664-672.

Carte, A.E., and van Rooyen, A.I.M. (1969) Further measurements of heat flow in South Africa. Upper mantle project. Geol. Soc. S. Afr. Spec. Pub. No. 2, 445-450.

Cherry, R.D., Hobbs, J.B.M., Erlank, A.J., and Willis, J.P. (1970) Thorium, uranium, potassium, lead, strontium and rubidium in silicate rocks by gamma - spectroscopy and X-ray fluorescence. Canadian Spectroscopy 15, 1-8.

Christensen, N.I. and Fountain D.M. (1975) Constitution of the lower continental crust based on experimental studies of seismic velocities in granulites. Geol. Soc. Amer. Bull. , 227-236.

Daly, R.A. (1947) The Vredefort ring structure of South Africa. J. Geol. 67, 496-506.

Davies, R.D., and Allsopp, H.L. Geochronological evidence relating to the evolution of the lower Precambrian granitic crust in Swaziland. Geol. , , 553-5 .

Davies, R.D., Allsopp, H.L., Erlank, A.J. and Manton, W.I. (1970) Sr-isotopic studies on variously layered intrusions in Southern Africa. Symposium on the Bushveld Igneous Complex and other layered intrusions. Geol. Soc. S. Afr. Spec. Pub. No. 1, 576-593.

Davies, R.H. (1971) Geochronology and isotopic evolution of the early Precambrian crustal rocks in Swaziland. Unpublished Ph.D. Thesis to the University of the Witwatersrand - Johannesburg.

De Gasparis, A.A. (1967) Rb-Sr studies relating to problems of geochronology on the Nelspruit and Lydenburg granites. Unpublished M.Sc. Thesis to the University of the Witwatersrand - Johannesburg.

Dietz, R.S. (1961) Vredefort ring structure : Meteorite impact scar? J. Geol. 69, 499-516.

Duchesne, J.C. (1968) Strontium vs. calcium and barium vs. potassium in plagioclase from Southern Rogaland Anorthosites. Ann. Sco. Geol. Belg. Bull. 90, pp 643.

Eade, K.E., Fahrig, W.E., and Maxwell, J.A. (1966) Composition of crystalline shield rocks and fractionating effects of regional metamorphism. Nature, 211, 1245-1249.

Engel, A.E.J. (1963) Geologic evolution of North America. Science., N.Y. 140, 143-152.

Erlank, A.J. (1968) The terrestrial abundance relationship between potassium and rubidium. In origin and distribution of the elements (editor L.H. Ahrens) 871-[illegible], Pergamon.

Erlank, A.J. (1971) Studies on the distribution of potassium and some geochemically related elements. Unpublished Ph.D. Thesis to the University of Cape Town - Cape Town.

Fisher, K., and Puchelt, H. (1972) [illegible] Handbook of Geochemistry (editor K.H. Wedepohl). Vol. II/3 Ch. 6. Springer-Verlag.

Flanagan, F.J. (1969) U.S. Geological Survey standard II. First compilation of data for the new U.S.G.S. rocks. Geochim. Cosmochim. Acta. 33, 81-120.

Gale, N.H. (1967) Delayed Neutron Activation: Development of delayed neutron technique as rapid and precise method for determination of U and Th at trace levels in rocks and minerals, with application to isotope geology. Radioactive dating and methods of low level counting. 531-552. Inter Atomic Energy agency. Vienna.

Gane, P.G., Collins, A.R., Stillwell, J.P.I., and Seligman, P. (1956) Crustal structure in the Transvaal. Bull. Seismol. Soc. Am. 46, 293-316.

Garner, E.L., Machlan, D.A., and Shields, W.R. (1971). Uranium isotopic standard reference materials. N.B.S. special publication 260-27, 1-162.

Gast, P.W. (1968b) Upper mantle chemistry and evolution of the earth's crust. In the History of the earth's crust, (editor R.A. Phinney) 15-27 Princeton University Press.

Green, T.H. (1970) High pressure experimental studies on the mineralogical constitution of the lower crust. Phys. Earth Planet. Interiors, 3, 441-450.

Hahn-Wein Heimer, P., and Johannin[illegible], H. (1968) Geochemical investigations on different granite plutons in the Black Forest. In origin and distribution of the elements (editor L.H. Ahrens).

Hall, A.L., and Molengra[illegible]ff, G.A.F. (1925) The Vredefort Mountain land in the southern Transvaal and Northern Orange Free State. Shaler Memorial Series. Verh. d. Kon. [illegible]d. V. Wetens. Amst. 2 Sec. deel 24, No. 3, 1-183.

Hall, A. (1967) The variati[illegible]n of [illegible]e tr[illegible] element[illegible] in the Roses granite complex. Done[illegible]al. Geol. Mag. [illegible], pp 99.

Hargraves, R.B. (1961) Sha'ter[illegible] in th[illegible]k[illegible] of the Vredefort ring. Trans. Geol. Soc. S. Afr. 64, 147-161.

Hargraves, R.B. (1970) Palae[illegible]magneti[illegible] relevant to the origin of the Vredefort Ring. J. Geol. 78, [illegible].

Haughton, S.H. (1969) Geological hi tory of [illegible]outhern Africa. Geol. Soc. of S. Afr., Cape Town. pp.535.

Hawkesworth, C.J. (1974) Vertical distribution of heat production in the basement of the E[illegible].tern Alp[illegible]. Natur[illegible] 249, 435-436.

Heier, K.S. (1976) Che[illegible]ical composition an[illegible]n igin of Archaean Granulites and charnockites : In the early hi tory of the earth (editor Brian Windley) John Wil[illegible]y and Son, 159 163.

Heier, K.S., and Rogers, J.J.W. (1[illegible]63) Radiometric determinations of thorium, uranium and potassium in ba[illegible]alt[illegible] and two magmatic differentiation series. Geochim. Cosm[illegible]him. Act[illegible]. 27, 137.

Heier, K.S., McDougall, I., and Adam, J.A.S. (1964) Thorium, Uranium and potassium concentrations in Hawaiian lavas. Nature 204, 254-256.

Heier, K.S. and Adams, J.A.S. (1965) Concentration of radioactive elements in deep crustal material. Geochim. Cosmochim. Acta. 29, 53.

Heier, K.S. and Thoresen, K. (1970) Geochemistry of high grade metamorphic rocks. Lofoten-Vesterålen, North Norway, Geochim. Cosmochim. Acta 35, 89-99.

Heier, K.S., and Billings, G.K. (1972) Rubidium : In handbook of Geochemistry (editor K.H. Wedepohl), Vol. II/2. Ch. 37, Springer-Verlag.

Hermann, A.G. (1970) Yttrium and the Lanthanides : In handbook of Geochemistry (editor K.W. Wedepohl, Vol. II/2. Ch. [illegible], 57-71.

Holland, J.G. and Lambert, R. St. J. (1975) The chemistry and origin of the Lewisian gneisses of the Scottish mainland: the Scourie and Inver assemblages and sub-crustal accretion. Precamb. Res. [illegible], 161-188.

Hunter, D.R. (1970) The ancient gneiss complex in Swaziland. Trans. Geol. Soc. S. Afr. 73, 107-1[illegible]

Hunter, D.R. (1972) The granitic rocks of the Precambrian in Swaziland. Spec. Publ. Geol. Soc. S. Afr., 3, 131-168.

Hunter, D.R. (1974b) Crustal development in the Kaap-Vaal craton, II. The proterozoic. Precambrian Research, 1, 295-326.

Hurley, P.M. (1968) Correction : Absolute abundance and distribution of Rb, K and Sr in the earth. Geochim. Cosmochim. Acta. 32, 1025-1030.

Jaffey, A.H., Flynn, K.F., Glendenin, L.E., Gentley, W.C. and Essling, A.M. (1971) Precision measurement of half lives and specific activities of ^{235}U and ^{238}U, Phys. Rev. C, 4, pp 1889.

Kranck, E.H., and Oja, R.V. (1960) Experimental studies on Anetexis. Int. Geol. Congr. rept. of the 2nd session. Norden, pt. XIV, 16-29.

Lachenbruch, A.H. (1968) Preliminary geothermal model of the Sierra Nevada. J. Geophys. Res. 73, 6977-6989.

Lachenbruch, A.H. (1970) Crustal temperature and heat production: Implications of the linear heat flow relation. J. Geophys. Res. 75, 3291-3300.

Lachenbruch, A.H. and Bunker, C.M. (1971) Vertical gradients of heat production in the continental crust [illegible] estimated from borehole data. J. Geophys. Res. [illegible] 6261-6271.

Lambert, I.B. and Heier, K.S. (1967) The vertical distribution of uranium, thorium and potassium in the continental crust. Geochim. Cosmochim. Acta, 31, 377-390.

Lambert, I.B. and Heier, K.S. (1968) Geochemical investigations of deep seated rocks in the Australian [illegible] Lithos, 1, 30-53.

Lambert, I.B. (1971) The composition and evolution of the deep continental crust. Spec. Publ. Geol. Soc. Aust. 3, 419-428.

Lambert, R. St. J. and Holland, J.G. (1[illegible] Yttrium geochemistry applied to petrogenesis utilizing [illegible]ium-yttrium relationships in minerals and rocks. Geochim Cosmochim Acta. [illegible], 1393-1414.

Mack, C. (1966) Essentials [illegible] and technologists. Heinemann educational books.

Manton, W.I. (1962) The origin and significance of shatter cones in the Vredefort ring structure : M.Sc. Thesis to the University of the Witwatersrand - Johannesburg.

Maree, B.D. (1944) The Vredefort structure as revealed by a gravimetric survey. Trans. [illegible]. S. Afr. [illegible] 97.

Maxwell, J. (1968) Rocks and mineral analysis. New York : Interscience 584.

McCarthy, T.S. (1976) Chemical interrelationships in a low pressure granulite terrain in Namaqualand, South Africa and their bearing on granite gneisses and the composition of the lower crust. Geochim. Cosmochim. Acta. 40, 1-11.

Moorbath, S. (1975) Evolution of Precambrian crust from strontium isotopic evidence. Nature. 254, 393-397.

Moorbath, S., Onions, R.K., Pankhurst, R.J., Gale, N.H. and McGregor, V.R. (1972) Further rubidium-strontium age determinations on the very early Precambrian rocks of the Godthaab district, West Greenland. Nature Phys. Sec. 240, 78-81.

Nel, L.T. (1927) The geology of the country around Vredefort. Geol. Surv. S. Afr. Spec. Pub. No. 6, 134.

Nicolaysen, L.O. Depth of "penetration" of radial profiles across the Vredefort structure. (ms. in preparation).

Nicolaysen, L.O., Burger, A.J., and van Niekerk, C.B. (1963) The origin of the Vredefort structure in the light of new isotopic data (abstract). Int. Union Geodesy and Geophysics. 13th General Assembly, Berkeley, Ca.

Nockolds, S.R., and Allen, R. (1953) The geochemistry of some igneous rock series. Geochim. Cosmochim Acta. 4, 105-142.

Nockolds, S.R., and Allen, R. (1956) The geochemistry of some igneous rock series - III. Geochim. Cosmochim. Acta. 9, 34-77.

Norrish, K., and Chappell, B. (1967) X-ray fluorescence spectrography. In physical methods in determinative mineralogy (editor J. Zeissman) 161-214. Academic Press, London.

Oosthuyzen, E.J. (1970) The geochronology of a suite of rocks from the granitic terrain surrounding the Barberton Mountain lands. Unpublished Ph.D. thesis to the University of the Witwatersrand - Johannesburg.

Pakiser, L.S. and Robinson, P. (1969) Composition of the continental crust as estimated from seismic observations. In the earth beaneath the continents (editor L.H. Steinhardt and T.J. Smith). Amer. Geophys. Union. Geophys. Monogr. 10.

Parker, R.L. and Fleisher, M. (1968) Geochemistry of Niobium and Tantalum. U.S. Geological Survey Professional papers. 612, 43.

Patterson, C. and Tatsumoto, M. (1964) The significance of lead isotopes

Moorbath, S. (1975) Evolution of Precambrian crust from strontium isotopic evidence. Nature. 254, 393-397.

Moorbath, S., Onions, R.K., Pankhurst, R.J., Gale, N.H. and McGregor, V.R. (1972) Further rubidium-strontium age determinations on the very early Precambrian rocks of the Godthaab district, West Greenland. Nature Phys. Sci. 240, 78-82.

Nel, L.T. (1927) The geology of the country around Vredefort. Geol. Surv. S. Afr. Spec. Pub. No. 6, 134.

Nicolaysen, L.O. Depth of "penetration" of radial profiles across the Vredefort structure. (ms. in preparation).

Nicolaysen, L.O., Burger, A.J., and van Niekerk, C.B. (1963) The origin of the Vredefort structure in the light of new isotopic data (abstract). Int. Union Geodesy and Geophysics. 13th General Assembly, Berkeley, Ca.

Nockolds, S.R , and Allen, R. (1953) The geochemistry of some igneous rock series. Geochim. Cosmochim Acta. 4, 105-142.

Nockolds, S.R., and Allen, R. (1956) The geochemistry of some igneous rock series - III. Geochim. Cosmochim. Acta. 9, 34-77.

Norrish, K.G., and Chappel, B. (1967) X-ray fluorescente spectrography. In physical methods in determinative mineralogy (editor J. Zeissman) 161-214. Academic Press, London.

Oosthuysen, E.J. (1970) The geochronology of a suite of rocks from the granitic terrain surrounding the Barberton Mountain lands. Unpublished Ph.D. thesis to the University of the Witwatersrand - Johannesburg.

Pakiser, L.S. and Robinson, R. (1969) Composition of the continental crust as estimated from seismic observations. In the earth beaneath the continents (editor J.S. Steinhardt and T.J. Smith). Amer. Geophys. Union. Geophys. Monogr. 10.

Parker, R.L. and Fleisher, M. (1968) Geochemistry of Niobium and Tantalum. U.S. Geological Survey Professional papers. 612, 43.

Patterson, C. and Tatsumoto, M. (1964) The significance of lead isotopes

in detrital feldspar with respect to chemical differentiation within the earth's mantle. Geochim. et. Cosmochim. Acta. 28, 1-[illegible].

Poldervaart, A. (1962) Notes on the Vredefort dome. Trans. Geol. Soc. S. Afr. 65, 231-251.

Rao, R.U.M. and Jessop, A.M. (197) Thermal characteristic. Can. J. Earth Sci. 12, 347-360.

Reynolds, R.C. (1967) Estimates of mass absorption coefficients by Compton scattering: improvement and extention of the existing method. Amer. Mineral. 52, 1693-1697.

Rogers, J.J.W. and Adams, J.A.S. (1969) Thorium : In handbook of geochemistry (editor K.H. Wedepohl) Vol. II/1 Ch. 90. Springer-Verlag.

Rogers, J.J.W. and Adams, J.A.S. (1969) Uranium : In handbook of geochemistry (editor K.H. Wedepohl) Vol. II/1 Ch. [illegible] Springer-Verlag.

Roy, R.F., Blackwell, D.D. and Birch, F. (1968) Heat generation of plutonic rocks and continental heat flow provinces. Earth Planet. Sci. Lett. 5, 1-12.

Sclater, J.G. and Francheteau, J. (1970) The implications of terrestrial heat flow observations on current tectonic and geochemical models of the crust and upper mantle of the earth. Geophys. J.R. astr. Soc. 20, 509-542.

Sclater, J.G. (1972) New perspectives in terrestrial heat flow. Tectonophysics 14, 257-291.

Shand, S.J. (1961) The pseudotachylite of Parys, (Orange Free State) and its relationship to 'trap-shotten gneiss' and 'flinty crush rock'. Quart. J. Geol. Soc. Lond. 7 , 198-221.

Shaw, D.M. (1968) Radioactive elements in the Canadian Precambrian crust. In origin and distribution of the elements, (editor L.H. Ahrens) 855-870. Pergamon.

Shimer, J.A. (1943) Spectrographic analysis of New England granites and pegmatites. Bull. Geol. Soc. Am. 54, 1049.

Slawson, W.F. (1976) Vredefort core : a cro ection of the upper crust. Geochim. Cosmochim. Acta. 40, 117-1 1.

Sighinolfi, G.P. (1971) Investigation inte d p crustal levels: fractionating effects and geochemical trend related to high grade metamorphism. Geochim. Cosmochim. Acta. 1005-1021.

Spooner, C.M. and Fairbairn, H.W.J. (1970) tium 87/ Strontium 86 initial ratios in pyr granulite 6706.

Stacey, J.S., and Kram , J.D. (19 5) Appr tion of terrestrial lead isotope evolution by a two-st del. Earth Planet. Sc . Lett. 26, 207-221.

Stepto, D. A Geological and Geophy l St f the Central portion of the Vredefort Dome Structure. (. in p paration).

Steuber, A.M., and Murthy, V.R. (Str i tope and alkali element abundance in ultram chim. Acta. 30, 1243-1259.

Sutton, J. (1967) The cat si n l l r rd into the Pre-cambrian. Pro . geol. A . Lond. , 49

Swanberg, C.A. (1972) Verti l di tribution of at eneration in the Idaho batholith. J. G phy.. R . 77, 25 13.

Tarney, J. (1976) G try of Ar an h ade gneiss, with implicati s a to the gin n luti n of the Precambrian crust: In the early hi tory f the earth (edit r Brian Windley) John Wiley and Son, 405-417.

Tatsumoto, M., Hedge, C.E. and Er l, A.J.J. (1 6) Potas ium, rubidium, strontium, thorium, uranium and the ratio of trontium 87 to strontium 86 in oceanic tholeiiti basalt . Science. 150, 886-888.

Taylor, S.R., Emeleus, C.H. and Ex . t.S. (19) Some anomalous K/Rb ratios in igneous roc and their p trolo l si nificance. Geochim. Cosmochim. Acta. 10, 224-229.

Taylor, S.R. (1969) Abundan[illegible] of chemi[illegible]l elements in the continental crust : a new table. Geochim. Cosmochim. Acta. 28, 1273-1285.

Viljoen, M.J. and Viljoen, R.P. (1969b) The geochemical evolution of the granitic rocks of the Barberton regi[illegible]n. Spec. Publ. 2, Geol. Soc. S. Afr., 189-218.

Wasserburg, G.J., Ma Donald, G.J.F., Houle, F., and Fowler, W.A. (1964) Relative contribution of uranium, th[illegible]rium and [illegible]ta[illegible]ium to heat production in the earth. Sci[illegible]nce [illegible]3, 5[illegible]-567.

Welke, H., [illegible]art, R.J. and Ni[illegible]y en L.O. Geochr[illegible]nology of a deep profile through Archi[illegible]an base[illegible]ent [illegible]t [illegible]f[illegible]rt, with i[illegible]li[illegible]ations for early crustal evolution. (ms. in prepar[illegible]ti[illegible]n).

Willemse, J. (1937) On the [illegible]a[illegible] te[illegible]r[illegible] t[illegible] Vrede[illegible]t region and some of its associati[illegible] r[illegible]. Tr[illegible]. Geol. [illegible]. S. Afr. 40, 43-119.

[illegible] Can. J. Phys. 44, 1079-108[illegible].

York, D. (1969) Le[illegible]t squar[illegible] ttin[illegible] a straight [illegible]ine with correlated error[illegible]. Earth. Planet. [illegible]. [illegible]t. 5, [illegible].0.

Author Hart R J
Name of thesis A study of the Isotopic and Geochemical Gradients in the Old Granite of the Vredefort Structure, with implications for continental heat flow 1978

PUBLISHER:
University of the Witwatersrand, Johannesburg
©2013

LEGAL NOTICES:

Copyright Notice: All materials on the University of the Witwatersrand, Johannesburg Library website are protected by South African copyright law and may not be distributed, transmitted, displayed, or otherwise published in any format, without the prior written permission of the copyright owner.

Disclaimer and Terms of Use: Provided that you maintain all copyright and other notices contained therein, you may download material (one machine readable copy and one print copy per page) for your personal and/or educational non-commercial use only.

The University of the Witwatersrand, Johannesburg, is not responsible for any errors or omissions and excludes any and all liability for any errors in or omissions from the information on the Library website.